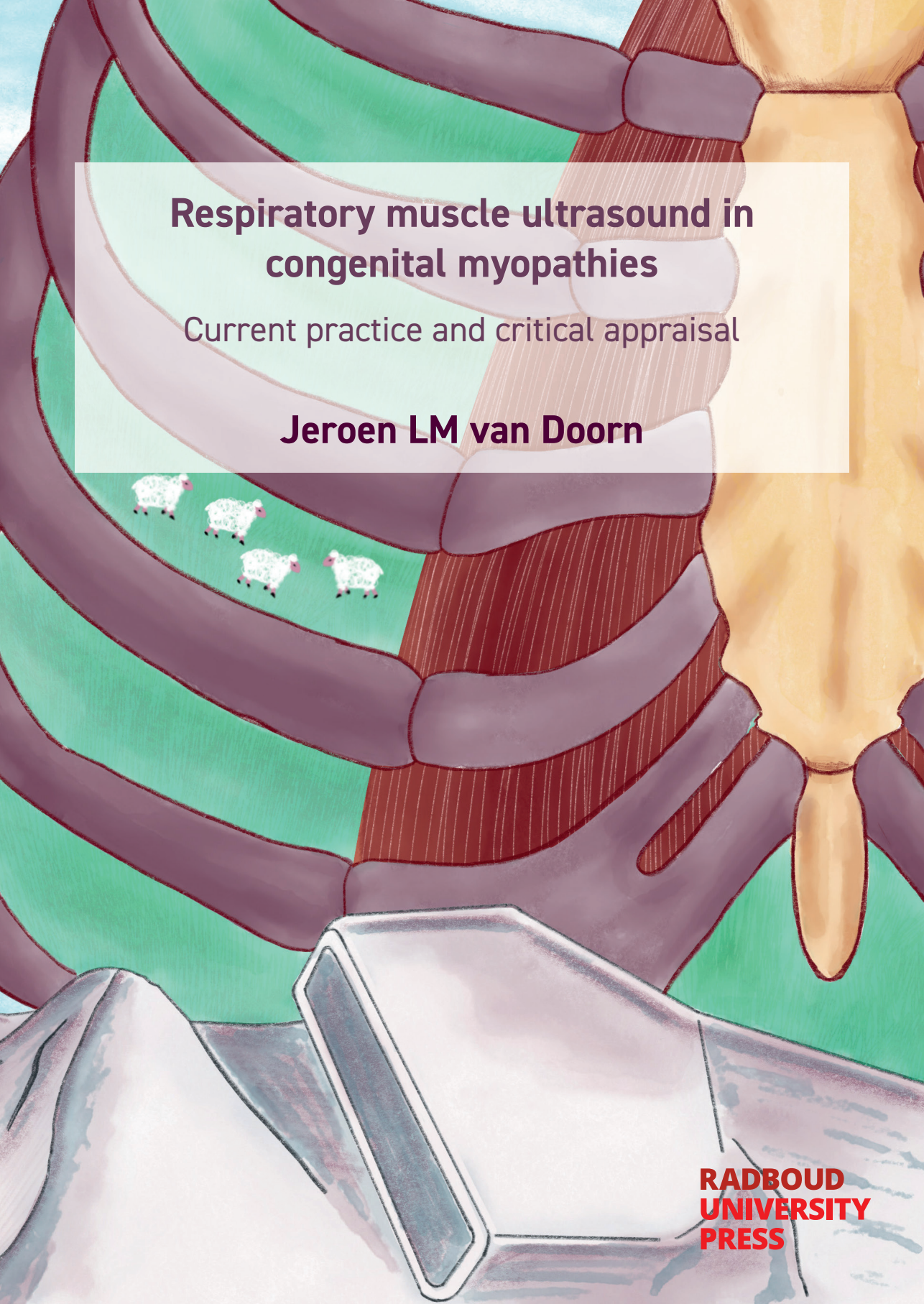


Respiratory muscle ultrasound in congenital myopathies

Current practice and critical appraisal

Jeroen LM van Doorn

RADBOUD UNIVERSITY PRESS

Respiratory muscle ultrasound in congenital myopathies

Current practice and critical appraisal

Jeroen Lambertus Maria van Doorn

Jeroen Lambertus Maria van Doorn

Respiratory muscle ultrasound in congenital myopathies

Current practice and critical appraisal

Radboud Dissertation Series

ISSN: 2950-2772 (Online); 2950-2780 (Print)

Published by RADBOUD UNIVERSITY PRESS

Postbus 9100, 6500 HA Nijmegen, The Netherlands

www.radbouduniversitypress.nl

Design: ProefschriftOntwerp.nl

Cover image: Daphne Akrum-Zoutendijk

Production coordination & prepress: ProefschriftOntwerp.nl

Printing: ProefschriftMaken/Pumbo

ISBN: 9789465153261

DOI: 10.54195/9789465153261

Free download at: https://doi.org/10.54195/9789465153261

© 2026 Jeroen Lambertus Maria van Doorn

RADBOUD
UNIVERSITY
PRESS

This is an Open Access book published under the terms of Creative Commons Attribution-Noncommercial-NoDerivatives International license (CC BY-NC-ND 4.0). This license allows reusers to copy and distribute the material in any medium or format in unadapted form only, for noncommercial purposes only, and only so long as attribution is given to the creator, see http://creativecommons.org/licenses/by-nc-nd/4.0/.

Respiratory muscle ultrasound in congenital myopathies

Current practice and critical appraisal

Proefschrift ter verkrijging van de graad van doctor
aan de Radboud Universiteit Nijmegen
op gezag van de rector magnificus prof. dr. J.M. Sanders,
volgens besluit van het college voor promoties
in het openbaar te verdedigen op
woensdag 2 december 2026
om 14.30 uur precies

door

Jeroen Lambertus Maria van Doorn
geboren op 1 september 1994
te Oss

Promotoren:
Prof. dr. N.C. Voermans
Prof. dr. C.A.C. Ottenheijm (Vrije Universiteit Amsterdam)
Prof. dr. ir. C.L. de Korte

Copromotor:
Dr. J. Doorduin

Manuscriptcommissie:
Prof. dr. D.H.J. Thijssen
Prof. dr. R.A.J. Nievelstein (Universiteit Utrecht)
Dr. S. Lassche (Zuyderland)

Respiratory muscle ultrasound in congenital myopathies

Current practice and critical appraisal

Dissertation to obtain the degree of doctor
from Radboud University Nijmegen
on the authority of the Rector Magnificus prof. dr. J.M. Sanders,
according to the decision of the Doctorate Board
to be defended in public on
Wednesday, December 2, 2026
at 2.30 pm

by

Jeroen Lambertus Maria van Doorn
born on September 1, 1994
in Oss (the Netherlands)

Supervisors:
Prof. dr. N.C. Voermans
Prof. dr. C.A.C. Ottenheijm (Vrije Universiteit Amsterdam)
Prof. dr. ir. C.L. de Korte

Co-supervisor:
Dr. J. Doorduin

Manuscript Committee:
Prof. dr. D.H.J. Thijssen
Prof. dr. R.A.J. Nievelstein (Utrecht University)
Dr. S. Lassche (Zuyderland)

Table of contents

Chapter 1	General introduction, aims and outline of the thesis	9
Part 1 – Current practice		**27**
Chapter 2	Respiratory muscle imaging by ultrasound and MRI in neuromuscular disorders	29
Chapter 3	Respiratory muscle function in patients with nemaline myopathy	55
Chapter 4	Respiratory function in LAMA2-related muscular dystrophy and SELENON-related congenital myopathy	77
Part 2 – Critical appraisal		**101**
Chapter 5	Association of diaphragm thickness and echogenicity with age, sex and body mass index in healthy subjects	103
Chapter 6	Interplay between diaphragm thickening, force generation, and lung volume change: a physiological study in health and diaphragm weakness	115
Chapter 7	Shear wave elastography to assess respiratory muscle function in congenital myopathies	133
Chapter 8	General discussion and future perspectives	153
Appendix		**165**
I – Summary		167
II – Nederlandse samenvatting | Dutch summary		171
III – Samenvatting in begrijpelijk Nederlands | Dutch plain language summary		175
IV – Research data management		179
V – Author's scientific contributions to this thesis		181
VI – List of publications		183
VII – Dankwoord | Acknowledgements		187
VIII – Curriculum Vitae		193



Chapter 1

General introduction, aims and outline of the thesis

General introduction

Breathing is a vital function that is driven by the respiratory muscles, which get weaker in neuromuscular disorders and lead to breathing difficulties. This can be a major contributor to death in individuals with a neuromuscular disorder, and has been identified as research focus by patient organizations [1]. Ultrasound is increasingly used to assess the respiratory muscles in diagnosis, clinical follow up and research in neuromuscular disorders, but also in other settings such as the intensive care unit and pulmonary medicine. Part 1 of this thesis focuses on the current application and interpretation of respiratory muscle ultrasound in patients with congenital myopathies. This is a specific group of neuromuscular disorders in which respiratory muscle weakness is common. Part 2 of this thesis critically appraises the methodology of respiratory muscle ultrasound. In this introduction, background information on congenital myopathies, the respiratory muscles and ultrasound are outlined. Then, respiratory muscle ultrasound will be extensively introduced in **Chapter 2**.

The respiratory muscles

The diaphragm is the main inspiratory muscle. The external and parasternal intercostal muscles, and neck muscles are accessory inspiratory muscles, while the abdominal wall muscles act as accessory expiratory muscles. See Figure 1 for an overview of the respiratory muscles.

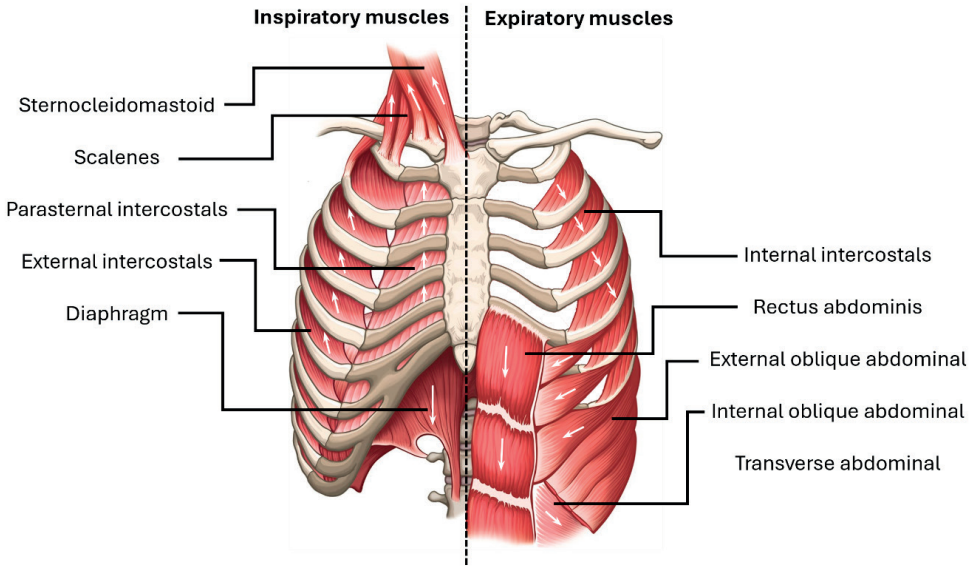


Figure 1: The respiratory muscles. The diaphragm is largely obscured by the ribcage and other respiratory muscles. The transverse abdominal muscle is deep to the external and internal oblique abdominal muscles.

The diaphragm

The diaphragm is an unique muscle, shaped as a dome and separating the thoracic and abdominal cavity. All muscle fibres originate from the entire circumference of the lowest ribs (costal part), sternum (sternal part) and vertebrae (crural part), and insert to a central tendon at the crest of the dome. The central tendon has apertures to let the oesophagus, aorta and inferior vena cava through. The diaphragm is typically very thin (± 2 mm). The insertion of the diaphragm at the lateral portions of the ribs is called the zone of apposition.

During contraction, the diaphragm flattens and with that, the lungs are pulled down. During normal day to day activities with base ventilatory demand, rested breathing is achieved by contraction of only the diaphragm during inhalation, and all respiratory muscles are inactive during exhalation during which the lungs deflate due to their elasticity and the elastic recoil of the chest wall. The diaphragm remains the most important contributor to generating negative pressure during increased ventilatory demand [2]. Movement of the diaphragm is not uniformly distributed over the diaphragm, rather, the dorsal parts have longer muscle bundles and will contract before the ventral parts.

The intercostal muscles

The intercostal muscles are two layers of muscle between each rib: the internal intercostal muscles and the external intercostal muscles. The intercostal muscles are oriented obliquely, where the insertion on the lower rib for each muscle fibre of the external intercostal muscles is more anterior than its insertion point on the upper rib. The fibres of the internal intercostal muscles are orientated opposite. From a biomechanical analysis, the contraction of the external intercostal muscles raises the ribs, increases thoracic volume, marking them as inspiratory muscles. Consequently, when the internal intercostal muscles contract, the ribs are lowered and thoracic volume is decreased, marking them as expiratory muscles.

This biomechanical model was already proposed in 1749 after nearly 2000 years of discussion and has been adopted into contemporary physiology textbooks [3]. However, solid experimental evidence was lacking, and more recent experiments suggest that both muscle layers contribute to both inhalation and exhalation, depending on their location on the thorax [3]. The exemption to this are the parasternal intercostal muscles, located directly lateral to the sternum, which is a single muscle layer that has been consistently described as inspiratory muscles [4].

The neck muscles

Four muscles in the neck contribute to breathing: the sternocleidomastoid muscle, the anterior scalene muscle, the middle scalene muscle and the posterior scalene muscle. The sternocleidomastoid muscle originates from the sternum and clavicula, inserts into the mastoid process and is the largest and most superficially located. The scalene muscles originates from the cervical vertebrae to the upper ribs.

Together, these muscles elevate the ribcage as accessory inspiratory muscles during increased ventilatory demand. By raising the ribs, the ribcage expands and lung volume is increased. Furthermore, these muscles contribute to cervical spine flexion and rotation when not recruited as accessory inspiratory muscles.

The abdominal wall muscles

The four abdominal wall muscles contribute to expiration and consist of the rectus abdominis muscle, the external oblique abdominal muscle, the internal oblique abdominal muscle and the transverse abdominal muscle. Together, they form a sheet over the abdominal organs between the lower ribs and the pelvic girdle. The rectus abdominis muscle lies medially, while the others form a three-layered structure and are referred to as the oblique abdominal muscles. The muscle fibres of all muscles are oriented differently.

The range in muscle fibre orientation enable these muscles to flex and rotate the lumbar spine, but by contracting simultaneously, they increase intra-abdominal pressure which forces the lungs to deflate. During increased ventilatory demand, the abdominal wall muscles accomplish a shorter exhalation period as accessory expiratory muscles. Furthermore, these muscles are primarily responsible for coughing.

Congenital myopathies

Congenital myopathies are a heterogeneous group of genetic neuromuscular disorders that typically present perinatally or in infancy with hypotonia and muscle weakness, usually non- or slowly progressive [5]. Congenital myopathies arise from defects in the muscles excitation-contraction coupling (box 1). All skeletal muscles may be affected in congenital myopathies, including the respiratory muscles. Weakness of the respiratory muscles lead to hypoventilation and impairs coughing. In turn, this may lead respiratory failure or to persistent lung infections, and may be an important contributor to death [6]. Given its clinical significance, respiratory management is integral to regular care, and respiratory outcome measures are used in clinical practice and drug-evaluating clinical trials (box 2). Secondary to respiratory muscle weakness, the chest wall and lungs are indirectly involved in breathing difficulties (box 3). Muscle weakness during bone development on a young age can lead to skeletal deformities in the ribcage such as a bell-shaped thorax and scoliosis, which impairs movement of the ribcage during breathing, or decreases total lung volume. Furthermore, weakness of the intercostal muscles may lead to collapse of the thorax during breathing and changes chest wall compliance, increasing the force needed to breathe. Hypoventilation leads to oedema and atelectasis in the less ventilated lung areas, increasing the effort required to breathe.

There are no curative options available for respiratory weakness in patients with congenital myopathies [7]. Therapeutic options aim at retaining as much function as possible and slow progression. Airstacking is used to passively inflate the lungs, preventing alveolar collapse,

oedema, and atelectasis. Inspiratory muscle training is being investigated to delay progression of respiratory muscle weakness [8]. The supportive approach to hypoventilation is mechanical ventilation, which can range from nocturnal non-invasive ventilation to fulltime invasive ventilation.

Currently, respiratory function in congenital myopathies is primarily assessed with pulmonary function testing However, this requires patient cooperation, which can be challenging in young children [9]. Furthermore, it is a global evaluation of respiratory function, and it does not provide information on specific respiratory muscles [10]. Moreover, significant weakness can develop before it is reflected in pulmonary function tests [11-13]. Therefore, new tests are needed that address these shortcomings to guide respiratory management and to be used as outcome measure in research. Respiratory muscle ultrasound is increasingly used in this capacity.

Ultrasound

Medical ultrasound imaging makes images of biological tissues by transmitting and receiving high frequency ultrasound waves. It operates with piezo-electric crystals, which have an unique property in that they deform when an electrical current is applied. By repeatedly applying electrical current, the crystal will vibrate and will emit sound. Alternatively, when not applying electrical current, when the crystal is deformed by an external force such as a soundwave, it will generate an electric voltage.

During scanning, the emitted sound wave will propagate through the medium. Each medium resist the passage of sound at different levels, known as the acoustic impedance. When sound encounters a change in acoustic impedance, such as between two different tissue types, in general a small part of the acoustic energy is reflected and a major part of it passes through. What portion of the acoustic intensity is reflected is based on the difference in acoustic impedance: the larger the difference, the larger the acoustic energy that is reflected. At a certain depth, most of the acoustic energy is reflected and/or attenuated and the remaining acoustic energy is too small to generate reflections detectable by the transducer. After emitting sound during the sending phase, the crystal is turned off and the listening phase is started. Reflected sound will deform the crystal, resulting in differences in electrical resistance. Since the speed of sound in biological tissues is around 1540 m/s for most tissues at 37 degrees Celsius, sound that is reflected close to the crystal will return quickly, while reflections from further away have a longer delay. Using the known speed of sound, the measured delay can be converted to a distance. Furthermore, the deformation of the crystal is proportional to the reflection intensity. By placing more crystals in a row, highly focussed beams can be generated and by switching subsequent subsets of these elements multiple parallel lines can be transmitted subsequently. In this way a 2D image can be acquired. The signals are processed and modulated until a real-time interpretable image emerges (see Figure 2).

Spatial resolution is mainly determined by the operation frequency: a lower frequency of the emitted sound penetrates the medium better, but at the cost of spatial resolution. Conversely, a higher frequency hampers penetration, but increases spatial resolution. Medical ultrasound operates typically between 1 and 20 MHz. Temporal resolution is mainly determined by the number of crystals used, as each crystal needs to send and listen independently and consecutively. Typically, transducers are composed of 192 to 256 crystals.

Furthermore, the imaged depth and temporal resolution are inverse related, as sound needs time to traverse the entire scan depth twice per transmitted signal.

One ultrasound beam, however, is never formed by a single crystal in modern ultrasound devices. Adjacent crystals coordinate their sending and listening phases, which can be used to focus the beam at a certain depth, steer the beam or amplify acoustic energy. By using different steering angles and different operating frequencies, image quality is enhanced considerably. Innovation lies in so-called plane wave imaging, where all crystals emit and listen simultaneously, and advanced signal processing techniques are used to reconstruct an image. This can accelerate from typically 30-60 images per second up to 2500 images per second.

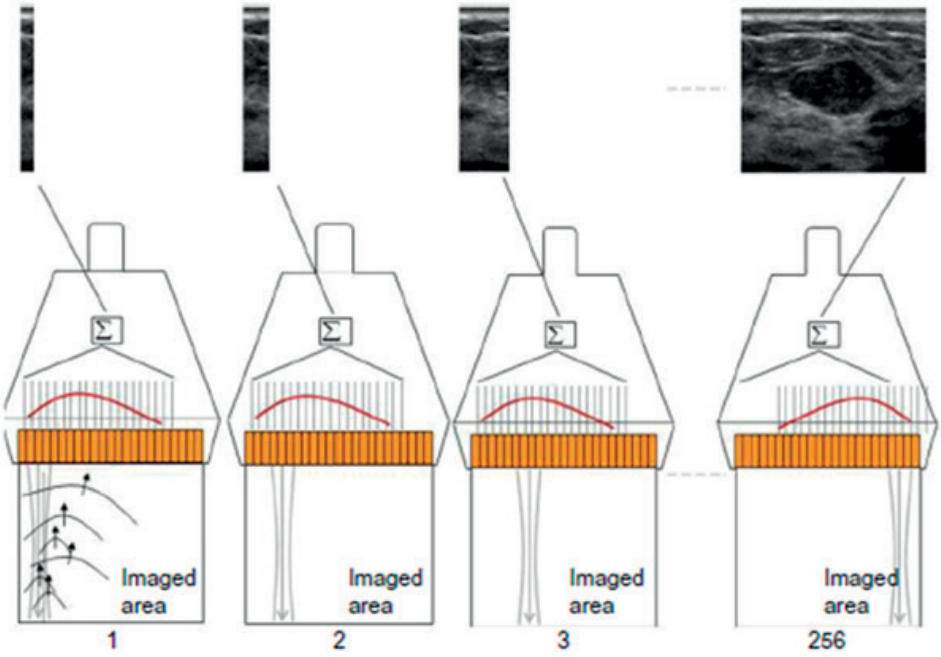


Figure 2: Image formation during conventional ultrasound scanning. The orange piezo-electric crystals consecutively emit high frequency acoustic energy, which is reflected at interfaces between mediums with different acoustic impedances. Image adapted from [14].

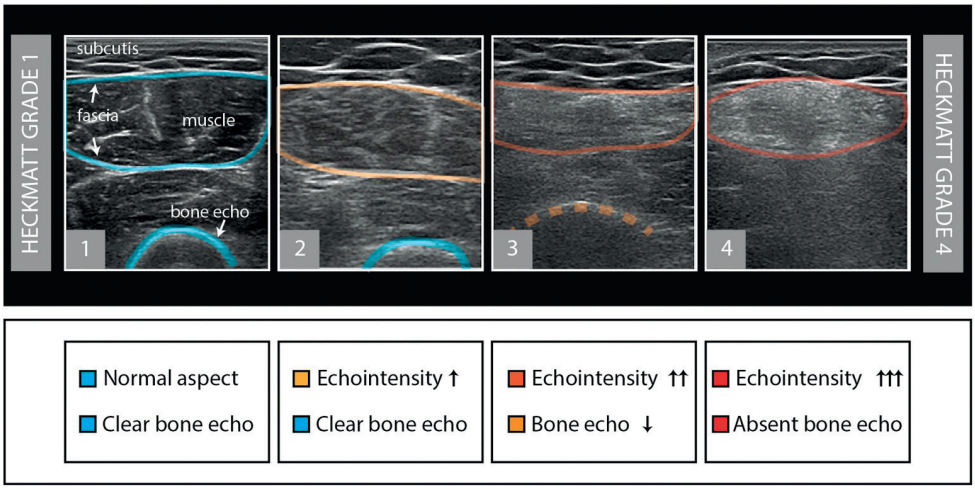


Figure 3: Echogenicity analysis of rectus femoris muscle and vastus intermedius muscle with ultrasound. With a progressive neuromuscular disorder (panel 1 to 4), muscle tissue gets progressively remodelled, which results in an increase in echogenicity within the region of interest. Image adapted from [17].

Advanced ultrasound modalities

Echogenicity is the mean pixel grey value of all pixels in a processed ultrasound image that represent a certain tissue (See Figure 3). An ultrasound image is typically in grey-scale where each pixel has a value between 0 (black) and 255 (white). When rigorously adhering to a pre-defined set of settings, this is a reliable and repeatable tissue characteristic. Echogenicity analysis has been to study the effects of tissue remodelling in neuromuscular disorders [15] or staging of liver steatosis [16]. Reference data obtained with the same device and setting are needed to interpret echogenicity measurements, or a matched control group should be included. These factors impede the widespread use of this technique.

Strain imaging using speckle tracking is an analysis method to track specific kernels of already acquired ultrasound image – speckles – through time (See Figure 4). By selecting kernels that represent specific tissue, a movement profile of that tissue can be acquired. Strain analysis aims to quantify tissue displacement, change in tissue volume – strain and strain rate – in the axial and lateral direction. Speckle tracking is dependent on speckles staying in the imaged plane and has its main application in echocardiography [18].

Shear wave elastography (SWE) is an advanced modality of ultrasound which aims to quantify tissue viscoelasticity (see Figure 5). This consists of two phases: the excitation phase and the tracking phase. During the excitation phase, emitted acoustic energy is amplified and focused in a single point. Tissue at that point will start to resonate with the acoustic energy and generate a so-called shear wave.

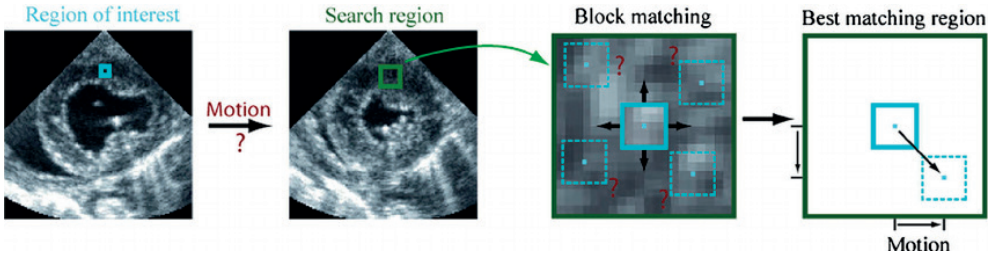


Figure 4: Strain imaging with speckle tracking. A speckle is defined by a small region of interest, which is tracked through subsequent ultrasound frames with a block matching algorithm. Image adapted from [19].

This shear wave propagates at a much lower speed through the tissue than conventional ultrasound waves. To track this wave, using speckle tracking, the tissue surrounding the excitation point is imaged using ultrafast acquisition, which has a framerate 2 orders of magnitude higher than conventional ultrasound. Typically, only a perpendicular line to the imaging direction in the imaging plane is tracked, hence the name shear wave. Shear wave propagation speed is proportional to tissue elasticity: higher propagation speed indicates stiffer tissue, while lower propagation speed indicates softer tissue. Dispersion measures how quickly acoustic energy is absorbed in the tissue when the shear wave is no longer trackable, which is proportional to tissue viscosity. SWE has been used in clinical practice for assessment of liver fibrosis, while making its way to assessment of breast, thyroid, prostate, kidney and lymph node tissue [20]. SWE is dependent on tissue isotropy which makes application in muscle tissue difficult.

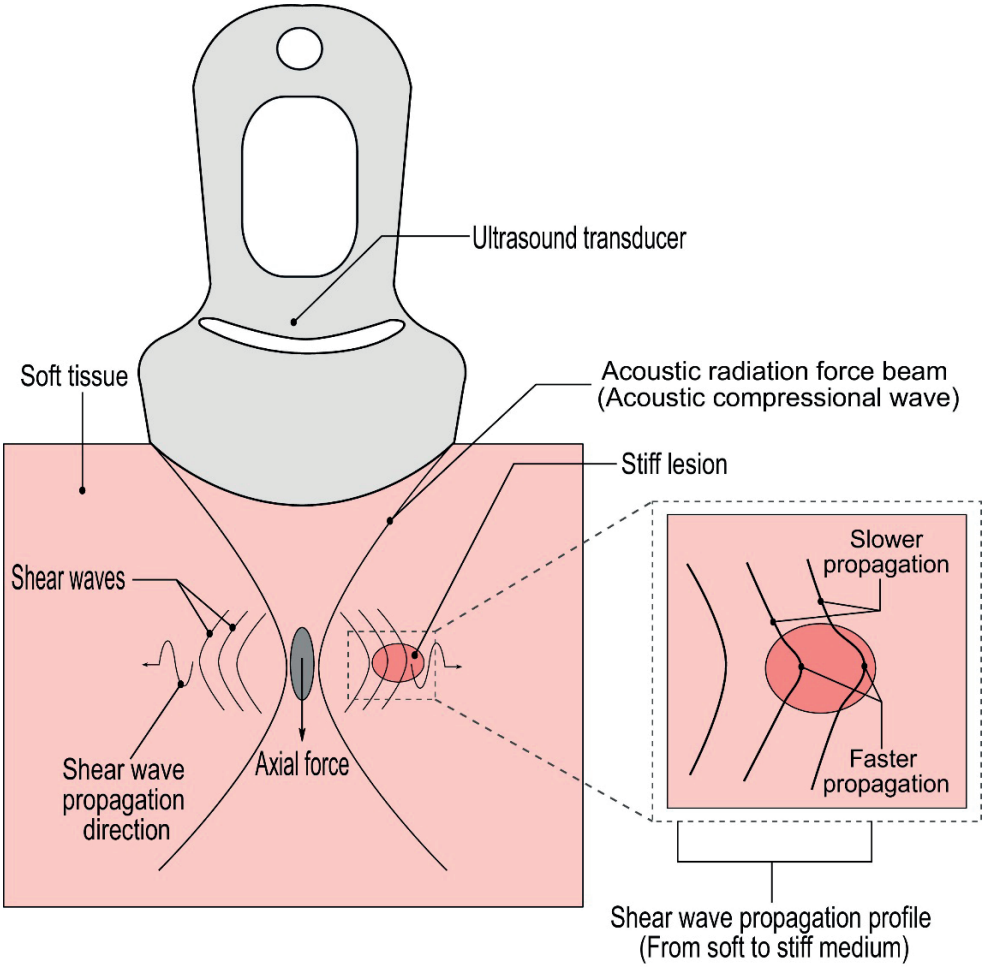


Figure 5: Shear wave elastography. Acoustic energy is focused on a point in tissue, from which a shear wave will originate. This shear wave will propagate through the tissue, displacing the ultrasound speckles that can be tracked with fast acquisition. Image adapted from [21].

Aims and outline of the thesis

Ultrasound is increasingly used to assess respiratory muscle function in neuromuscular disorders, the intensive care unit and pulmonary medicine, both in clinical practice and as outcome measure in research. The first part of this thesis – **Current practice** – aims to provide an overview of the current state of respiratory muscle ultrasound in congenital myopathies and its interpretation. The second part of this thesis – **Critical appraisal** – aims to scrutinize respiratory muscle ultrasound methodology. This thesis thus aims to determine the current status and future perspectives of respiratory muscle ultrasound in clinical practice and research.

Part 1 – Current practice

Chapter 2 is a review of the literature on methodology, technological developments, clinical applications and limitations of ultrasound and magnetic resonance imaging of the respiratory muscles in neuromuscular disorders. **Chapter 3** comprehensively assesses respiratory muscle function in 42 patients with nemaline myopathy. Besides common clinical methods, thickness, thickening, and echogenicity of the diaphragm and intercostal muscles are assessed. These are non-volitional methods which give additional insight in respiratory muscle functioning compared to volitional testing. These tests are also included in the longitudinal study of **Chapter 4** with 26 patients with *LAMA2* related muscular dystrophy and 11 patients with *SELENON (SEPN1)* related congenital myopathy to characterize respiratory involvement and its change over time.

Part 2 – Critical appraisal

Diaphragm ultrasound is used in many centres worldwide as a clinical or research tool. Although standardized protocols exist to aim for uniformity, different normative values are not uniform. **Chapter 5** is a cross-sectional study with 83 healthy participants to determine normative values of diaphragm echogenicity, thickness, and thickening in our centre. **Chapter 6** contains two experiments with 21 healthy participants and with 21 patients with a congenital myopathy. Diaphragm thickening is assessed during unloaded and loaded concentric contractions, and isometric contractions, to determine the physiological value of diaphragm thickening as measured with ultrasound. There has been considerable debate on which physiological parameters are reflected by diaphragm ultrasound, and this chapter aims to establish a shift in its interpretation. In **Chapter 7**, shear wave elastography (SWE) is performed on all respiratory muscles in 21 healthy participants and 21 patients with a congenital myopathy during quiet breathing, deep breathing, and isometric contractions. This is repeated after two weeks and by a different observer. SWE is proposed as alternative to diaphragm thickening for measuring diaphragm contractility, and this chapter investigates its validity and reliability.

Box 1: excitation-contraction coupling and congenital myopathies

Individual muscle fibres are elongated, multinucleated cells packed with myofibrils, which consist of repeating units called sarcomeres (figure B1-1). The sarcomere is the fundamental structural and functional unit of muscle, consisting of thin filaments which are mainly composed of actin, and thick filaments which are mainly composed of myosin. The thin filaments are connected to a central skeleton called the Z-disc, where the thick filaments are interwoven and connected to the Z-disc through the elastic filaments, titin. Surrounding each myofibril is the sarcoplasmatic reticulum, serving as reservoirs for intracellular calcium. At regular intervals, the sarcoplasmatic reticulum forms enlarged regions, terminal cisternae, adjacent to transverse (T-) tubules. T-tubules are invaginations of the muscle fibre membranes (sarcolemma) that penetrate the fibre (Figure B1-2).

An alpha-motor neuron axon carries an action potential when a contraction is initiated. That action potential is transmitted through the neuromuscular junction to the fibre membrane and into the T-tubules. The action potential triggers voltage-gated channel proteins at the interface between the T-tubule and the terminal cisternae to release calcium into the cytosol. An increase in intracellular calcium will initiate binding of thick filaments to thin filaments, generating force. If the produced force is larger than the external load, the filaments slide against each other, opening up more binding sites and therefore, producing more force. This results in a shortening and thickening of the muscle. This process, from signal transduction through the T-tubule to the filaments sliding is called the excitation-contraction coupling.

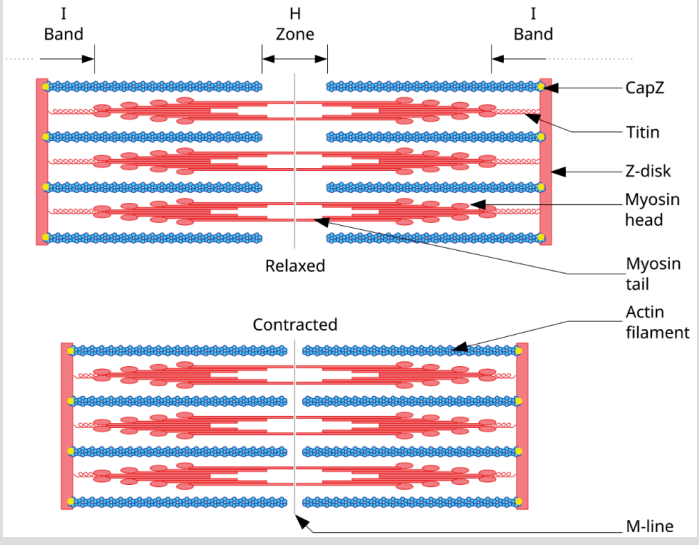


Figure B1-1: A sarcomere in relaxed and contracted state. Image adapted from [22].

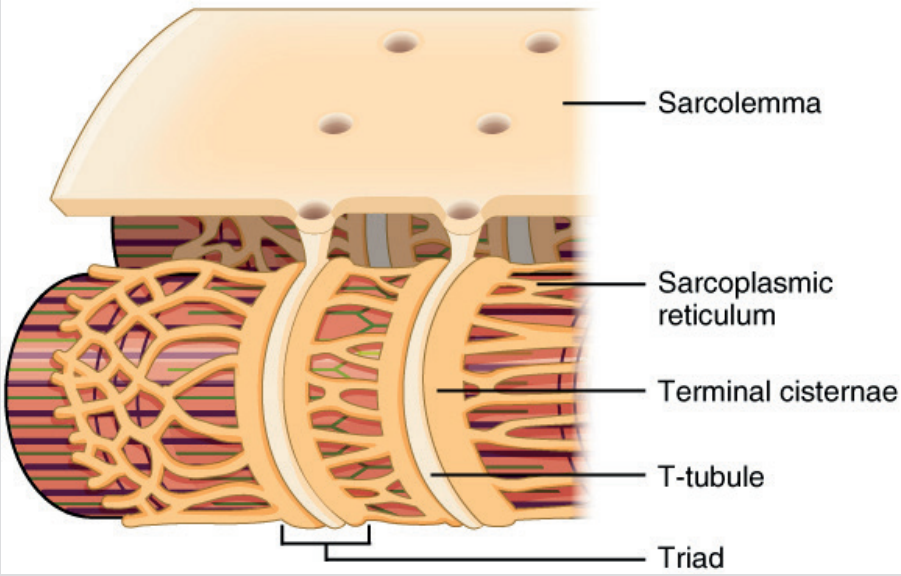


Figure B1-2: Schematic overview of and individual muscle fibre with the sarcoplasmatic reticulum, terminal cisternae and T-tubules coming from the sarcolemma. Image adapted from [23].

At the cellular level, congenital myopathies arise from defects in excitation–contraction coupling [24]. Congenital myopathies are different from muscular dystrophies by which proteins are affected: in muscular dystrophies, proteins that are associated with fibre structure and extracellular matrix are affected. Besides genetic classification based on affected proteins, congenital myopathies are classified based on histopathological features upon muscle biopsy. Histopathological and genetic classification do not match: one variant gene can present as multiple histopathological features in different patients, or change between histopathological features during the lifespan of an individual patient. A new classification system was proposed by a recent consensus meeting that includes inheritance pattern, variant gene and main histopathological findings for each patient [5].

Box 2: trial readiness

Only one in ten candidate drugs that start clinical trials reach market approval. From a financial perspective, developing drugs carries an enormous risk which is covered by increasing costs of market approved drugs, leading to unsustainable financing of healthcare. From a patient perspective, participation in a clinical trial may be harmful and presents significant burden on time investment and psychological wellbeing. It is therefore of interest to increase efficiency of clinical trials, and reduce the number of trials and participants needed in each trial.

Trial efficiency can be increased through trial readiness, which encompasses all efforts to increase validity of a clinical trial. This can be achieved by, among others, a strong knowledge of natural history of a patient population to inform clinical trial duration and sample size, extensive patient registries to quickly identify patients that fall in the intended therapeutic window, and meaningful and validated outcome measures. Together, these factors increase the likelihood of drawing the correct conclusion on the effectiveness of a candidate drug, while simultaneously minimizing the number of clinical trials and patient burden.

Several candidate drugs for specific congenital myopathies are currently being tested in the preclinical phase, while a few have proceeded to clinical testing already. The majority of these clinical trials failed to reach market approval. One of the factors that lead to failure is the lack of sufficient trial readiness. Several efforts are being pursued by the Radboudumc Centre of Expertise for Neuromuscular Disorders to increase trial readiness for congenital myopathies by setting up registries of Dutch congenital myopathy patients, performing an extensive natural history study and investigate meaningful and valid outcome measures. This thesis adds to that by investigating one of those outcome measures, respiratory muscle ultrasound.

Box 3: physiology of breathing

The primary aim of breathing is to exchange oxygen and carbon dioxide between air and blood. Breathing is enabled by the respiratory system, which consists of four distinct components that nonetheless interact very strongly: the lungs, the thoracic wall, the central and peripheral nervous system, and the respiratory muscles.

Exchange of oxygen and carbon dioxide takes place in the lungs, which increases in volume when they are stretched, and deflate due to their elastic recoil. The lungs are not physically attached to the thoracic wall but interacts through the pleura, which are membranes on the lungs and on the thoracic wall, with fluid in between. As long as the pleural space is sealed airtight, the lungs stick to the thoracic wall, but are able to slide against each other during breathing with minimal friction. The chest wall is formed by the rib cage and the intercostal muscles, providing the stability needed.

Breathing is controlled by the respiratory centres in the brainstem, specifically the medulla and pons. Physiological ventilatory demand is controlled by arterial chemoreceptors that sense partial pressure of oxygen and the dissolved product of carbon dioxide, H^+. Furthermore, central chemoreceptors close to the respiratory centres sense partial pressure of H^+ only. When H^+ levels are too high or oxygen levels are too low, breathing is increased in intensity and vice versa. Furthermore, muscle and lung stretch reflexes modulate breathing intensity to overcome resistance in the respiratory system, and prevent overstretching. Breathing is an autonomous process, but is unique in its ability to be influenced by higher cortical regions to become volitional. Cognitive responses such as stress, fear or emotion also influence breathing.

References

1. van Esch, C., et al., *What is on the agenda? About the importance of a collaborative research agenda set by Dutch neuromuscular patients, their families and the neuromuscular field.* Neuromuscular Disorders, 2026. 62.
2. Mead, J. and S.H. Loring, *Analysis of volume displacement and length changes of the diaphragm during breathing.* J Appl Physiol Respir Environ Exerc Physiol, 1982. 53(3): p. 750-5.
3. De Troyer, A., P.A. Kirkwood, and T.A. Wilson, *Respiratory action of the intercostal muscles.* Physiol Rev, 2005. 85(2): p. 717-56.
4. Tagliabue, G., et al., *Parasternal intercostal, costal, and crural diaphragm neural activation during hypercapnia.* J Appl Physiol (1985), 2021. 131(2): p. 672-680.
5. Villar-Quiles, R.N., et al., *277th ENMC international workshop: Congenital myopathies: revising and revisiting nomenclature and diagnostic guidelines, 21-23 June 2024, Hoofddorp, The Netherlands.* Neuromuscul Disord, 2026. 60: p. 106328.
6. Laghi, F. and M.J. Tobin, *Disorders of the respiratory muscles.* Am J Respir Crit Care Med, 2003. 168(1): p. 10-48.
7. Smith, B.K., M. Goddard, and M.K. Childers, *Respiratory assessment in centronuclear myopathies.* Muscle Nerve, 2014. 50(3): p. 315-26.
8. van Kleef, E.S.B., et al., *Future Directions for Respiratory Muscle Training in Neuromuscular Disorders: A Scoping Review.* Respiration, 2024. 103(10): p. 601-621.
9. Gauld, L.M., et al., *Spirometry is affected by intelligence and behavior in Duchenne muscular dystrophy.* Pediatr Pulmonol, 2005. 40(5): p. 408-13.
10. Doorduin, J., et al., *Monitoring of the respiratory muscles in the critically ill.* Am J Respir Crit Care Med, 2013. 187(1): p. 20-7.
11. Jackson, C.E., et al., *A preliminary evaluation of a prospective study of pulmonary function studies and symptoms of hypoventilation in ALS/MND patients.* J Neurol Sci, 2001. 191(1-2): p. 75-8.
12. Gayraud, J., et al., *Ventilatory parameters and maximal respiratory pressure changes with age in Duchenne muscular dystrophy patients.* Pediatr Pulmonol, 2010. 45(6): p. 552-9.
13. Guimarães-Costa, R., et al., *Human diaphragm atrophy in amyotrophic lateral sclerosis is not predicted by routine respiratory measures.* Eur Respir J, 2019. 53(2).
14. Couade, M., *The advent of ultrafast ultrasound in vascular imaging: a review.* Journal of Vascular Diagnostics and Interventions, 2016: p. 9.
15. Wijntjes, J. and N. van Alfen, *Muscle ultrasound: Present state and future opportunities.* Muscle Nerve, 2021. 63(4): p. 455-466.
16. Weijers, G., et al., *Noninvasive Staging of Hepatic Steatosis Using Calibrated 2D US with Liver Biopsy as the Reference Standard.* Radiology, 2023. 306(3): p. e220104.
17. Wijntjes, J., et al., *Improving Heckmatt muscle ultrasound grading scale through Rasch analysis.* Neuromuscul Disord, 2024. 42: p. 14-21.
18. Kersten, J., et al., *Applications of Speckle Tracking Echocardiography in Stress Echocardiography: A Systematic Review on Feasibility, Diagnostic, and Clinical Utility.* Echocardiography, 2025. 42(8): p. e70251.

19. Opdahl, A., et al., *Strain, Strain Rate, Torsion, and Twist: Echocardiographic Evaluation.* Current cardiology reports, 2015. 17: p. 568.
20. Sigrist, R.M.S., et al., *Ultrasound Elastography: Review of Techniques and Clinical Applications.* Theranostics, 2017. 7(5): p. 1303-1329.
21. Lim, W.T.H., et al., *Shear Wave Elastography: A Review on the Confounding Factors and Their Potential Mitigation in Detecting Chronic Kidney Disease.* Ultrasound in Medicine and Biology, 2021. 47(8): p. 2033-2047.
22. Richfield, D., *Sarcomere*. 2014, WikiJournal of Medicine.
23. J. Gordon Betts, K.A.Y., James A. Wise, Eddie Johnson, Brandon Poe, Dean H. Kruse, Oksana Korol, Jody E. Johnson, Mark Womble, Peter DeSaix, *Anatomy and Physiology*. 2013, Houston, Texas: OpenStax.
24. Jungbluth, H., et al., *Congenital myopathies: disorders of excitation-contraction coupling and muscle contraction.* Nat Rev Neurol, 2018. 14(3): p. 151-167.

Part I

Current practice



Chapter 2

Respiratory muscle imaging by ultrasound and MRI in neuromuscular disorders

Jeroen LM van Doorn
Francesca Pennati
Hendrik HG Hansen
Baziel GM van Engelen
Andrea Aliverti
Jonne Doorduin

Published in:
European Respiratory Journal, 2021

Abstract

Respiratory muscle weakness is common in neuromuscular disorders and leads to significant respiratory difficulties. Therefore, reliable and easy assessment of respiratory muscle structure and function in neuromuscular disorders is crucial. In the last decade, ultrasound and MRI emerged as promising imaging techniques to assess respiratory muscle structure and function. Respiratory muscle imaging directly measures the respiratory muscles and, in contrast to pulmonary function testing, is independent of patient effort. This makes respiratory muscle imaging suitable to use as tool in clinical respiratory management and as outcome parameter in upcoming drug trials for neuromuscular disorders, particularly in children. In this narrative review, we discuss the latest studies and technological developments in imaging of the respiratory muscles by US and MR, and its clinical application and limitations. We aim to increase understanding of respiratory muscle imaging and facilitate its use as outcome measure in daily practice and clinical trials.

Introduction

Respiratory muscle dysfunction is a common feature in many neuromuscular disorders (NMDs) that leads to significant respiratory difficulties, such as dyspnoea, sleep disturbances, lung infections and is often the primary cause of death [1]. Therefore, reliable assessment of respiratory muscle function in NMDs is crucial. For patients it is of vital importance to identify early signs of respiratory insufficiency, to monitor disease progression, and to guide individual respiratory management. From a scientific perspective, exciting new gene-modifying and drug therapies are currently being developed for specific NMDs that hold promise for effective treatment [2]. To evaluate these therapies, clinical trials are in urgent need of relevant and reliable respiratory outcome measures instead of motor outcome measures, such as the Six Minute Walking Test or Motor Function Measure.

Currently, pulmonary function testing is recommended to assess respiratory muscle function. However, it has several limitations [3]. First, it provides merely a global evaluation of pulmonary function. Performance on pulmonary function testing results from the interaction between respiratory muscles, chest wall and lungs. Hence, it does not provide specific information on respiratory muscle structure and function, such as the diaphragm, abdominal muscles or intercostal muscles [4]. Second, considerable respiratory muscle weakness may occur before it is reflected in pulmonary function tests [5-7]. Third, pulmonary function testing is effort-dependent, affected by active participation and cognitive function, and moreover cannot be performed in early-childhood [8]. The latter is of utter importance because the decline in respiratory muscle function already starts at early-childhood in many NMDs such as Duchenne muscular dystrophy (DMD) or Pompe disease.

In the last decade, ultrasound (US) imaging and magnetic resonance (MR) imaging emerged as techniques to evaluate the respiratory muscles. These imaging techniques can be used to examine structural and functional characteristics of the respiratory muscles. In this review, we discuss the latest studies and developments in imaging of the respiratory muscles by US and MR, and its clinical application and limitations. The pathophysiology of respiratory failure in NMDs will be described briefly. Our goal is to increase understanding of respiratory muscle imaging and facilitate its use as outcome measure in daily practice and clinical trials.

Methods

A systematic literature search was carried out in the Medline, Embase and Cochrane databases to find relevant studies on the 24th of September, 2020. Search terms included MeSH terms or Emtree terms, synonyms and specifications of NMDs, respiratory muscles and ultrasound or MRI. The identified studies are discussed narratively in this review.

Respiratory failure in neuromuscular disorders

NMDs are a heterogeneous group of disorders that are inherited or acquired, resulting from an impairment in the anterior horn motor cells, peripheral nerves, neuromuscular junctions, or muscles. In parallel with their respective aetiology, respiratory muscles are progressively affected by NMDs. In Figure 1 we present an overview of well-known NMDs according to their level of impairment. For a detailed description of respiratory muscle dysfunction in NMDs, we refer to excellent reviews on this topic [9, 10].

In most NMDs both inspiratory and expiratory muscles are affected and subsequently put patients at risk for respiratory failure. Diaphragm and accessory inspiratory muscle weakness leads to hypoventilation, rapid shallow breathing, and sleep-disordered breathing [11-13]. Whereas, weakness of the expiratory muscles leads to ineffective cough and therefore mucus stasis, which in turn increases the risk for pneumonia [11, 14]. In addition to the respiratory muscles, weakness of the trunk muscles (leading to chest wall deformities and scoliosis) and bulbar muscles (leading to swallowing impairment) may contribute to respiratory failure in NMDs.

Depending on the specific aetiology, respiratory muscles of patients with NMDs are characterized by muscle atrophy, replacement of muscle tissue by fat or fibrosis, or contractile dysfunction. Respiratory muscle imaging aims to evaluate these structural and functional changes.

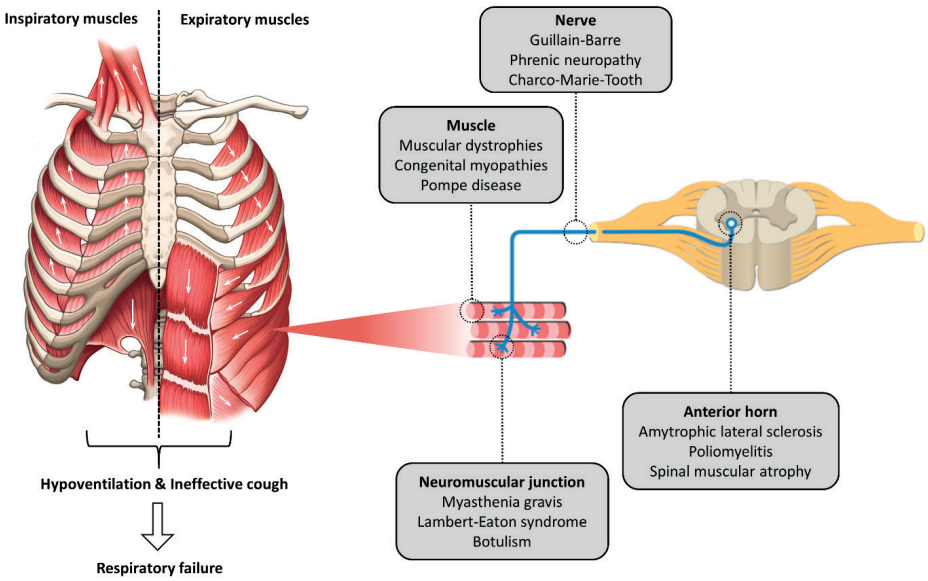


Figure 1: Overview of well-known NMDs that affect respiratory muscle function according to their level of impairment.

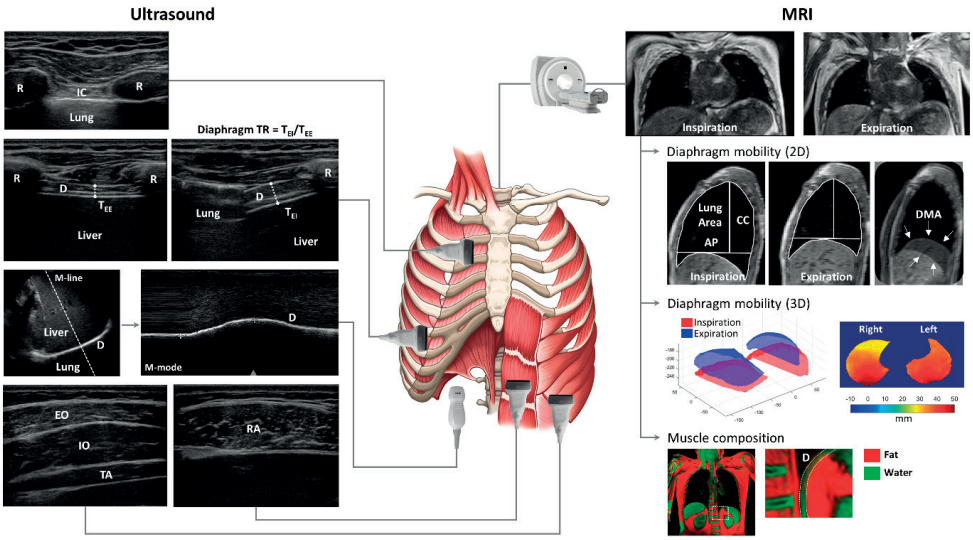


Figure 2: Overview of currently used respiratory muscle imaging techniques. Abbreviations: AP, antero-posterior; CC, cranio-caudal; D, diaphragm; DMA, diaphragmatic movement area; EO, external oblique muscle; IO, internal oblique muscle; IC, intercostal muscles; R, rib; TA, transverse abdominal muscle; T_{EE}, thickness end-expiratory; T_{EI}, thickness end-inspiratory; TR, thickening ratio; RA, rectus abdominis muscle. Original MRI data are from [52], acquired at Scientific Institute, IRCCS E. Medea, Bosisio Parini, Italy.

Current ultrasound and MRI techniques

An overview of currently available respiratory muscle imaging techniques is shown in Figure 2 and will be discussed in detail in this section.

US imaging

Currently, two approaches to US imaging of the diaphragm are most practised in NMDs. An intercostal approach to measure thickness and thickening of the diaphragm, and a subcostal approach to measure diaphragm excursion. Surprisingly, the extra-diaphragmatic respiratory muscles have not yet been studied in NMDs using US. However, considering the important role of these muscles in NMDs, we will describe the approaches that have been used in other settings to visualize the parasternal intercostal muscles and abdominal wall muscles.

Intercostal approach: diaphragm thickness and thickening

Using the intercostal approach, a linear array transducer (10-15 MHz) is positioned perpendicular to the skin in the zone of apposition of the diaphragm. Using this approach, the diaphragm can be identified as three hyperechoic (white) bands with two hypoechoic (black) bands in-between. The most superficial hyperechoic band is caused by reflections at the interface between the pleural layer and the diaphragm, the middle band by reflections at the tendinous structure inside the diaphragm and the deepest band by reflections at the interface between the diaphragm

and the peritoneal layer. The two hypoechoic bands in-between represent the muscular parts of the diaphragm. Please note that the middle hyperechoic band is not always visible, or may be interrupted throughout the entire diaphragm image. Variations in transducer placement, subject positions and thickness measurement exist between studies.

In medio-lateral direction, different transducer placements between the midclavicular line and the posterior axillary line have been reported [15-33]. Most often the transducer is placed in the anterior-axillary or mid-axillary line. In cranio-caudal direction the transducer placement varies in studies between the 7th and 10th intercostal space [15, 19, 20, 24-26, 30-33] or described as the intercostal level where the diaphragm is best imaged [16-18, 21-23, 27-29].

Different subject positions have been reported during diaphragm US examination. Most studies report that subjects are in the supine position [15-18, 21, 24, 25, 27, 28, 30-34], while others report that subjects are sitting [19, 22-24, 29, 35] or in semi-recumbent position [26]. Importantly, subject position has a considerable effect on lung function [36]. From our experience, examination in supine position is not always feasible in patients with orthopnoea due to diaphragm paralysis or severe weakness.

An important aspect in calculation of diaphragm thickness is placement of the callipers. Most practiced is to place the callipers at the inner borders of the pleural and peritoneal lines [17, 23, 30-33]. However, some studies report to place callipers in the middle of the hyperechoic pleural and peritoneal line [20-22] or at the inside of the pleural line and the outside of the peritoneal line [15]. Furthermore, the majority of studies calculate diaphragm thickness on one location in the image, repeat the measurement at least three times and average thickness [15, 16, 20, 22-24, 26, 29-33, 35]. However, some studies report to use only a single image, but perform thickness calculation on three locations, and average these [17, 21].

Table 1

	n (m/f)	Age (years)	Thickness end-expiration (mm)		Thickness end-inspiration (mm)		Thickening ratio		Excursion tidal breathing (cm)		Excursion deep breathing (cm)	
			right	left	right	left	right	left	right	left	right	left
Boussuges et al., 2009 [39]	210 (150/60)	50 ± 14							1.8 ± 0.3	1.8 ± 0.4	6.6 ± 1.3	7.3 ± 1.0
Hiwatani et al., 2013 [21]	19 (12/7)	63 ± 11	1.9 ± 0.7		3.9 ± 1.1		2.2 ± 0.8					
Boon et al., 2013 [38]	150	51 ± 18	3.3 ± 0.1	3.4 ± 0.2			1.8 ± 0.5	1.9 ± 0.6				
Fantini et al., 2016 [29]	30 (20/10)	57 [46–72]			5.3* [0.46–0.61]		3.1#* [2.8–3.5]					
Carrillo-Esper et al., 2016 [97]	109 (55/54)	26 ± 7	1.6 ± 0.04									
Fayssoil, Chaffaut et al., 2019 [27]	17 (17/0)	33 [27–46]	1.8 [1.5–2.3]	1.5 [1.2–2.1]			1.7# [1.5–1.8]	1.7# [1.6–2.1]	1.6 [1.4–2.0]	1.2 [1.0–1.5]	8.4 [7.3–9.1]	7.5 [7.0–8.3]
Fayssoil, Nguyen et al., 2019 [28]	27 (14/14)	31 [26–39]	1.5 [1.3–1.9]	1.5 [1.1–1.9]							7.2 [6.2–8.8]	6.2 [6.1-9.7]
Sartucci et al., 2019 [24]	30 (15/15)	63 ± 10	2.0 ± 0.4		4.5 ± 0.4							
Spiesshoefer et al., 2019 [31]	19 (5/14)	47 ± 11	2.1 [1.5–2.2]		4.4 [3.8–6.5]		2.5 [2.1–3.1]		1.6 ± 0.6		7.8 ± 2.0	
Henke et al., 2020 [33]	21 (11/10)	42 ± 13	2.0 ± 0.6		5.5 ± 20.		2.7 ± 0.6		1.5 ± 0.5		7.8 ± 2.0	
Ruggeri et al., 2020 [26]	17 (8/9)	47 ± 15	2.0 ± 0.2		5.4 ± 0.6		2.8# ± 1.5				7.8 ± 0.4	

Normal values of diaphragm ultrasound parameters. Values are reported as mean ± standard deviation or median [interquartile range]. Only studies with more than 15 healthy subjects are reported. Abbreviations: f, female; m, male; n, number of subjects. * Highest value from bilateral measurement. # Reported thickening fraction (TF) was converted to thickening ratio (TR): TR = (TF / 100) + 1.

During inspiration the diaphragm thickens as a result of muscle contraction. The thickening fraction (TF) of the diaphragm can be calculated as the difference between end-expiratory thickness and end-inspiratory thickness divided by end-expiratory thickness. Alternatively, thickening ratio (TR) is calculated as end-inspiratory thickness divided by end-expiratory thickness. End-inspiratory thickness can be calculated at different lung volumes. Most studies measure end-inspiratory thickness during tidal breathing or a manoeuvre to total lung capacity (TLC) [16, 18, 20, 21, 24-33, 35]. The lung volume at which end-inspiratory thickness is measured greatly affects diaphragm thickening fraction [37].

The differences in measurement technique cause variability in reported diaphragm thickness. This variability is shown in Table 1, where we summarize normal values for diaphragm ultrasound from different studies. Furthermore, differences in sex have been reported [38, 39]. If repeat measurements are performed on the exact same anatomical position the reliability of diaphragm ultrasound is high: intra-class correlation coefficients of intra-rater operability of 0.89-0.96 [19, 38] and inter-observer operability of 0.74-0.99 have been reported [19, 21, 38].

Subcostal approach: diaphragm excursion

Diaphragm excursion is measured with low-frequency phased-array or curved-array transducers (1.5-5 MHz) using a subcostal approach. With this anterior subcostal view, the diaphragm is imaged with the liver or spleen as acoustic window. The diaphragm is identified as a broad hyperechoic band covering the liver or spleen. An M-line is manually selected perpendicular to the diaphragmatic dome. Diaphragm excursion can be measured in M-mode during tidal breathing, deep inhalation or sniff manoeuvres. Probe placement [25-28, 30-34, 40] in medio-lateral direction is between the mid-clavicular and anterior axillary line [26-28, 30-34, 40]. Evaluation of left diaphragm excursion can be more challenging than the right side, due to the small acoustic window of the spleen. While most subjects are in supine position during excursion measurements [25, 27, 28, 30-33], some measure in semi-recumbent position [26, 34, 40].

Parasternal intercostal muscles

Typically, a 10-15 MHz linear array transducer is used, positioned at the level of the second intercostal space in a cranio-caudal orientation, 3-8 cm lateral to the sternum [41-44]. The parasternal intercostal muscles are visible as two hyperechoic bands running from the anterior and posterior aspects of the ribs with a more hypoechoic muscular portion in between. Similar to diaphragm US imaging, thickness of the parasternal intercostal muscles can be determined at expiration and inspiration, and thickening ratio can be derived.

Abdominal wall muscles

The rectus abdominus muscle is typically imaged using a 10-15 MHz linear array transducer in a transverse orientation, placed 2 cm above the umbilicus and 2 cm lateral to the midline [45, 46]. The transducer is then moved laterally, to the anterior axillary line. The external oblique,

internal oblique and transverse abdominis muscles can be identified here as three muscles separated by hyperechoic bands (fasciae) [45, 46]. Thickness at FRC and during forced expiratory manoeuvres to residual volume or with open glottis against a closed airway can be measured for each muscle, or compounded, to assess expiratory muscle function [47].

MR imaging

Current approaches to image respiratory muscles in NMDs using MR include both imaging of muscle structure and function.

Respiratory muscle structure: qualitative approach and quantitative approach

To estimate the extent of respiratory muscle involvement, both qualitative and quantitative approaches to MRI have been used.

T1-weighted images can be used to visualize intramuscular fat, which appears hyperintense compared to healthy muscle tissue and water. T2-weighted images can be used to visualize both fat and water increase within muscle, due to fat infiltration, oedema and inflammation. Using multi-sequence imaging protocols, including T1-weighted and T2-weighted spin echo sequences, as well as fat-suppressed T2-weighted sequences (T2WFS), respiratory muscles degeneration can be scored according to established rating scales. Fatty infiltration is scored from normal appearance to complete fatty degeneration [48, 49]. Adaptation of this scale has been proposed for rating the diaphragm, due to its thin muscle size [50]. Semi-quantitative scoring scales allow a fast and reproducible assessment of the degree of each muscle involvement but is not sensitive to subtle changes over time. As quantitative and objective methods to measure respiratory muscles damage, T2 mapping and 3-point Dixon technique have been investigated.

T2 relaxation time mapping (T2 mapping) measures the distribution of the T2 relaxation time throughout the tissue of interest, which is increased by both inflammation, oedema and fatty infiltration. To date T2 mapping has only been investigated in the sternocleidomastoid muscle [51, 52]. A coronal plane where both sternocleidomastoid muscles were adequately imaged was acquired and T2 relaxation time measurements were obtained in three regions of interest selected in the centre of the muscle [51]. Dixon MRI techniques [53] quantify the individual contributions of fat and water in each voxel of tissue to calculate the muscle's fat fraction. Dixon MRI has been recently applied to quantify fatty replacement of the accessory respiratory muscles and of the diaphragm [54, 55]. Intercostal muscles were quantified on coronal images of the chest, bisecting the rib cage at its widest point, whereas the rectus abdominis, the external and the internal obliques were evaluated on an axial image acquired at the level of the umbilicus [55]. The diaphragm was evaluated on volumetric acquisitions in the coronal plane, on 3D regions of interest over the costal and the crural parts of the diaphragm [54].

Diaphragm function: static and dynamic approach

The cranio-caudal, antero-posterior and left-right length changes of the lungs between inspiration and expiration have been investigated as a hallmark of respiratory muscle function.

Using static MRI, 2D or 3D breath-hold images are acquired at TLC and FRC, while subjects are holding breath [54, 56, 57]. Breath-holding times range from 0.6 s for 2D image acquisition, to 10-12 s for 3D image acquisition, with total scan time varying from 2 min to 15-20 min [54, 56, 57], respectively. After manual or automatic lung segmentation, lung area using 2D or volume using 3D, maximum lung diameters in cranio-caudal (CC) and in antero-posterior (AP) directions are measured both at maximal inspiration and expiration, and their changes are calculated [56, 57]. Other proposed measures include diaphragmatic movement area (DMA) and chest wall movement area (CWMA), defined respectively as the area bordered by diaphragm edges after subtracting the expiratory from the inspiratory scan and the area calculated subtracting DMA from inspiration [56]. To correct for inter-subject anatomical variations, each length at inspiration is divided by the length at expiration [56, 57]. A 3D map of apico-caudal diaphragm excursion has also been proposed to investigate regional diaphragm motion [54]. Diaphragm surfaces are reconstructed as the bottom surfaces of the segmented left and right lungs, both in expiration and inspiration and aligned via a nonrigid iterative closest point algorithm [58].

Using dynamic MRI, respiratory muscle function can be monitored over multiple breathing cycles, during free- and deep- breathing conditions, by acquiring multiple images at different time points both in 2D (in the sagittal, coronal and axial plane) and in 3D. Measures derived from dynamic imaging include lung area (using 2D) or volume (using 3D), lung length in AP, CC and left-right directions and diaphragm length using 2D or diaphragm surface area using 3D [55, 59-62]. All measures are computed in every frame of each cine MRI dataset, to extract the temporally varying profiles of each measure. Maximal inspiration and maximal expiration are identified as the frames with the maximum and minimum lung area, respectively. DMA and CWMA are calculated on the superimposed frames of the maximal inspiration and expiration from each breathing cycle. In 3D, additional measures are derived, including the volume displaced by the diaphragmatic and the costal surface, to determine the independent contribution of the diaphragm and thoracic muscles, and the orientation of the right diaphragm dome, as a measure of diaphragm shape [62].

Clinical studies and applications

US and MR imaging have been used to characterize respiratory muscle function in several NMDs. Below, we will summarize the findings from these studies. Figure 3 illustrates an example of different degrees of diaphragm dysfunction that can be seen in NMDs.

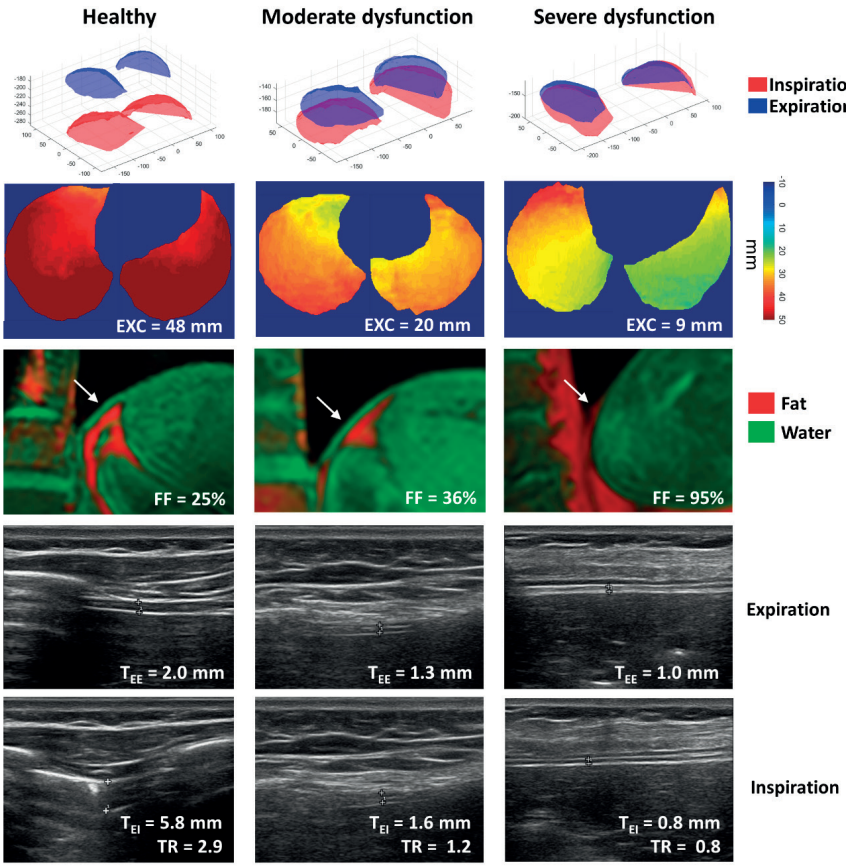


Figure 3: Results of ultrasound and MR imaging measurements in neuromuscular disorder patients with different degrees of diaphragm dysfunction. Note, images are not from the same patients. Abbreviations: T_{EE}, thickness end-expiratory; T_{EI}, thickness end-inspiratory; TR, thickening ratio; EXC = median excursion from full-expiration to full-inspiration; FF = fat fraction. Original MRI data are from [52], acquired at Scientific Institute, IRCCS E. Medea, Bosisio Parini, Italy.

Motor neuron diseases

In ALS, diaphragm thickness at FRC [17, 21, 29] and TLC [21] and thickening ratio [21, 29] are decreased compared to age-matched healthy controls. In ALS patients with a predicted vital capacity below 80%, diaphragm thickening ratio was found to be 1.6 [21]. Whereas patients above this threshold have a thickening ratio of 2.1, which is comparable to the 2.2 observed in healthy controls [21]. No differences in diaphragm thickness at FRC and TLC were found between patients with bulbar-onset ALS and spinal-onset ALS [22]. Furthermore, no changes in diaphragm thickness were found after a follow-up period of four months [23]. In spinal muscular atrophy (SMA), no structural or functional differences of the diaphragm could be found with ultrasound between SMA subtype 1 and other NMD, including SMA subtype 2 and 3 [25, 63].

Muscular dystrophies

In patients with myotonic dystrophy, diaphragm thickness at FRC and TLC, thickening ratio and excursion amplitude at TLC were decreased compared to healthy controls [33]. In facioscapulohumeral dystrophy, diaphragm thickness at TLC, thickening ratio and diaphragm excursion amplitude at TLC were decreased [30]. In both studies thickening ratio was 2.0, while healthy controls showed thickening ratios of 2.7 and 2.9, respectively [30, 33].

In DMD patients under the age of fourteen diaphragm thickness at FRC is increased compared to healthy controls, while thickness at TLC and thickening ratio were reduced [15, 20]. This increase can be explained as pseudohypertrophy by fat infiltration. This changes in older boys with DMD, thickness at FRC and TLC, and thickening ratio are all decreased [15]. Excursion amplitude during quiet breathing and sniff manoeuvres are reduced, as well as excursion velocity during sniff manoeuvres [28]. Diaphragm fat fraction obtained with MRI reaches 50% at around 17 years old [54], with a slower increase compared to paraspinal muscles [54], quadriceps, hamstrings and adductors [64], which reaches 50% fat fraction before 15 years old. Functionally, diaphragm fat fraction is reflected by lower excursion of the diaphragm, with early signs of weakness visible in DMD patients younger than 15 years old when regional excursion is investigated [54, 60]. Both diaphragm fat fraction and excursion are strongly related to spirometry and age [54, 60]. Expiratory muscles show elevated fat fraction, with the internal oblique muscle showing the earliest signs of involvement, reaching 50% fat fraction around 13 years old, whereas the rectus abdominis muscle was the least affected [55]. The sternocleidomastoid muscle shows on T2 maps decreased times in DMD patients compared to controls over 12 years old and decreasing times with age, but no correlation with FVC [51].

Pompe disease

In late-onset Pompe disease (LOPD), diaphragm thickness at FRC and TLC, and thickening ratio were decreased [26, 32]. Furthermore, excursion velocity during a sniff manoeuvre was decreased, as well as excursion amplitude at TLC. Thickening ratio was 1.8 in LOPD patients, compared to 2.6 in healthy controls. [26, 32]. On MRI, paravertebral and abdominal muscles at all stages of the disease demonstrated some degree of involvement, also in asymptomatic patients [65]. In axial and coronal MRI images, prominent atrophy of the diaphragm and abdominal muscles was found, but to a lesser extent of the intercostal muscles [50]. A correlation was found between diaphragm atrophy and FVC in supine position, FVC drop, peak cough flow and PImax [50]. From a functional point of view, significant differences of lung diameter in the cranio-caudal and antero-posterior direction, and diaphragmatic movement area were observed between LOPD patients and controls [56, 57, 66], showing that diaphragm movement is deteriorated in patients and mild diaphragm weakness is compensated by increasing ribcage expansion. This was confirmed in a 3D study with dynamic MRI, which shows that at early disease stage the increased chest wall movement can compensate for diaphragm weakness, leading to relatively normal pulmonary function [62]. Furthermore, diaphragm dysfunction was

found to alter both the ability to generate static force but also the ability to preserve minute ventilation during transient or sustained inspiratory loads [66].

Other neuromuscular disorders

In a heterogenous group of patients with different myopathies, diaphragm thickness at FRC was found to be decreased compared to healthy controls [17]. In Charcot-Marie-Tooth disease type 1A (CMT1A), excursion amplitude at TLC, diaphragm thickness at TLC and thickening fraction were reduced [31]. Thickness at FRC was not different, which was consistent with findings in other neuropathies [17].

Clinical applications

A few studies reported application of respiratory muscle imaging as a diagnostic tool to guide respiratory management or as outcome measure. Diaphragm ultrasound had a 93% sensitivity and 100% specificity for diagnosis of diaphragm dysfunction in patients with dyspnoea referred for evaluation of neuromuscular respiratory failure [16]. In patients with ALS, serial assessment of diaphragm thickening by ultrasound was found to be an accurate method to predict the initiation of non-invasive ventilation (NIV) [35]. In a study to assess the effects of the steroid deflazacort in DMD, T2 relaxation times of the sternocleidomastoid muscle were used as outcome measure [52]. The use of diaphragm ultrasound in the intensive care unit to predict weaning failure and clinical outcome is beyond the scope of this review, but a good example of the clinical utility of diaphragm ultrasound [67-69].

Taken together, US and MR imaging have been utilized to characterize respiratory muscles in NMDs. Most NMDs show impaired diaphragm structure and function. Measurements of extra-diaphragmatic respiratory muscles are included sporadically. To date, only limited studies used respiratory muscle imaging in clinical practice or as outcome measure in clinical trials.

Limitations and challenges

Clinical

Currently, studies on respiratory muscle imaging evaluating natural progression of respiratory muscle function in NMDs are lacking. The low prevalence of each NMD requires collaborative research between different study groups to achieve a sufficient cohort of patients at different clinical stages (from presymptomatic to advanced patients). Collection of these data are essential to unlock the potential of respiratory muscle imaging as respiratory outcome measure and to guide respiratory management. Additionally, the collection of data from a large population of healthy subjects is necessary to establish reference values and normal patterns of diaphragm and chest wall motion.

Note that the non-invasive, portable, and effort independent character of ultrasound makes this technique particularly well suitable for evaluation of respiratory muscle function in early childhood. On the contrary, MRI of the respiratory muscles is more dependent on patient's motivation, attention and coordination but is more reproducible across clinical centres.

Most of the studies evaluating respiratory muscle function report correlation with spirometry, but other measures should be included in future studies, such as sniff nasal inspiratory pressures or transdiaphragmatic pressures.

The focus of respiratory muscle imaging in NMDs is mainly limited to the diaphragm. Although the diaphragm is our most important respiratory muscle, dysfunction of accessory inspiratory muscles and expiratory muscles also greatly contributes to respiratory failure in NMD. In fact, prominent respiratory difficulties in NMDs originate from extra-diaphragmatic respiratory muscle weakness, such as cough impairment. For example, in Duchenne muscular dystrophy, accessory inspiratory muscles and expiratory muscles are earlier and more severely affected than the diaphragm [51, 70]. Furthermore, the diaphragm is relatively spared in spinal muscular atrophy (SMA) type I with more severely affected expiratory muscles [71]. Remarkably, no studies have been published that assess extra-diaphragmatic respiratory muscles in NMDs using US, and only a few studies using MRI. In patients with Duchenne muscular dystrophy, early fatty infiltration in the expiratory muscles was found using MRI. Fatty infiltration of the expiratory muscles were reflected functionally as decreased maximal expiratory pressures. Interestingly, in some cases, elevated fat-fraction was present prior to decreases in maximal expiratory pressure [55]. Furthermore, sternocleidomastoid muscle tissue composition was altered in DMD compared to healthy controls, as assessed by T2 relaxation times, and was more preserved in DMD patients on the steroid deflazacort [51, 52].

Technical

US imaging

A major concern in respiratory muscle ultrasound is the trade-off between resolution and penetration. Respiratory muscles are relatively thin, especially the diaphragm (~2-3 mm). Moreover, in many NMDs, diaphragm thickness is even less. High resolution is therefore paramount for diaphragm ultrasound. However, due to the physical nature of ultrasound, when increasing the resolution using higher ultrasound frequencies, penetration of ultrasound decreases. As a consequence, deeper structures are not visualized. Penetration is further diminished when imaging through tissue with a high density of transitions between high and low acoustic impedance, such as muscle tissue with high fat or fibrous tissue contents. The latter is present in many NMDs and should be accounted for in the resolution/penetration trade-off. Furthermore, the presence of unrelated pathology, such as pleural effusion or fluid between the liver and diaphragm, may contribute to an image that is more difficult to interpret.

As discussed, there are large differences in diaphragm ultrasound techniques and normal values (Table 1). This leads to poor comparability between labs and studies. Therefore, for research and clinical evaluation it is of uttermost importance to use the same measurement technique as was used for the normal values. Best practice is to collect own lab normal values with a strict protocol and training, because differences may even occur when apparently using the same approach [33, 38].

MR imaging

Contraindications to MRI such as metal implants, invasive ventilation, and claustrophobia make it impossible to scan certain patients. Furthermore, some patients, due to reduced pulmonary function, are unable to lay in supine position without mechanical ventilation. Even if MR compatible mechanical ventilation is available, the longer acquisition protocols limit the use of MRI in these patients.

The duration of the image acquisition protocol represents a traditional concern. Providing shorter scan durations represents the main challenge for imaging respiratory muscles, especially for patients who cannot lay supine in the scanner for a long time or cannot perform multiple deep-breath cycles. When designing a clinical study protocol, a balance must be achieved between the measures that could be obtained and the minimization of patient discomfort.

When measuring diaphragm excursion and chest wall movement, both static and dynamic MRI methods have inherited limitations. Static MRI techniques are dependent on patients' capability to perform vital capacity manoeuvres in supine position. Although this requirement makes MRI measures sensitive to early signs of diaphragm weakness, it can be challenging in some patients. On the other hand, free-breathing MRI does not require breath-holds acquisitions, but longer scan time and irregular breathing become the limiting factors.

A further challenge is represented by the MR image processing techniques associated to the measure of the fat infiltration of the respiratory muscles. Dixon images are still analysed by manually tracing the muscle borders, or regions of interests within the muscle, slice by slice, which is a time-consuming process, not feasible in a large, multisite setting. Moreover, due to the non-uniform distribution of fat within the muscle, the accurate description of fat replacement process over time would require the delineation of the same region of interest at different time points or the volumetric segmentation of individual muscles. No automated techniques for respiratory muscle segmentation have been reported, but recent automatic algorithms for muscle segmentation and quantification of fat infiltration have been described in patients on other muscle groups [72, 73].

Novel techniques and future developments

US imaging

Advances in respiratory muscle ultrasound lag behind on developments in other fields. Most prominent are the increasing technological advances in cardiac or gynaecological ultrasound [74, 75]. Furthermore, ultrasound is increasingly applied to general skeletal muscles in the diagnostic workup of NMDs [76]. Several efforts have been attempted to apply new ultrasound techniques to the respiratory muscles.

First, strain imaging, which is a technique to estimate and visualize local tissue deformation. This technique is clinically used in echocardiography to detect systolic dysfunction [77]. Strain imaging is based on speckle tracking. Speckle tracking is the estimation of local tissue displacement as a function of time by following small kernels of ultrasound image signals throughout successively acquired images. This is possible because of the characteristic grainy patterns inherent to ultrasound, so-called speckle patterns, that provide local footprints of a tissue. Spatial derivation of the estimated displacement maps, directly provides a strain image representing the deformation of the tissue relative to its initial length [78]. No dedicated ultrasound equipment is required as a recorded ultrasound video can be processed afterwards. Speckle tracking has been applied to diaphragm ultrasound. With the intercostal approach deformation of the diaphragm can be visualized as an outcome for contractility [79-81]. Diaphragm strain and strain rate using speckle tracking in healthy subjects showed high correlations with transdiaphragmatic pressure (Pdi), which is considered the gold standard of diaphragm function [4, 79]. In contrast, diaphragm thickening fraction was poorly correlated to Pdi [82].

Second, ultrafast shear wave elastography (UF-SWE) is the latest and most advanced type of elastography [83]. In short, a temporary mechanical disturbance is introduced to a specific location in the tissue of interest using an acoustic force generated by focussed ultrasound. This initiates a mechanical wave to propagate through the tissue. The tissue motion which is induced as the wave propagates can be measured and with ultrafast ultrasound. The magnitude and velocity of this wave is directly linked to tissue stiffness. In general the wave propagates faster, but with a lower amplitude, for stiffer tissue. Stiffness of the diaphragm as assessed by UF-SWE can be measured reliably and showed high correlation to Pdi [84, 85]. Changes in muscle architecture due to fat infiltration or fibrous tissue in NMDs are also reflected in tissue stiffness as assessed by UF-SWE in skeletal muscles [86-88].

Third, quantitative muscle ultrasound (QMUS) is a well-established approach in the diagnostic workup of NMDs [76]. QMUS evaluates the echogenicity of muscles. Healthy muscles appear relatively black on ultrasound images, interspersed with thin white fascial lines. In NMDs, where muscle tissue is replaced by fat or fibrous tissue, echogenicity is increased. To date, echogenicity of respiratory muscles in NMDs has not been assessed.

Overall, strain imaging, UF-SWE and QMUS may be potentially interesting techniques to assess diaphragm structure and function in NMDs.

MR imaging

Advances in respiratory muscle MRI may follow the advances in image processing techniques and their recent application in NMDs. Texture analysis and machine learning techniques have shown the potential of improving muscular tissue characterization in NMDs [89, 90]. The distribution of grey-intensities of voxels provides additional features able to describe the full muscular water/fat signal distribution in MRI, which may not be caught by fat fraction or visual scoring only.

No study using T2-weighted fat-saturated sequences, such as short τ inversion recovery (STIR) sequences, has been reported on respiratory muscles. Hypertense signal abnormalities on STIR sequences are consistent with the presence of oedema or inflammation and have been observed on skeletal muscles that appear normal on T1 images, suggesting that both oedema and inflammation are associated with early stage of involvement [91-93]. With these techniques, early respiratory muscle involvement may be investigated.

A comprehensive protocol including short and ultra-short echo time acquisitions, would also provide information about regional ventilation. Non-contrast enhanced MRI has been proposed to infer ventilation from signal changes occurring within the lung between different lung volumes [94-96]. In NMDs, ventilation maps would emphasize early ventilatory impairment due to respiratory muscles' weakness and would provide an additional tool to understand how structural impairment and dysfunction of respiratory muscles affect ventilation.

Conclusion

Different US and MR imaging techniques have been demonstrated useful to detect impaired respiratory muscle structure and function in patients with NMDs. Moreover, new technological developments in US and MR imaging will further increase its value. However, a lack of standardization in measurement procedures, data on extra-diaphragmatic respiratory muscles and clinical data from natural history studies impede its widespread clinical use. To unlock the potential of respiratory muscle imaging to monitor disease progression, to guide respiratory management and as respiratory outcome measure in clinical trials these limitation should be addressed by an international working group on respiratory muscle imaging.

References

1. Laghi F, Tobin MJ. Disorders of the respiratory muscles. *Am J Respir Crit Care Med* 2003: 168(1): 10-48.
2. Scoto M, Finkel R, Mercuri E, Muntoni F. Genetic therapies for inherited neuromuscular disorders. *Lancet Child Adolesc* 2018: 2(8): 600-609.
3. LoMauro A, D'Angelo MG, Aliverti A. Assessment and management of respiratory function in patients with Duchenne muscular dystrophy: current and emerging options. *Ther Clin Risk Manag* 2015: 11: 1475-1488.
4. Doorduin J, van Hees HW, van der Hoeven JG, Heunks LM. Monitoring of the respiratory muscles in the critically ill. *Am J Respir Crit Care Med* 2013: 187(1): 20-27.
5. Jackson CE, Rosenfeld J, Moore DH, Bryan WW, Barohn RJ, Wrench M, Myers D, Heberlin L, King R, Smith J, Gelinas D, Miller RG. A preliminary evaluation of a prospective study of pulmonary function studies and symptoms of hypoventilation in ALS/MND patients. *J Neurol Sci* 2001: 191(1-2): 75-78.
6. Gayraud J, Ramonatxo M, Rivier F, Humberclaude V, Petrof B, Matecki S. Ventilatory parameters and maximal respiratory pressure changes with age in Duchenne muscular dystrophy patients. *Pediatr Pulmonol* 2010: 45(6): 552-559.
7. Guimarães-Costa R, Similowski T, Rivals I, Morélot-Panzini C, Nierat M-C, Bui MT, Akbar D, Straus C, Romero NB, Michel PP, Menegaux F, Salachas F, Gonzalez-Bermejo J, Bruneteau G. Human diaphragm atrophy in amyotrophic lateral sclerosis is not predicted by routine respiratory measures. *European Respiratory Journal* 2019: 53(2): 1801749.
8. Gauld LM, Boynton A, Betts GA, Johnston H. Spirometry is Affected by Intelligence and Behavior in Duchenne Muscular Dystrophy. *Pediatric Pulmonology* 2005: 40(5): 408-413.
9. Boentert M, Wenninger S, Sansone VA. Respiratory involvement in neuromuscular disorders. *Curr Opin Neurol* 2017: 30(5): 529-537.
10. Benditt JO, Boitano LJ. Pulmonary Issues in Patients with Chronic Neuromuscular Disease. *American Journal of Respiratory and Critical Care Medicine* 2013: 187(10): 1046-1055.
11. Benditt JO. The neuromuscular respiratory system: physiology, pathophysiology, and a respiratory care approach to patients. *Respir Care* 2006: 51(8): 829-837; discussion 837-829.
12. LoMauro A, Romei M, Gandossini S, Pascuzzo R, Vantini S, D'Angelo MG, Aliverti A. Evolution of respiratory function in Duchenne muscular dystrophy from childhood to adulthood. *European Respiratory Journal* 2018: 51(2): 1701418.
13. LoMauro A, D'Angelo MG, Aliverti A. Sleep Disordered Breathing in Duchenne Muscular Dystrophy. *Curr Neurol Neurosci Rep* 2017: 17(5): 44.
14. LoMauro A, Romei M, D'Angelo MG, Aliverti A. Determinants of cough efficiency in Duchenne muscular dystrophy. *Pediatr Pulmonol* 2014: 49(4): 357-365.
15. Laviola M, Priori R, D'Angelo MG, Aliverti A. Assessment of diaphragmatic thickness by ultrasonography in Duchenne muscular dystrophy (DMD) patients. *PLoS ONE* 2018: 13(7).
16. Boon AJ, Sekiguchi H, Harper CJ, Strommen JA, Ghahfarokhi LS, Watson JC, Sorenson EJ. Sensitivity and specificity of diagnostic ultrasound in the diagnosis of phrenic neuropathy. *Neurology* 2014: 83(14): 1264-1270.

17. Noda Y, Sekiguchi K, Kohara N, Kanda F, Toda T. Ultrasonographic diaphragm thickness correlates with compound muscle action potential amplitude and forced vital capacity. *Muscle and Nerve* 2016: 53(4): 522-527.
18. O'Gorman CM, O'Brien T G, Boon AJ. Utility Of diaphragm ultrasound in myopathy. *Muscle and Nerve* 2017: 55(3): 427-429.
19. Pathak S, Caress JB, Wosiski-Kuhn M, Milligan C, Williams D, Cartwright MS. A pilot study of neuromuscular ultrasound as a biomarker for amyotrophic lateral sclerosis. *Muscle and Nerve* 2019: 59(2): 181-186.
20. De Bruin PF, Ueki J, Bush A, Khan Y, Watson A, Pride NB. Diaphragm thickness and inspiratory strength in patients with Duchenne muscular dystrophy. *Thorax* 1997: 52(5): 472-475.
21. Hiwatani Y, Sakata M, Miwa H. Ultrasonography of the diaphragm in amyotrophic lateral sclerosis: Clinical significance in assessment of respiratory functions. *Amyotrophic Lateral Sclerosis and Frontotemporal Degeneration* 2013: 14(2): 127-131.
22. Pinto S, Alves P, Pimentel B, Swash M, de Carvalho M. Ultrasound for assessment of diaphragm in ALS. *Clinical Neurophysiology* 2016: 127(1): 892-897.
23. Pinto S, Alves P, Swash M, de Carvalho M. Phrenic nerve stimulation is more sensitive than ultrasound measurement of diaphragm thickness in assessing early ALS progression. *Neurophysiol Clin* 2017: 47(1): 69-73.
24. Sartucci F, Pelagatti A, Santin M, Bocci T, Dolciotti C, Bongioanni P. Diaphragm ultrasonography in amyotrophic lateral sclerosis: a diagnostic tool to assess ventilatory dysfunction and disease severity. *Neurological Sciences* 2019: 40(10): 2065-2071.
25. Buonsenso D, Berti B, Palermo C, Leone D, Ferrantini G, De Sanctis R, Onesimo R, Curatola A, Fanelli L, Forcina N, Norcia G, Carnicella S, Lucibello S, Mercuri E, Pane M. Ultrasound assessment of diaphragmatic function in type 1 spinal muscular atrophy. *Pediatric Pulmonology* 2020.
26. Ruggeri P, Lo Monaco L, Musumeci O, Tavilla G, Gaeta M, Caramori G, Toscano A. Ultrasound assessment of diaphragm function in patients with late-onset Pompe disease. *Neurological Sciences* 2020.
27. Fayssoil A, Chaffaut C, Ogna A, Stojkovic T, Lamothe L, Mompoint D, Meng P, Prigent H, Clair B, Behin A, Laforet P, Bassez G, Carlier R, Orlikowski D, Amthor H, Quijano Roy S, Crenn P, Chevret S, Eymard B, Lofaso F, Annane D. Echographic assessment of diaphragmatic function in duchenne muscular dystrophy from childhood to adulthood. *Journal of Neuromuscular Diseases* 2019: 6(1): 55-64.
28. Fayssoil A, Nguyen LS, Ogna A, Stojkovic T, Meng P, Mompoint D, Carlier R, Prigent H, Clair B, Behin A, Laforet P, Bassez G, Crenn P, Orlikowski D, Annane D, Eymard B, Lofaso F. Diaphragm sniff ultrasound: Normal values, relationship with sniff nasal pressure and accuracy for predicting respiratory involvement in patients with neuromuscular disorders. *PLoS ONE* 2019: 14(4).
29. Fantini R, Mandrioli J, Zona S, Antenora F, Iattoni A, Monelli M, Fini N, Tonelli R, Clini E, Marchioni A. Ultrasound assessment of diaphragmatic function in patients with amyotrophic lateral sclerosis. *Respirology* 2016.
30. Henke C, Spiesshoefer J, Kabitz HJ, Herkenrath S, Randerath W, Brix T, Gorlich D, Young P, Boentert M. Respiratory muscle weakness in facioscapulohumeral muscular dystrophy. *Muscle and Nerve* 2019: 60(6): 679-686.

31. Spiesshoefer J, Henke C, Kabitz HJ, Akova-Oeztuerk E, Draeger B, Herkenrath S, Randerath W, Young P, Brix T, Boentert M. Phrenic nerve involvement and respiratory muscle weakness in patients with Charcot-Marie-Tooth disease 1A. *Journal of the Peripheral Nervous System* 2019: 24(3): 283-293.
32. Spiesshoefer J, Henke C, Kabitz HJ, Brix T, Gorlich D, Herkenrath S, Randerath W, Young P, Boentert M. The nature of respiratory muscle weakness in patients with late-onset Pompe disease. *Neuromuscular Disorders* 2019: 29(8): 618-627.
33. Henke C, Spiesshoefer J, Kabitz HJ, Herkenrath S, Randerath W, Brix T, Gorlich D, Young P, Boentert M. Characteristics of respiratory muscle involvement in myotonic dystrophy type 1. *Neuromuscular Disorders* 2020: 30(1): 17-27.
34. Ayoub J, Milane J, Targhetta R, Prioux J, Chamari K, Arbeille P, Jonquet O, Bourgeois JM, Prefaut C. Diaphragm kinetics during pneumatic belt respiratory assistance: a sonographic study in Duchenne muscular dystrophy. *Neuromuscul Disord* 2002: 12(6): 569-575.
35. Fantini R, Tonelli R, Castaniere I, Tabbi L, Pellegrino MR, Cerri S, Livrieri F, Giaroni F, Monelli M, Ruggieri V, Fini N, Mandrioli J, Clini E, Marchioni A. Serial ultrasound assessment of diaphragmatic function and clinical outcome in patients with amyotrophic lateral sclerosis. *BMC Pulmonary Medicine* 2019: 19(1).
36. Fromageot C, Lofaso F, Annane D, Falaize L, Lejaille M, Clair B, Gajdos P, Raphaël JC. Supine fall in lung volumes in the assessment of diaphragmatic weakness in neuromuscular disorders. *Arch Phys Med Rehabil* 2001: 82(1): 123-128.
37. Cohn D, Benditt JO, Eveloff S, McCool FD. Diaphragm thickening during inspiration. *J Appl Physiol (1985)* 1997: 83(1): 291-296.
38. Boon AJ, Harper CJ, Ghahfarokhi LS, Strommen JA, Watson JC, Sorenson EJ. Two-dimensional ultrasound imaging of the diaphragm: quantitative values in normal subjects. *Muscle Nerve* 2013: 47(6): 884-889.
39. Boussuges A, Gole Y, Blanc P. Diaphragmatic motion studied by m-mode ultrasonography: methods, reproducibility, and normal values. *Chest* 2009: 135(2): 391-400.
40. Carrie C, Bonnardel E, Vally R, Revel P, Marthan R, Biais M. Vital Capacity Impairment due to Neuromuscular Disease and its Correlation with Diaphragmatic Ultrasound: A Preliminary Study. *Ultrasound in Medicine and Biology* 2016: 42(1): 143-149.
41. Dres M, Dubé BP, Goligher E, Vorona S, Demiri S, Morawiec E, Mayaux J, Brochard L, Similowski T, Demoule A. Usefulness of Parasternal Intercostal Muscle Ultrasound during Weaning from Mechanical Ventilation. *Anesthesiology* 2020: 132(5): 1114-1125.
42. Umbrello M, Formenti P, Lusardi AC, Guanziroli M, Caccioppola A, Coppola S, Chiumello D. Oesophageal pressure and respiratory muscle ultrasonographic measurements indicate inspiratory effort during pressure support ventilation. *British Journal of Anaesthesia* 2020: 125(1): e148-e157.
43. Wallbridge P, Parry S, Das S, Law C, Hammerschlag G, Irving L, Hew M, Steinfort D. Parasternal intercostal muscle ultrasound measurements correlate with disease severity in chronic obstructive pulmonary disease: a pilot study. *European Respiratory Journal* 2018: 52(suppl 62): PA3895.
44. Cala SJ, Kenyon CM, Lee A, Watkin K, Macklem PT, Rochester DF. Respiratory Ultrasonography of Human Parasternal Intercostal Muscle In Vivo. *Ultrasound in Medicine & Biology* 1998: 24(3): 313-326.

45. Tahan N, Khademi-Kalantari K, Mohseni-Bandpei MA, Mikaili S, Baghban AA, Jaberzadeh S. Measurement of superficial and deep abdominal muscle thickness: an ultrasonography study. *J Physiol Anthropol* 2016: 35(1): 17-17.
46. Pirri C, Todros S, Fede C, Pianigiani S, Fan CL, Foti C, Stecco C, Pavan P. Inter-rater reliability and variability of ultrasound measurements of abdominal muscles and fasciae thickness. *Clin Anat* 2019: 32(7): 948-960.
47. Misuri G, Colagrande S, Gorini M, Iandelli I, Mancini M, Duranti R, Scano G. In vivo ultrasound assessment of respiratory function of abdominal muscles in normal subjects. *European Respiratory Journal* 1997: 10(12): 2861-2867.
48. Mercuri E, Talim B, Moghadaszadeh B, Petit N, Brockington M, Counsell S, Guicheney P, Muntoni F, Merlini L. Clinical and imaging findings in six cases of congenital muscular dystrophy with rigid spine syndrome linked to chromosome 1p (RSMD1). *Neuromuscul Disord* 2002: 12(7-8): 631-638.
49. Fischer D, Kley RA, Strach K, Meyer C, Sommer T, Eger K, Rolfs A, Meyer W, Pou A, Pradas J, Heyer CM, Grossmann A, Huebner A, Kress W, Reimann J, Schröder R, Eymard B, Fardeau M, Udd B, Goldfarb L, Vorgerd M, Olivé M. Distinct muscle imaging patterns in myofibrillar myopathies. *Neurology* 2008: 71(10): 758-765.
50. Gaeta M, Barca E, Ruggeri P, Minutoli F, Rodolico C, Mazziotti S, Milardi D, Musumeci O, Toscano A. Late-onset Pompe disease (LOPD): correlations between respiratory muscles CT and MRI features and pulmonary function. *Mol Genet Metab* 2013: 110(3): 290-296.
51. Mavrogeni S, Tzelepis GE, Athanasopoulos G, Maounis T, Douskou M, Papavasiliou A, Cokkinos DV. Cardiac and sternocleidomastoid muscle involvement in Duchenne muscular dystrophy: an MRI study. *Chest* 2005: 127(1): 143-148.
52. Mavrogeni S, Papavasiliou A, Douskou M, Kolovou G, Papadopoulou E, Cokkinos DV. Effect of deflazacort on cardiac and sternocleidomastoid muscles in Duchenne muscular dystrophy: a magnetic resonance imaging study. *Eur J Paediatr Neurol* 2009: 13(1): 34-40.
53. Dixon WT. Simple proton spectroscopic imaging. *Radiology* 1984: 153(1): 189-194.
54. Pennati F, Arrigoni F, LoMauro A, Gandossini S, Russo A, D'Angelo MG, Aliverti A. Diaphragm Involvement in Duchenne Muscular Dystrophy (DMD): An MRI Study. *J Magn Reson Imaging* 2020: 51(2): 461-471.
55. Barnard AM, Lott DJ, Batra A, Triplett WT, Forbes SC, Riehl SL, Willcocks RJ, Smith BK, Vandenborne K, Walter GA. Imaging respiratory muscle quality and function in Duchenne muscular dystrophy. *J Neurol* 2019: 266(11): 2752-2763.
56. Gaeta M, Musumeci O, Mondello S, Ruggeri P, Montagnese F, Cucinotta M, Vinci S, Milardi D, Toscano A. Clinical and pathophysiological clues of respiratory dysfunction in late-onset Pompe disease: New insights from a comparative study by MRI and respiratory function assessment. *Neuromuscul Disord* 2015: 25(11): 852-858.
57. Wens SC, Ciet P, Perez-Rovira A, Logie K, Salamon E, Wielopolski P, de Bruijne M, Kruijshaar ME, Tiddens HA, van Doorn PA, van der Ploeg AT. Lung MRI and impairment of diaphragmatic function in Pompe disease. *BMC Pulm Med* 2015: 15: 54.
58. Amberg B, Romdhani S, Vetter T. Optimal Step Nonrigid ICP Algorithms for Surface Registration. In: 2007 IEEE Conference on Computer Vision and Pattern Recognition; 2007 17-22 June 2007; 2007. p. 1-8.

59. Mankodi A, Kovacs W, Norato G, Hsieh N, Bandettini WP, Bishop CA, Shimellis H, Newbould RD, Kim E, Fischbeck KH, Arai AE, Yao J. Respiratory magnetic resonance imaging biomarkers in Duchenne muscular dystrophy. *Ann Clin Transl Neurol* 2017: 4(9): 655-662.
60. Bishop CA, Ricotti V, Sinclair CDJ, Evans MRB, Butler JW, Morrow JM, Hanna MG, Matthews PM, Yousry TA, Muntoni F, Thornton JS, Newbould RD, Janiczek RL. Semi-Automated Analysis of Diaphragmatic Motion with Dynamic Magnetic Resonance Imaging in Healthy Controls and Non-Ambulant Subjects with Duchenne Muscular Dystrophy. *Front Neurol* 2018: 9: 9.
61. Smith BK, Martin AD, Lawson LA, Vernot V, Marcus J, Islam S, Shafi N, Corti M, Collins SW, Byrne BJ. Inspiratory muscle conditioning exercise and diaphragm gene therapy in Pompe disease: Clinical evidence of respiratory plasticity. *Exp Neurol* 2017: 287(Pt 2): 216-224.
62. Mogalle K, Perez-Rovira A, Ciet P, Wens SC, van Doorn PA, Tiddens HA, van der Ploeg AT, de Bruijne M. Quantification of Diaphragm Mechanics in Pompe Disease Using Dynamic 3D MRI. *PLoS One* 2016: 11(7): e0158912.
63. LoMauro A, Aliverti A, Mastella C, Arnoldi MT, Banfi P, Baranello G. Spontaneous Breathing Pattern as Respiratory Functional Outcome in Children with Spinal Muscular Atrophy (SMA). *PLoS One* 2016: 11(11): e0165818.
64. Fischmann A, Hafner P, Gloor M, Schmid M, Klein A, Pohlman U, Waltz T, Gonzalez R, Haas T, Bieri O, Fischer D. Quantitative MRI and loss of free ambulation in Duchenne muscular dystrophy. *J Neurol* 2013: 260(4): 969-974.
65. Alejaldre A, Díaz-Manera J, Ravaglia S, Tibaldi EC, D'Amore F, Morís G, Muelas N, Vílchez JJ, García-Medina A, Usón M, Martínez García FA, Illa I, Pichiecchio A. Trunk muscle involvement in late-onset Pompe disease: study of thirty patients. *Neuromuscul Disord* 2012: 22 Suppl 2: S148-154.
66. Smith BK, Allen S, Mays S, Martin AD, Byrne BJ. Dynamic respiratory muscle function in late-onset Pompe disease. *Sci Rep* 2019: 9(1): 19006.
67. Li C, Li X, Han H, Cui H, Wang G, Wang Z. Diaphragmatic ultrasonography for predicting ventilator weaning: A meta-analysis. *Medicine (Baltimore)* 2018: 97(22): e10968.
68. Medrinal C, Combret Y, Hilfiker R, Prieur G, Aroichane N, Gravier FE, Bonnevie T, Contal O, Lamia B. ICU outcomes can be predicted by noninvasive muscle evaluation: a meta-analysis. *Eur Respir J* 2020: 56(4).
69. Llamas-Álvarez AM, Tenza-Lozano EM, Latour-Pérez J. Diaphragm and Lung Ultrasound to Predict Weaning Outcome: Systematic Review and Meta-Analysis. *Chest* 2017: 152(6): 1140-1150.
70. Khirani S, Ramirez A, Aubertin G, Boulé M, Chemouny C, Forin V, Fauroux B. Respiratory muscle decline in Duchenne muscular dystrophy. *Pediatr Pulmonol* 2014: 49(5): 473-481.
71. Schroth MK. Special considerations in the respiratory management of spinal muscular atrophy. *Pediatrics* 2009: 123 Suppl 4: S245-249.
72. Gadermayr M, Disch C, Müller M, Merhof D, Gess B. A comprehensive study on automated muscle segmentation for assessing fat infiltration in neuromuscular diseases. *Magn Reson Imaging* 2018: 48: 20-26.
73. Ogier AC, Heskamp L, Michel CP, Fouré A, Bellemare ME, Le Troter A, Heerschap A, Bendahan D. A novel segmentation framework dedicated to the follow-up of fat infiltration in individual muscles of patients with neuromuscular disorders. *Magn Reson Med* 2020: 83(5): 1825-1836.

74. Dave JK, Mc Donald ME, Mehrotra P, Kohut AR, Eisenbrey JR, Forsberg F. Recent technological advancements in cardiac ultrasound imaging. *Ultrasonics* 2018: 84: 329-340.
75. Nawapun K, Phithakwatchara N, Jaingam S, Viboonchart S, Mongkolchat N, Wataganara T. Advanced ultrasound for prenatal interventions. *Ultrasonography* 2018: 37(3): 200-210.
76. van Alfen N, Gijsbertse K, de Korte CL. How useful is muscle ultrasound in the diagnostic workup of neuromuscular diseases? *Curr Opin Neurol* 2018: 31(5): 568-574.
77. Smiseth OA, Torp H, Opdahl A, Haugaa KH, Urheim S. Myocardial strain imaging: how useful is it in clinical decision making? *Eur Heart J* 2016: 37(15): 1196-1207.
78. Ophir J, Céspedes I, Ponnekanti H, Yazdi Y, Li X. Elastography: a quantitative method for imaging the elasticity of biological tissues. *Ultrason Imaging* 1991: 13(2): 111-134.
79. Oppersma E, Hatam N, Doorduin J, van der Hoeven JG, Marx G, Goetzenich A, Fritsch S, Heunks LMA, Bruells CS. Functional assessment of the diaphragm by speckle tracking ultrasound during inspiratory loading. *J Appl Physiol (1985)* 2017: 123(5): 1063-1070.
80. Orde SR, Boon AJ, Firth DG, Villarraga HR, Sekiguchi H. Diaphragm assessment by two dimensional speckle tracking imaging in normal subjects. *BMC Anesthesiol* 2016: 16(1): 43-43.
81. Hatam N, Goetzenich A, Rossaint R, Karfis I, Bickenbach J, Autschbach R, Marx G, Bruells CS. A novel application for assessing diaphragmatic function by ultrasonic deformation analysis in noninvasively ventilated healthy young adults. *Ultraschall Med* 2014: 35(6): 540-546.
82. Goligher EC, Laghi F, Detsky ME, Farias P, Murray A, Brace D, Brochard LJ, Bolz SS, Rubenfeld GD, Kavanagh BP, Ferguson ND. Measuring diaphragm thickness with ultrasound in mechanically ventilated patients: feasibility, reproducibility and validity. *Intensive Care Med* 2015: 41(4): 642-649.
83. Sarvazyan A, Hall TJ, Urban MW, Fatemi M, Aglyamov SR, Garra BS. AN OVERVIEW OF ELASTOGRAPHY - AN EMERGING BRANCH OF MEDICAL IMAGING. *Curr Med Imaging Rev* 2011: 7(4): 255-282.
84. Bachasson D, Dres M, Niérat MC, Gennisson JL, Hogrel JY, Doorduin J, Similowski T. Diaphragm shear modulus reflects transdiaphragmatic pressure during isovolumetric inspiratory efforts and ventilation against inspiratory loading. *J Appl Physiol (1985)* 2019: 126(3): 699-707.
85. Flatres A, Aarab Y, Nougaret S, Garnier F, Larcher R, Amalric M, Klouche K, Etienne P, Subra G, Jaber S, Molinari N, Matecki S, Jung B. Real-time shear wave ultrasound elastography: a new tool for the evaluation of diaphragm and limb muscle stiffness in critically ill patients. *Crit Care* 2020: 24(1): 34-34.
86. Lacourpaille L, Gross R, Hug F, Guével A, Péréon Y, Magot A, Hogrel JY, Nordez A. Effects of Duchenne muscular dystrophy on muscle stiffness and response to electrically-induced muscle contraction: A 12-month follow-up. *Neuromuscul Disord* 2017: 27(3): 214-220.
87. Lacourpaille L, Hug F, Guével A, Péréon Y, Magot A, Hogrel JY, Nordez A. Non-invasive assessment of muscle stiffness in patients with Duchenne muscular dystrophy. *Muscle Nerve* 2015: 51(2): 284-286.
88. Bachasson D, Dubois GJR, Allenbach Y, Benveniste O, Hogrel JY. Muscle Shear Wave Elastography in Inclusion Body Myositis: Feasibility, Reliability and Relationships with Muscle Impairments. *Ultrasound Med Biol* 2018: 44(7): 1423-1432.
89. Cai J, Xing F, Batra A, Liu F, Walter GA, Vandenborne K, Yang L. Texture Analysis for Muscular Dystrophy Classification in MRI with Improved Class Activation Mapping. *Pattern Recognit* 2019: 86: 368-375.

90. Nasel C, Klickovic U, Cetin H, Struhal W, Moser E. Advanced Analysis of the Water/Fat Distribution in Skeletal Muscle Tissue Using Magnetic Resonance Imaging in Patients With Neuromuscular Disease. *Frontiers in Physics* 2020: 8(195).
91. Pichiecchio A, Alessandrino F, Bortolotto C, Cerica A, Rosti C, Raciti MV, Rossi M, Berardinelli A, Baranello G, Bastianello S, Calliada F. Muscle ultrasound elastography and MRI in preschool children with Duchenne muscular dystrophy. *Neuromuscul Disord* 2018: 28(6): 476-483.
92. Degardin A, Morillon D, Lacour A, Cotten A, Vermersch P, Stojkovic T. Morphologic imaging in muscular dystrophies and inflammatory myopathies. *Skeletal Radiol* 2010: 39(12): 1219-1227.
93. Tasca G, Monforte M, Iannaccone E, Laschena F, Ottaviani P, Leoncini E, Boccia S, Galluzzi G, Pelliccioni M, Masciullo M, Frusciante R, Mercuri E, Ricci E. Upper girdle imaging in facioscapulohumeral muscular dystrophy. *PloS one* 2014: 9(6): e100292-e100292.
94. Zapke M, Topf HG, Zenker M, Kuth R, Deimling M, Kreisler P, Rauh M, Chefd'hotel C, Geiger B, Rupprecht T. Magnetic resonance lung function--a breakthrough for lung imaging and functional assessment? A phantom study and clinical trial. *Respir Res* 2006: 7(1): 106.
95. Pennati F, Quirk JD, Yablonskiy DA, Castro M, Aliverti A, Woods JC. Assessment of regional lung function with multivolume (1)H MR imaging in health and obstructive lung disease: comparison with (3)He MR imaging. *Radiology* 2014: 273(2): 580-590.
96. Bauman G, Puderbach M, Deimling M, Jellus V, Chefd'hotel C, Dinkel J, Hintze C, Kauczor HU, Schad LR. Non-contrast-enhanced perfusion and ventilation assessment of the human lung by means of fourier decomposition in proton MRI. *Magn Reson Med* 2009: 62(3): 656-664.
97. Carrillo-Esper R, Pérez-Calatayud Á A, Arch-Tirado E, Díaz-Carrillo MA, Garrido-Aguirre E, Tapia-Velazco R, Peña-Pérez CA, Espinoza-de Los Monteros I, Meza-Márquez JM, Flores-Rivera OI, Zepeda-Mendoza AD, de la Torre-León T. Standardization of Sonographic Diaphragm Thickness Evaluations in Healthy Volunteers. *Respir Care* 2016: 61(7): 920-924.



Chapter 3

Respiratory muscle function in patients with nemaline myopathy

Esmee SB van Kleef
Jeroen LM van Doorn
Michael A Gaytant
Willemien de Weerd
Bettine AH Vosse
Carina Wallgren-Pettersson
Baziel GM van Engelen
Coen AC Ottenheijm
Nicol C Voermans
Jonne Doorduin

Published in:
Neuromuscular Disorders, 2022

Abstract

In this cross-sectional study, we comprehensively assessed respiratory muscle function in various clinical forms of nemaline myopathy (NM) including non-volitional tests for diaphragm function. Forty-two patients with NM were included (10 males (25-74 y/o); 32 females (11-76 y/o)). The NM forms were typical (n=11), mild (n=7), or childhood-onset with slowness of movements (n=24). Forced vital capacity (FVC) and maximal inspiratory pressure were decreased in typical NM in comparison with childhood-onset NM with slowness (32.0 [29.0-58.5] vs 81.0 [75.0-87.0]%, $p<0.01$, and 35.0 [24.0-55.0] vs 81.0 [65.0-102.5] cmH_2O, $p<0.01$). Eight patients with childhood-onset NM with slowness had respiratory muscle weakness. There was a low correlation between FVC and Motor Function Measure scores (r=0.48, $p<0.01$). End-inspiratory diaphragm thickness and twitch mouth pressure were decreased in patients requiring home mechanical ventilation compared to non-ventilated patients with normal lung function (1.8 [1.5-2.4] vs 3.1 [2.0-4.6] mm, $p=0.049$, and -7.9 [-10.9- -4.0] vs -14.9 [-17.3- -12.6], $p=0.04$). Our results show that respiratory muscle weakness is present in all NM forms, including childhood-onset NM with slowness, and may be present irrespective of the degree of general motor function impairment. These findings highlight the importance for screening of respiratory function in patients with NM to guide respiratory management.

Introduction

Nemaline myopathy (NM) is a congenital myopathy with characteristic nemaline rods in the muscle biopsy [1, 2] with clinical manifestation ranging from severe NM to childhood-onset NM with slowness of movements. Causative mutations in at least 12 genes have been identified *[3-17]*, with *NEB* and *ACTA1* mutations being the most prevalent worldwide [1, 2]. The most prevalent NM form in the Netherlands is childhood-onset NM with slowness of movements caused by mutations in the *KBTBD13* gene [18-21].

Respiratory muscle weakness is a common feature in patients with NM and can lead to respiratory failure [22, 23]. In previous clinical studies, the physiological impact of respiratory muscle weakness was mostly assessed by spirometry or based on the presence of clinically evident respiratory insufficiency [9, 24-28]. A recent NM cohort study also assessed respiratory muscle strength [29]. These studies did not assess respiratory involvement in relation to the clinical NM forms, the relationship between respiratory muscle function and motor function, or specific measures of diaphragm function and structure. Furthermore, respiratory muscle weakness in childhood-onset NM with slowness has not been reported in the cohort studies [20, 30, 31], although it was tested in only one study [31]. Detailed knowledge of respiratory muscle involvement in the different forms of NM is important for respiratory management and for the development of outcome measures for clinical trials.

This cross-sectional study comprehensively assessed the degree of respiratory muscle involvement in different NM forms and genotypes using global measures of respiratory muscle function (spirometry, respiratory muscle strength testing). Moreover, compared to previous work we used non-volitional measures, i.e. ultrasound imaging of diaphragm and intercostal muscles and twitch mouth pressure ($P_{mo,tw}$) elicited by magnetic stimulation of the phrenic nerves. Furthermore, we explored the relationship between respiratory muscle function and motor function, and included patients with childhood-onset NM with slowness of movements.

Methods

Study design and patients

This cross-sectional study was performed between October 2018 and September 2020 at the Radboud University Medical Centre, Nijmegen, the Netherlands. Ethical approval (NL65214.091.18) was obtained from the local ethical committee and written informed consent was obtained from all patients or legal representatives.

Recruitment was performed by contacting patients with NM who had previously visited the outpatient clinic. Moreover, we reached out to clinicians in neuromuscular centres in the Netherlands and to patients via the Dutch patient organisation. The inclusion criteria were

genetically confirmed NM or the combination of an NM clinical phenotype, a biopsy confirming NM, and a first degree family member with genetically confirmed NM. The age range included was six to 80 years to increase the likelihood for patients to be cognitively and physically able to carry out the tests. Patients with other conditions affecting pulmonary or respiratory muscle function were excluded. Patient demographics (age, sex, BMI) and genotype were systematically collected.

Outcome measures

The form of NM, ambulation, requirement for home mechanical ventilation (HMV), and spinal deformity were systematically collected. We used the recently proposed revised classification, which distinguishes five forms of NM based on the age of onset and severity [1, 2]:

1) severe NM (contractures, fractures, no respiratory effort or no movements at birth); 2) typical NM (perinatal onset and motor milestones delayed but reached); 3) mild NM (childhood or juvenile onset); 4) distal NM (distal weakness); 5) childhood-onset NM with slowness (slowness of movements and core-rod histology, caused by the *KBTBD13* mutation [18-20]); and 6) recessive *TNNT1* (former Amish) NM. Ambulation was classified as unaided, using walking aids including intermittent wheelchair use, or wheelchair-dependent. HMV was categorised as none, nocturnal non-invasive, nocturnal and daytime non-invasive, and invasive ventilation. The presence of scoliosis was assessed by physical examination and by the Adam's forward bend test [32], and dichotomized as present or absent. The 32-item Motor Function Measure (MFM) was used to examine motor function. The total score is expressed as percentage of the maximum score. In case the patients were not able or willing to visit the Radboud University Medical Centre, a limited protocol consisting of MFM assessment and respiratory muscle strength testing was performed during home visits.

Spirometry was carried out with a handheld electronic spirometer (SpiroUSB, Vyaire Medical, Mettawa, IL, USA connected to PC Spirometry software, Spida CareFusion 2.3.0.10 for Windows 7). Forced vital capacity (FVC) and vital capacity (VC) upright and supine, and forced expiratory volume in the first second (FEV1) were measured and compared with reference values [33]. Peak cough flow (PCF) was also measured. Respiratory muscle strength testing, including maximal inspiratory pressure (MIP), maximal expiratory pressure (MEP), and sniff nasal inspiratory pressure (SNIP), was performed with a handheld electronic manometer (Micro RPM, Micro Medical, Rhymney, UK connected to Puma software version 1.4.2) and compared with reference values [34, 35]. Both spirometry and respiratory muscle strength tests were performed in accordance with the standards of the American Thoracic Society and the European Respiratory Society [36-38].

Right hemidiaphragm and intercostal muscle thickness and echogenicity was measured in supine position using an Esaote MyLab Twice ultrasound machine (Esaote SpA, Genoa, Italy)

equipped with a 3-13 MHz LA533 linear transducer (Esaote SpA, Genoa, Italy) according to previously described standards [**Chapter 2**][39].The ultrasound probe was placed near the zone of apposition of the diaphragm, typically in the 8th or 9th intercostal space, on the antero-axillary line. Thickness was measured at resting end-expiration (DT_{EE}), i.e. at functional residual capacity, and at maximal end-inspiration (DT_{EI}), i.e. at total lung capacity, from the inner part of the peritoneal layer to the inner part of the pleural layer. An average value was calculated from three separate measurements. Thickening ratio (DTR) was calculated as DT_{EI} / DT_{EE} [39] and absolute change in thickness was calculated as DT_{EI} - DT_{EE}. Thickness of the intercostal muscles was measured at resting end-expiration (IT_{EE}). Muscle echogenicity was measured by manually selecting a region of interest, using the trace method [40], in the diaphragm or intercostal muscular tissue in the images at end-expiration using custom developed software in Matlab (R2018a, Mathworks, Natick, MA, USA). Echogenicity cannot be reliably measured in a diaphragm thickness of less than 1 mm, leading to exclusion of echogenicity analysis. Three measurements were averaged to calculate the mean echogenicity in grey values. Echogenicity evaluates the muscle structure and increased echogenicity may result from fibrosis, inflammation or fatty degeneration of the muscle [41]. As the reference values of echogenicity are dependent of the ultrasound machine and its settings, standardised scores (z-scores) were calculated as the number of standard deviations from the predicted value. These predicted values were calculated using a linear regression equation including age. This linear regression was obtained from diaphragm ultrasound images from 83 healthy subjects (2-80 y/o) measured in our lab with an even distribution of males and females.

$P_{mo,tw}$ was measured to obtain a nonvolitional measurement of diaphragm function. To measure $P_{mo,tw}$ we used an automated inspiratory-pressure trigger device, as described previously [42]. The patient wore a nose clip in a seated position and breathed through a flanged mouthpiece connected to a two-way non-rebreathing valve with an inflatable balloon connected to the inspiratory port (Series 9300, Hans Rudolph Inc, Kansas City, MO, USA). Mouth pressure was recorded from a small port near the mouthpiece that was connected to a pressure transducer (MP160 equipped with DA100C and TSD160E, connected to AcqKnowledge software version 5.0.2, Biopac systems Inc. Goleta, CA, USA). Two small figure-of-eight coils (D40 Alpha Branding Iron Coil 4179-00, Magstim, Whitland, UK) were placed bilaterally on the phrenic nerves at the posterior border of the sternomastoid muscle at the level of the cricoid cartilage. The pulses were simultaneously generated by two magnetic stimulators (Magstim 200^2, Magstim, Whitland, UK). Optimal coil position and intensity were determined by varying the position of the coils and increasing the intensity. The stimulations were automatically delivered at a predetermined inspiratory pressure trigger of -5 cmH_2O to ensure an open glottis. We performed five measurements with 30 seconds in between to avoid twitch potentiation[43]. The highest value was chosen. The compound muscle action potential of the diaphragm was recorded using electrodes (MP160 equipped with BIO100C and MEC110C, connected to AcqKnowledge software version 5.0.2, Biopac systems Inc. Goleta, CA, USA) positioned at the costal margin to

check for correct stimulation of the diaphragm. $P_{mo,tw}$ values below -11 cmH_2O were considered abnormal, indicating diaphragm dysfunction [44].

We explicitly asked for the presence of respiratory symptoms and symptoms of sleep-related hypoventilation as part of the medical history. We systematically asked about exertional dyspnoea (dyspnoea when washing, dressing and/or walking), orthopnoea, and dyspnoea when bending forward. Symptoms of sleep-related hypoventilation were waking up more often in comparison with five years ago, restlessness during sleep, nightmares, morning headache, and daytime sleepiness (all at multiple days a week).

Data analysis

The data was stored in Castor EDC (Castor clinical data management platform, Amsterdam, The Netherlands) and the statistical analysis was performed using GraphPad Prism software version 5.03 (GraphPad Software, San Diego, CA, USA). Results are presented in two different categorisations: form of NM and degree of respiratory involvement. The latter is based on the presence of a restrictive lung pattern, i.e. FVC < 80% of predicted, and use of HMV.

Results are expressed as median [interquartile range (IQR)]. Kruskal-Wallis tests with Dunns post-test analysis were used to compare the groups. Chi-squared tests were used to compare categorical data. Spearman tests assessed correlation analyses. A p-value < 0.05 was considered to be statistically significant.

Results

Patients

Forty-three female patients and 21 male patients with NM were identified, of whom five patients did not fulfil the inclusion criteria because their diagnosis had not been genetically verified. Seventeen patients declined to participate because of various reasons, including the visit considered to be too strenuous or time-consuming. Forty-two patients with NM participated in this study, including ten male patients (24%; aged 25 to 74 years) and 32 female patients (76%; aged 11 to 76 years).

Form of NM and motor function

The forms of NM were either typical (n=11), mild (n=7), or childhood-onset with slowness (n=24). Walking aids were used by 12 patients and six patients were wheelchair-dependent. A total of 11 patients required HMV. Within this group, seven patients required only nocturnal non-invasive HMV, two NEB patients required daytime and nocturnal non-invasive HMV, and two ACTA1 patients required continuous invasive HMV via tracheostomy. The initial indication for HMV in these 11 patients was sleep-related hypoventilation in seven patients and daytime hypercapnia in three patients. *In one patient it was not specified other than respiratory insufficiency. Scoliosis was present in 11 patients.* Seven patients were visited at home. The patient demographics and characteristics subdivided based on NM form are displayed in Table 1.

Spirometry and respiratory muscle strength testing

Results of spirometry and respiratory muscle strength testing are presented in Table 2 and Figure 1, subdivided based on NM forms. At group level, patients with a typical form showed a lower FVC, VC, PCF, MIP, MEP and SNIP in comparison with patients with childhood-onset NM with slowness. However, a large variation in the degree of respiratory muscle involvement was observed within the three groups. All *NEB* (n=4) and *ACTA1* (n=3) patients and eight of the 19 *KBTBD13* patients had an FVC < 80% of predicted. FEV1/FVC was above 70% in all patients, thus no obstructive lung pattern was present. MIP was correlated with FVC (Figure 2A). There was a low correlation between MFM scores and FVC (Figure 2B).

Table 1: Demographics and characteristics of included patients with nemaline myopathy.

	Typical NM (n=11)	Mild NM (n=7)	Childhood-onset NM with slowness (n=24)	Total (n=42)	*p*-value
Genotype (n)					
NEB	3	2	-	5	
ACTA1	4	1	-	5	
TPM2	1	1	-	2	
TPM3	1	-	-	1	
RYR1	-	2	-	2	
CFL2	1	-	-	1	
LMOD3	1	-	-	1	
MYPN	-	1	-	1	
KBTBD13	-	-	24	24	
Female (n (%))	8 (73%)	5 (71%)	19 (79%)	32 (76%)	ns
Age (years)	21 [18.0-47.0]	63 [28.0-67.0]	49 [31.0-56.8]	40 [26.5-58.3]	ns
BMI (kg/m^2)	20.6 [16.6-24.0]*	22.8 [19.4-37.6]	24.7 [23.5-27.2]	24.0 [20.6-26.7]	0.01
MFM (%)	55.0 [49.0-94.0]*	88.0 [72.0-93.0]	90.5 [83.5-95.3]	88.5[66.0-93.3]	0.02
Ambulation (n)					
Unaided	2	3	19	24	
Walking aids (including intermittent wheelchair use)	3	4	5	12	
Wheelchair-dependent	6	-	-	6	
Mechanical ventilation(n)					
None	2	5	24	31	
Nocturnal non-invasive	6	1	-	7	
Nocturnal and daytime non-invasive	1	1	-	2	
Invasive	2	-	-	2	
Scoliosis (n)					
No	5	5	21	31	
Yes	6	2	3	11	

The data are categorised on the form of NM of the patients. NM form is classified according to Laitila et al., 2021 [1]. Data are presented as median [IQR]. *Significant difference in comparison with childhood-onset NM with slowness. NM: nemaline myopathy. BMI: body mass index. MFM: Motor Function Measure. IQR: interquartile range.

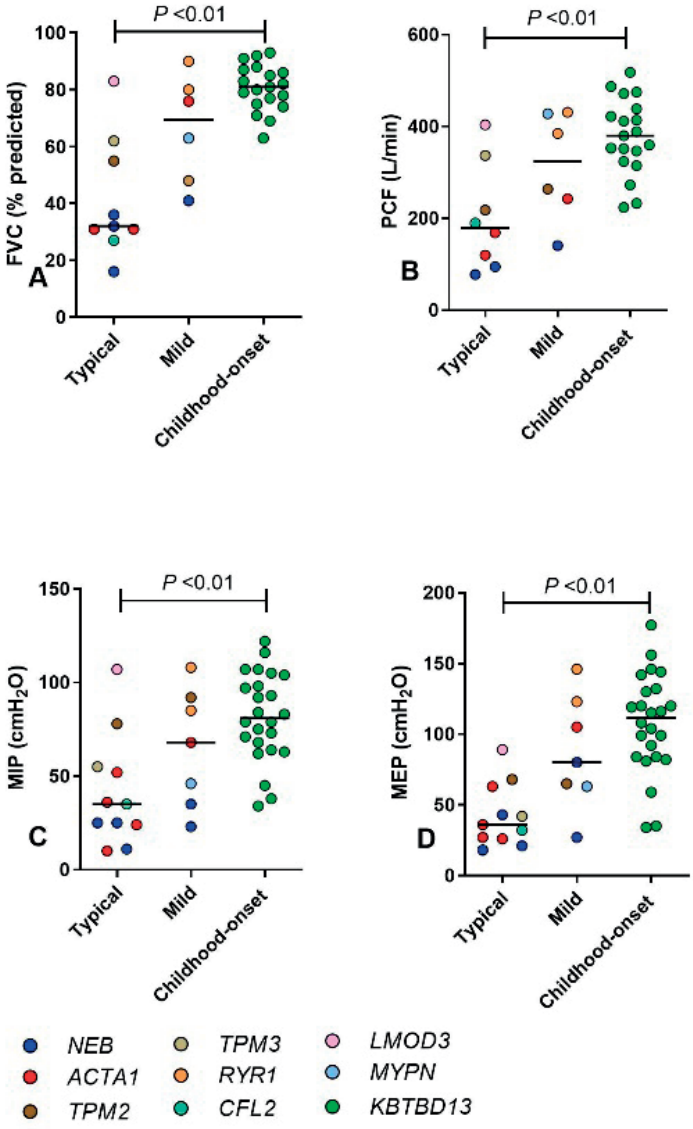


Figure 1: FVC (A), PCF (B), MIP (C) and MEP (D) in patients with a typical, mild or childhood-onset NM with slowness form. The genotypes are represented by different colours and the horizontal bars represent the median. Significant differences are indicated by ***p***-values of the Dunns post-test. FVC: forced vital capacity. PCF: peak cough flow. MIP: maximal inspiratory pressure. MEP: maximal expiratory pressure. NM: nemaline myopathy.

,

Table 2: Spirometry, respiratory muscle strength tests, diaphragm and intercostal muscle ultrasound, and twitch mouth pressure results in patients with a typical, mild, or a childhood-onset NM with slowness form.

	Typical NM (n=11)	Mild NM (n=7)	Childhood-onset NM with slowness (n=24)	Total (n=42)	*p*-value
Spirometry					
FVC (L)	1.1 [1.0-2.3]*	2.3 [1.8-2.9]	3.0 [2.8-3.5]	2.7 [2.2-3.2]	<0.01
FVC (% predicted)	32.0 [29.0-58.5]*	69.5 [46.3-82.5]	81.0 [75.0-87.0]	76.5 [53.3-83.5]	<0.01
VC (L)	1.1 [0.9-2.2]*	2.2 [1.7-2.9]	3.0 [2.8-3.6]	2.8 [2.0-3.3]	<0.01
Change VC upright and supine (%)	-9.0 [-18.8- -1.3]	-2.0 [-10.8- -0.5]	-6.0 [-9.0- -2.0]	-5.0 [-10.0- -1.5]	ns
FEV1/FVC	90.0 [82.0-95.0]	80.5 [72.5-88.8]	80.0 [78.0-88.0]	82.5 [77.8-90.0]	ns
PCF (L/min)	179.5 [101.3-307.3]*	324.5 [217.5-428.8]	380.0 [324.0-439.0]	352.0 [228.5-418.0]	0.01
Respiratory muscle testing					
MIP (cmH_2O)	35.0 [24.0-55.0]*	68.0 [35.0-92.0]	81.0 [65.0-102.5]	72.0 [37.5-94.0]	<0.01
MIP (% predicted)	50.0 [32.0-77.0]*	103.0 [42.0-122.0]	102.0 [84.3-127.0]	90.5 [49.8-116.5]	<0.01
MEP (cmH_2O)	36.0 [26.0-63.0]*	80.0 [63.0-123.0]	111.5 [84.0-131.5]	86.5 [42.8-120.0]	<0.01
MEP (% predicted)	35.0 [28.0-46.0]*	79.0 [42.0-135.0]	105.0 [87.8-122.0]	88.5 [42.0-115.0]	<0.01
SNIP(cmH_2O)	34.5 [18.8-60.3]*	55.0 [50.0-83.0]	76.0 [61.8-82.0]	68.0 [48.5-79.5]	<0.01
SNIP (% predicted)	36.0 [19.5-63.5]*	59.0 [48.0-102.0]	81.0 [72.3-94.5]	73.0 [50.5-90.0]	<0.01
Diaphragm ultrasound					
DT_{EE} (mm)	1.4 [1.1-1.7]	1.4 [1.0-2.7]	1.4 [1.1-1.7]	1.4 [1.1-1.7]	ns
DT_{EI} (mm)	2.4 [1.5-2.8]	3.5 [1.8-5.8]	2.2 [1.9-3.6]	2.3 [1.8-3.7]	ns
DT_{EI} - DT_{EE} (mm)	0.7 [0.2-1.3]	1.8 [0.8-3.2]	0.9 [0.7-1.7]	1.0 [0.6-1.8]	ns
DTR	1.5 [1.2-1.9]	2.1 [1.6-2.6]	1.7 [1.5-2.1]	1.7 [1.5-2.1]	ns
Echogenicity (z-scores)	2.4 [1.5-3.0]	0.6 [-0.2-1.9]	1.2 [0.0-1.9]	1.4 [0.0-2.3]	ns
Intercostal muscle ultrasound					
IT_{EE} (mm)	2.0 [1.8-2.2]	2.5 [1.7-3.4]	2.0 [1.7-2.6]	2.0 [1.8-2.6]	ns
Echogenicity (z-scores)	1.4 [0.8-2.6]	0.8 [-0.7-2.1]	1.6 [0.9-2.2]	1.4 [0.6-2.1]	ns
$P_{mo,tw}$ (cmH_2O)	-8.7 [-12.2--4.7]*	-10.0 [-10.1--9.3]	-15.2 [-19.3--10.9]	-13.6 [-17.8--8.8]	0.02

The spirometry and diaphragm and intercostal muscle ultrasound results are obtained from patients who visited the hospital, i.e. 10 patients with a typical, 5 patient with a mild, and 19 patients with a childhood-onset NM with slowness form. The PCF result of one patient with a typical form is missing. Three patients

were excluded from diaphragm echogenicity measurement due to a diaphragm thickness of less than 1 mm. $P_{mo,tw}$ was measured in 5, 3 and 17 adult patients, respectively. Data are presented as median [IQR]. *Significant difference in comparison to patients with childhood-onset NM with slowness. NM: nemaline myopathy. HMV: home mechanical ventilation. FVC: forced vital capacity. VC: vital capacity. FEV1: forced expiratory volume in first second. PCF: peak cough flow. MIP: maximal inspiratory pressure. MEP: maximal expiratory pressure. SNIP: sniff nasal inspiratory pressure. $DT_{EE:}$ end-expiratory diaphragm thickness. DT_{EI}: maximal end-inspiratory diaphragm thickness. DT_{EI}-DT_{EE}: absolute change in diaphragm thickness. DTR: diaphragm thickening ratio. IT_{EE}: end-expiratory intercostal muscle thickness. $P_{mo,tw}$: twitch mouth pressure. IQR: interquartile range.

To further characterise the patients, they were subdivided based on the presence of a restrictive lung pattern, i.e. an FVC of less than 80% predicted, and requirement for HMV. One *ACTA1* patient was excluded from this subdivision as spirometry could not be performed due to severe respiratory muscle weakness. MIP and MEP were decreased in patients requiring HMV compared to non-ventilated patients with FVC ≥ 80% of predicted (Table 3, Figure 3A and 3B). MEP was decreased in comparison with patients with FVC < 80% of predicted without HMV too.

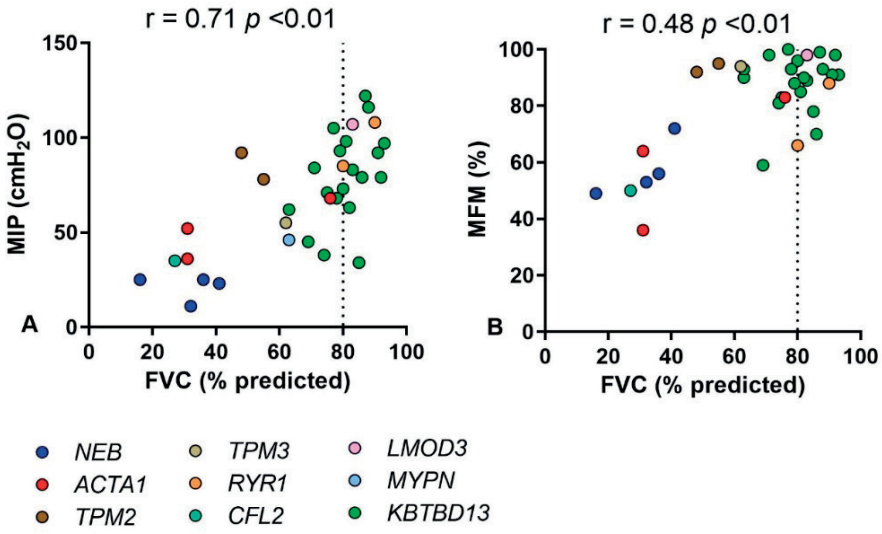


Figure 2: Correlation between MIP and FVC (A), and MFM and FVC (B). The genotypes are represented by different colours. The dotted vertical line represents the definition of restrictive lung pattern (less than 80% of predicted FVC). FVC: forced vital capacity. MIP: maximal inspiratory pressure. MFM: Motor Function Measure.

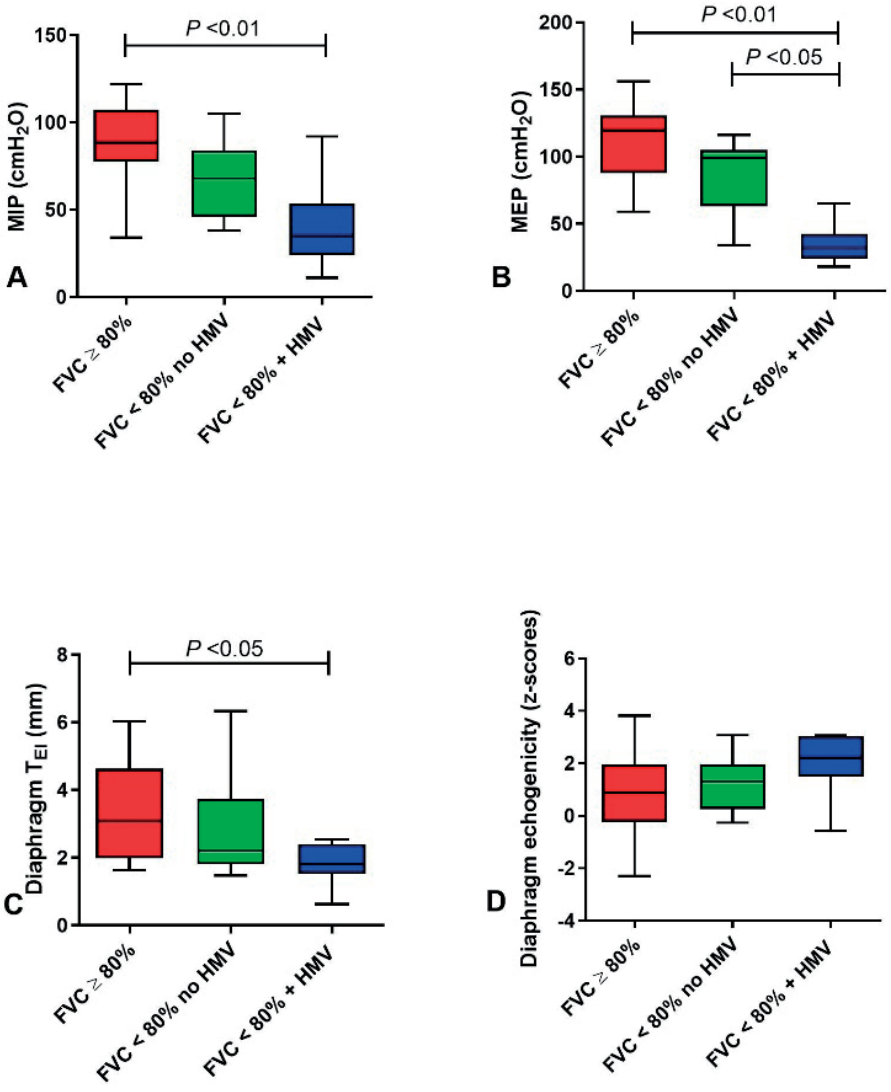


Figure 3: MIP (A), MEP (B), Diaphragm T_{EI} (C), and echogenicity of the diaphragm (D) in patients with FVC ≥ 80% predicted, FVC < 80% predicted without HMV, and FVC < 80% predicted with HMV. The horizontal bars indicate the median. Significant differences are indicated by ***p***-values of the Dunns post-test. HMV, home mechanical ventilation. FVC, forced vital capacity. MIP, maximal inspiratory pressure. MEP, maximal expiratory pressure. T_{EI}, maximal end-inspiratory thickness.

Table 3: Results from respiratory muscle strength testing, diaphragm and intercostal muscle ultrasound, twitch mouth pressure, and respiratory symptoms in patients with FVC ≥ 80% predicted, FVC < 80% predicted without HMV, and FVC < 80% predicted with HMV.

	FVC ≥80% (n=14)	FVC <80% no HMV (n=11)	FVC <80% + HMV (n=9)	*p*-value
Genotype (n)				
NEB	-	-	4	
ACTA1	-	1	2	
TPM2	-	1	1	
TPM3	-	-	1	
RYR1	2	-	-	
CFL2	-	-	1	
LMOD3	1	-	-	
MYPN	-	1	-	
KBTBD13	11	8	-	
NM form (n)				
Typical	1	2	7	
Mild	2	1	2	
Childhood-onset with slowness	11	8	-	
Female (n (%))	11 (79%)	9 (82%)	8 (89%)	ns
Age (years)	55 [39.5-59.8]	34 [28.0-58.0]	28 [18.0-60.5]	ns
BMI (kg/m^2)	26.3 [24.4-32.6]	23.7 [22.2-24.5]	19.4 [16.6-21.9]*	<0.01
MFM (%)	90.5 [83.3-96.5]	90.0 [83.0-95.0]	56.0 [49.5-82.0]*†	0.01
Respiratory muscle testing				
MIP (cmH_2O)	88.5 [77.5-107.3]	68.0 [46.0-84.0]	35.0 [24.0-53.5]*	<0.01
MIP(% predicted)	114.0 [102.3-130.8]	96.0 [55.0-103.]	50.0 [32.0-76.5]*	<0.01
MEP (cmH_2O)	119.5 [87.8-130.5]	99.0 [63.0-105.0]	32.0 [24.0-42.5]*†	<0.01
MEP(% predicted)	117.0 [84.3-132.0]	93.0 [42.0-111.0]	35.0 [23.5-43.5]*†	<0.01
SNIP (cmH_2O)	77.5 [71.3-81.5]	68.0 [55.0-83.0]	20.0 [17.0-57.0]*†	<0.01
SNIP(% predicted)	85.5 [71.5-99.0]	77.0 [52.0-95.0]	24.0 [19.0-56.5]*†	<0.01
Diaphragm ultrasound				
DT_{EE} (mm)	1.4 [1.3-2.0]	1.3 [1.0-1.7]	1.3 [1.0-1.6]	ns
DT_{EI} (mm)	3.1 [2.0-4.6]	2.2 [1.8-3.7]	1.8 [1.5-2.4]*	0.049
DT_{EI} - DT_{EE} (mm)	1.6 [0.7-2.8]	1.1 [0.7-1.9]	0.5 [0.2-1.0]*	0.02
DTR	1.9 [1.6-2.6]	1.7 [1.6-2.1]	1.4 [1.2-1.7]*	0.03
Echogenicity (z-scores)	0.9 [-0.2-2.0]	1.3 [0.3-2.0]	2.2 [1.5-3.0]	ns
Intercostal muscle ultrasound				
IT_{EE} (mm)	2.0 [1.7-3.1]	2.1 [1.3-2.6]	1.9 [1.8-2.2]	ns
Echogenicity (z-scores)	1.1 [0.5-1.7]	1.9 [0.9-2.4]	1.4 [1.0-2.6]	ns

$P_{mo,tw}$ (cmH_2O)	-14.9 [-17.3- -12.6]	-9.0 [-19.4- -8.4]	-7.9 [-10.9- -4.0]*	0.04
Respiratory symptoms (n (%))				
Exertional dyspnoea	5 (36%)	3 (27%)	6 (67%)	
Orthopnoea	0 (0%)	1 (9%)	3 (33%)	
Dyspnoea when bending forward	2 (14%)	3 (27%)	3 (33%)	
Waking up more often	6 (43%)	3 (27%)	2 (22%)	
Restlessness	4 (29%)	1 (9%)	1 (11%)	
Nightmares	0 (0%)	1 (9%)	3 (33%)	
Morning headache	3 (21%)	4 (36%)	1 (11%)	
Daytime sleepiness	6 (43%)	0 (0%)	2 (22%)	

Three patients were excluded from diaphragm echogenicity measurement due to a diaphragm thickness of less than 1 mm. $P_{mo,tw}$ was measured in 11 patients with FVC ≥ 80% predicted, 10 with FVC < 80% predicted without HMV, and 4 with FVC < 80% predicted with HMV. Data are presented as median [IQR]. *Significant in comparison to patients with FVC ≥ 80%. † Significant in comparison to patients with FVC < 80% without HMV. HMV: home mechanical ventilation. FVC: forced vital capacity. NM: nemaline myopathy. BMI: body mass index. MFM: Motor Function Measure. MIP: maximal inspiratory pressure. MEP: maximal expiratory pressure. SNIP: sniff nasal inspiratory pressure. DT_{EE}: end-expiratory diaphragm thickness. DT_{EI}: maximal end-inspiratory diaphragm thickness. DT_{EI}-$DT_{EE,}$: absolute change in diaphragm thickness. DTR: diaphragm thickening ratio. IT_{EE}: end-expiratory intercostal muscle thickness. $P_{mo,tw}$: twitch mouth pressure. IQR: interquartile range.

Diaphragm and intercostal muscle function

At group level, there was no difference in diaphragm and intercostal muscle thickness, and echogenicity between the different forms of NM (Table 2). Due to declination and contraindications for magnetic stimulation, $P_{mo,tw}$ was measured in a selected number of adult patients (n=25). $P_{mo,tw}$ was decreased in typical NM in comparison with childhood-onset NM with slowness. In Table 3, results of diaphragm and intercostal muscle measurements are shown in patients with and without restrictive lung pattern and HMV. There was no difference in DT_{EE} between groups, but DT_{EI}, absolute change in thickness, and DTR in patients requiring HMV were lower in comparison with patients with FVC ≥ 80% predicted (Figure 3C). IT_{EE} showed no difference between the groups. Three patients were excluded from diaphragm echogenicity measurement due to a diaphragm thickness of less than 1 mm. There were no differences in echogenicity of the diaphragm and intercostal muscles between patients, but the majority had a higher echogenicity than predicted, indicated by a z-score > 0 (Figure 3D). $P_{mo,tw}$ was decreased in patients requiring HMV in comparison with patients with FVC ≥ 80% predicted.

Respiratory symptoms

Table 3 shows the respiratory symptoms in groups with different degrees of respiratory muscle weakness. Complaints indicative of respiratory muscle weakness were present in all patients.

Discussion

This study showed that respiratory muscle weakness is present in a large proportion (59%) of patients with NM of all clinical forms. In contrast to previous findings, we found that respiratory muscle weakness is also present in patients with childhood-onset NM with slowness of movements. There was a low correlation between motor function and the degree of respiratory muscle weakness in our cohort, indicating that respiratory muscle function can be compromised independently of motor performance. Furthermore, we showed, using diaphragm ultrasound and twitch mouth pressure, that impaired diaphragm function is a key component of respiratory muscle weakness in NM.

Respiratory muscle function was most severely compromised in the typical form of NM. However, within the different forms a large variability was observed. This variability is partly explained by distinct differences in respiratory muscle function in relation to genotypes, but also by variation within genotypes. All patients with *NEB* and *ACTA1* mutations included had respiratory muscle weakness and most of these patients required non-invasive or invasive HMV, which is in accordance with previous studies [45, 46]. In contrast, respiratory muscle function varied widely in the patients with *TPM2, TPM3, RYR1, CFL2, LMOD3,* and *MYPN* mutations. The adult *RYR1* patients and the adult *LMOD3* patient had no respiratory muscle weakness. These findings stand out from previously described patients with severe or typical NM forms with respiratory insufficiency [3, 5, 6], which adds to the variability of the clinical spectrum of these genotypes. Another contrasting finding is that the included *TPM2* patients showed respiratory muscle weakness with a high MFM score, while mildly affected patients with mutations in this gene usually do not have respiratory muscle weakness [14]. Interestingly, we found mild respiratory muscle weakness in eight of the 24 patients with the childhood-onset with slowness form caused by a mutation in the *KBTBD13* gene, which has not been observed in previous cohort studies [20, 30, 31]. However, respiratory function tests were not systematically performed in these studies. A case report assessing FVC in a patient with a mutation in the *KBTBD13* gene did find respiratory muscle weakness [47]. Overall, the variability in respiratory muscle weakness between different NM forms and genotypes in our cohort emphasises the need for regular screening of respiratory muscle function in all patients with NM.

Importantly, we found a low correlation between motor function and spirometry. This may partly be explained by a known ceiling effect of the MFM in mildly affected patients [48]. However, 20 patients with high MFM scores (90% or more) showed a broad range of FVC values (48-93% predicted). Moreover, two *NEB* patients and one *ACTA1* patient with respiratory involvement in our study had a mild form of NM. This confirms the clinical observation that the degree of motor function impairment is not representative for respiratory muscle function in all patients with NM, as shown previously in case reports [49-51]. The low correlation could also be caused by the heterogeneity in genotypes. For example, the *TPM2* patients stand out with a high MFM

score and a decreased FVC. Moreover, the correlation is influenced by a large group of mildly affected *KBTBD13* patients. We cannot exclude that there is a stronger correlation between motor function and spirometry in specific genotypes or clinical forms of NM. The monocentric nature of our study and consequently the relatively low number of patients per genotype or clinical form of NM limits these subgroup analyses.

Diaphragm and intercostal muscle thickness and echogenicity did not differ between the different forms of NM. However, echogenicity of these respiratory muscles was higher than their predicted normal value in most patients. This finding is in line with a previous study which found high muscle echogenicity in peripheral muscles in NM caused by fatty degeneration [52]. A possible explanation for the lack of difference between the forms of NM might be that structural changes in the respiratory muscles precede changes in pulmonary function. In patients receiving HMV impaired diaphragm function is a key component of impaired respiratory function, shown by a decreased diaphragm thickness (end-inspiration) and a decreased $P_{mo,tw}$. In line with these results, previous post-mortem studies in cases with severe respiratory insufficency have found a high concentration of nemaline rods in the diaphragm, indicating an important role of diaphragm involvement [53, 54]. Whether respiratory muscle ultrasound is suitable as an outcome measure for respiratory function in NM patients should be evaluated in future studies.

All patients reported respiratory symptoms regardless of the degree of respiratory muscle weakness. Thus, in our study respiratory symptoms were not indicative of the severity of respiratory muscle weakness.

This study has several limitations. First, the number of patients for each form of NM, except childhood-onset NM with slowness, was limited. Second, genetically unresolved cases were not included. Third, no patients with severe NM were included. This led to a bias towards less severely affected patients. Fourth, there was a female predominance, which cannot be explained by a selection bias. This predominance of female patients was not reported in other studies [24, 29]. Hence, because of this coincidence, these data are more representative for female patients. Last, we were unable to perform a quantitative analysis on the reported respiratory symptoms, as we did not use a validated questionnaire.

Given that respiratory muscle weakness is an important feature in all forms of NM, future longitudinal studies and clinical trials should evaluate respiratory muscle function as well as general motor function. Longitudinal studies will be able to determine the intervals needed for respiratory monitoring by assessing the progression of respiratory muscle weakness. Relevant outcome measures for a longitudinal study of nemaline myopathy, including respiratory outcomes, have also been discussed [55]. Furthermore, these studies should also focus on which measurements and corresponding cut-off values can predict the need for HMV. Interestingly,

diaphragm ultrasound has recently been shown as a novel predictor of nocturnal hypercapnia in slowly progressive myopathies [56].

In conclusion, respiratory muscle weakness in NM is present in all clinical forms and genotypes, and may be present irrespective of the degree of motor function impairment. Diaphragm dysfunction was identified as an important contributor to respiratory muscle weakness. In contrast to previous findings, we also found respiratory muscles weakness in patients with childhood-onset NM with slowness of movements. Therefore, screening of respiratory function is important to guide respiratory management in all patients with NM.

References

1. Laitila, J. and C. Wallgren-Pettersson, *Recent advances in nemaline myopathy.* Neuromuscul Disord, 2021. 31(10): p. 955-967.
2. Sewry, C.A., J.M. Laitila, and C. Wallgren-Pettersson, *Nemaline myopathies: a current view.* J Muscle Res Cell Motil, 2019. 40(2): p. 111-126.
3. Yuen, M., et al., *Leiomodin-3 dysfunction results in thin filament disorganization and nemaline myopathy.* J Clin Invest, 2014. 124(11): p. 4693-708.
4. Sambuughin, N., et al., *Dominant mutations in KBTBD13, a member of the BTB/Kelch family, cause nemaline myopathy with cores.* Am J Hum Genet, 2010. 87(6): p. 842-7.
5. Hernandez-Lain, A., et al., *De novo RYR1 heterozygous mutation (I4898T) causing lethal core-rod myopathy in twins.* Eur J Med Genet, 2011. 54(1): p. 29-33.
6. Kondo, E., et al., *Recessive RYR1 mutations in a patient with severe congenital nemaline myopathy with ophthalomoplegia identified through massively parallel sequencing.* Am J Med Genet A, 2012. 158a(4): p. 772-8.
7. Gupta, V.A., et al., *Identification of KLHL41 Mutations Implicates BTB-Kelch-Mediated Ubiquitination as an Alternate Pathway to Myofibrillar Disruption in Nemaline Myopathy.* Am J Hum Genet, 2013. 93(6): p. 1108-17.
8. Ravenscroft, G., et al., *Mutations in KLHL40 are a frequent cause of severe autosomal-recessive nemaline myopathy.* Am J Hum Genet, 2013. 93(1): p. 6-18.
9. Miyatake, S., et al., *Biallelic Mutations in MYPN, Encoding Myopalladin, Are Associated with Childhood-Onset, Slowly Progressive Nemaline Myopathy.* Am J Hum Genet, 2017. 100(1): p. 169-178.
10. Nilipour, Y., et al., *Ryanodine receptor type 3 (RYR3) as a novel gene associated with a myopathy with nemaline bodies.* Eur J Neurol, 2018. 25(6): p. 841-847.
11. Sandaradura, S.A., et al., *Nemaline myopathy and distal arthrogryposis associated with an autosomal recessive TNNT3 splice variant.* Hum Mutat, 2018. 39(3): p. 383-388.
12. Agrawal, P.B., et al., *Nemaline myopathy with minicores caused by mutation of the CFL2 gene encoding the skeletal muscle actin-binding protein, cofilin-2.* Am J Hum Genet, 2007. 80(1): p. 162-7.
13. Kiphuth, I.C., et al., *Autosomal dominant nemaline myopathy caused by a novel alpha-tropomyosin 3 mutation.* J Neurol, 2010. 257(4): p. 658-60.
14. Davidson, A.E., et al., *Novel deletion of lysine 7 expands the clinical, histopathological and genetic spectrum of TPM2-related myopathies.* Brain, 2013. 136(Pt 2): p. 508-21.
15. Pelin, K., et al., *Refined localisation of the genes for nebulin and titin on chromosome 2q allows the assignment of nebulin as a candidate gene for autosomal recessive nemaline myopathy.* Eur J Hum Genet, 1997. 5(4): p. 229-34.
16. Johnston, J.J., et al., *A novel nemaline myopathy in the Amish caused by a mutation in troponin T1.* Am J Hum Genet, 2000. 67(4): p. 814-21.
17. Nowak, K.J., et al., *Mutations in the skeletal muscle alpha-actin gene in patients with actin myopathy and nemaline myopathy.* Nat Genet, 1999. 23(2): p. 208-12.

18. Pauw-Gommans, I.M., et al., *Muscle slowness in a family with nemaline myopathy.* Neuromuscul Disord, 2006. 16(8): p. 477-80.
19. Gommans, I.M., et al., *A locus on chromosome 15q for a dominantly inherited nemaline myopathy with core-like lesions.* Brain, 2003. 126(Pt 7): p. 1545-51.
20. Gommans, I.M., et al., *A new phenotype of autosomal dominant nemaline myopathy.* Neuromuscul Disord, 2002. 12(1): p. 13-8.
21. de Winter, J.M., et al., *KBTBD13 is an actin-binding protein that modulates muscle kinetics.* J Clin Invest, 2020. 130(2): p. 754-767.
22. Wallgren-Pettersson, C., et al., *Nemaline myopathies.* Semin Pediatr Neurol, 2011. 18(4): p. 230-8.
23. Smith, B.K., et al., *Inspiratory muscle training in a child with nemaline myopathy and organ transplantation.* Pediatr Crit Care Med, 2011. 12(2): p. e94-8.
24. Ryan, M.M., et al., *Nemaline myopathy: a clinical study of 143 cases.* Ann Neurol, 2001. 50(3): p. 312-20.
25. Yin, X., et al., *Clinical and pathological features of patients with nemaline myopathy.* Mol Med Rep, 2014. 10(1): p. 175-82.
26. Yin, X., et al., *Clinico-pathological features and mutational spectrum of 16 nemaline myopathy patients from a Chinese neuromuscular center.* Acta Neurol Belg, 2021.
27. Wang, Q., et al., *Mutational and clinical spectrum in a cohort of Chinese patients with hereditary nemaline myopathy.* Clin Genet, 2020. 97(6): p. 878-889.
28. Nagata, R., et al., *A case of nemaline myopathy with associated dilated cardiomyopathy and respiratory failure.* Int Heart J, 2011. 52(6): p. 401-5.
29. Amburgey, K., et al., *A Cross-Sectional Study of Nemaline Myopathy.* Neurology, 2021. 96(10): p. e1425-e1436.
30. Kang, Z.X., et al., *A family with nemaline myopathy type 6 caused by hseterozygous mutation (c.1222C>T) in the KBTBD13 gene in China: A case report.* Neuropathology, 2020. 40(1): p. 104-108.
31. Olivé, M., et al., *Nemaline myopathy type 6: clinical and myopathological features.* Muscle Nerve, 2010. 42(6): p. 901-7.
32. Côté, P., et al., *A study of the diagnostic accuracy and reliability of the Scoliometer and Adam's forward bend test.* Spine (Phila Pa 1976), 1998. 23(7): p. 796-802; discussion 803.
33. Quanjer, P.H., et al., *Multi-ethnic reference values for spirometry for the 3-95-yr age range: the global lung function 2012 equations.* Eur Respir J, 2012. 40(6): p. 1324-43.
34. Wilson, S.H., et al., *Predicted normal values for maximal respiratory pressures in caucasian adults and children.* Thorax, 1984. 39(7): p. 535-8.
35. Uldry, C. and J.W. Fitting, *Maximal values of sniff nasal inspiratory pressure in healthy subjects.* Thorax, 1995. 50(4): p. 371-5.
36. Laveneziana, P., et al., *ERS statement on respiratory muscle testing at rest and during exercise.* Eur Respir J, 2019. 53(6).
37. Graham, B.L., et al., *Standardization of Spirometry 2019 Update. An Official American Thoracic Society and European Respiratory Society Technical Statement.* Am J Respir Crit Care Med, 2019. 200(8): p. e70-e88.
38. American Thoracic Society/European Respiratory, S., *ATS/ERS Statement on respiratory muscle testing.* Am J Respir Crit Care Med, 2002. 166(4): p. 518-624.

39. Boon, A.J., et al., *Two-dimensional ultrasound imaging of the diaphragm: quantitative values in normal subjects.* Muscle Nerve, 2013. 47(6): p. 884-9.
40. Sarwal, A., et al., *Interobserver Reliability of Quantitative Muscle Sonographic Analysis in the Critically Ill Population.* J Ultrasound Med, 2015. 34(7): p. 1191-200.
41. Pillen, S., I.M. Arts, and M.J. Zwarts, *Muscle ultrasound in neuromuscular disorders.* Muscle Nerve, 2008. 37(6): p. 679-93.
42. Santos, D.B., et al., *Twitch mouth pressure for detecting respiratory muscle weakness in suspicion of neuromuscular disorder.* Neuromuscul Disord, 2017. 27(6): p. 518-525.
43. Wragg, S., et al., *Potentiation of diaphragmatic twitch after voluntary contraction in normal subjects.* Thorax, 1994. 49(12): p. 1234-7.
44. Laghi, F. and M.J. Tobin, *Relationship between transdiaphragmatic and mouth twitch pressures at functional residual capacity.* Eur Respir J, 1997. 10(3): p. 530-6.
45. Moreno, C.A.M., et al., *Clinical and Histologic Findings in ACTA1-Related Nemaline Myopathy: Case Series and Review of the Literature.* Pediatr Neurol, 2017. 75: p. 11-16.
46. Piga, D., et al., *New Mutations in NEB Gene Discovered by Targeted Next-Generation Sequencing in Nemaline Myopathy Italian Patients.* J Mol Neurosci, 2016. 59(3): p. 351-9.
47. Garibaldi, M., et al., *Core-rod myopathy due to a novel mutation in BTB/POZ domain of KBTBD13 manifesting as late onset LGMD.* Acta Neuropathol Commun, 2018. 6(1): p. 94.
48. Mul, K., et al., *Rasch analysis to evaluate the motor function measure for patients with facioscapulohumeral muscular dystrophy.* Int J Rehabil Res, 2021. 44(1): p. 38-44.
49. Befort, P., et al., *[Adult onset nemaline myopathy revealed by respiratory insufficiency].* Rev Neurol (Paris), 2006. 162(12): p. 1260-2.
50. Kelly, E., M.A. Farrell, and N.G. McElvaney, *Adult-onset nemaline myopathy presenting as respiratory failure.* Respir Care, 2008. 53(11): p. 1490-4.
51. Whitaker, J., et al., *Idiopathic adult-onset nemaline myopathy presenting with isolated respiratory failure.* Muscle Nerve, 2009. 39(3): p. 406-8.
52. Wallgren-Pettersson, C., et al., *Ultrasonography, CT, and MRI of muscles in congenital nemaline myopathy.* Pediatr Neurol, 1990. 6(1): p. 20-8.
53. Shafiq, S.A., et al., *Nemaline myopathy: report of a fatal case, with histochemical and electron microscopic studies.* Brain, 1967. 90(4): p. 817-28.
54. Tsujihata, M., et al., *Fatal neonatal nemaline myopathy: a case report.* J Neurol Neurosurg Psychiatry, 1983. 46(9): p. 856-9.
55. Neuhaus, S.B., et al., *250th ENMC International Workshop: Clinical trial readiness in nemaline myopathy 6-8 September 2019, Hoofdorp, the Netherlands.* Neuromuscul Disord, 2020. 30(10): p. 866-875.
56. Spiesshoefer, J., et al., *Respiratory Muscle Function Tests and Diaphragm Ultrasound Predict Nocturnal Hypoventilation in Slowly Progressive Myopathies.* Front Neurol, 2021. 12: p. 731865.



Chapter 4

Respiratory function in LAMA2-related muscular dystrophy and SELENON-related congenital myopathy, a 1.5-year natural history study

Karlijn Bouman
Jeroen LM van Doorn
Jan T Groothuis
Peter J Wijkstra
Baziel GM van Engelen
Corrie E Erasmus
Jonne Doorduin
Nicol C Voermans

Published in:
European Journal of Paediatric Neurology, 2024

Abstract

Introduction: LAMA2-related muscular dystrophy (LAMA2-MD) and SELENON(SEPN1)-related congenital myopathy (SELENON-RM) are rare neuromuscular diseases with respiratory impairment from a young age. Prospective natural history studies are needed for prevalence estimations, respiratory characterization, optimizing clinical care and selecting outcome measures for trial readiness.

Methods: Our prospective 1.5-year natural history study included spirometry (forced vital capacity (FVC); difference between upright and supine vital capacity (dVC)), respiratory muscle strength tests (sniff nasal inspiratory pressure (SNIP)) (age≥5 years), and diaphragm ultrasound (thickness; thickening; echogenicity; all ages).

Results: Twenty-six LAMA2-MD patients (M=8, median 21 [9; 31] years) and 11 SELENON-RM patients (M=8, 20 [10; 33] years) were included. At baseline, 17 (85%) LAMA2-MD (FVC%: 59% [33; 68]) and all SELENON-RM patients (FVC%: 34% [31; 46]) had an impaired respiratory function (FVC%<80%). Nine (35%) LAMA2-MD and eight (73%) SELENON-RM patients received mechanical ventilation at baseline, and two additional SELENON-RM patients started during follow-up. Contrarily to LAMA2-MD, SELENON-RM patients had severe diaphragm atrophy (diaphragm thickness z-score: -2.5 [-3.1; -2.1]) and dysfunction (diaphragm thickening ratio: 1.2 [1.0; 1.7]; dVC: 30% [7.7; 41]). SNIP was low in both neuromuscular diseases and correlated with motor function. In SELENON-RM, respiratory function decreased during follow-up.

Conclusion: The majority of LAMA2-MD and all SELENON-RM patients had respiratory impairment. SELENON-RM patients showed lower respiratory function which was progressive, more prevalent mechanical ventilation, and more severe diaphragm atrophy and dysfunction than LAMA2-MD patients. Spirometry (FVC%, dVC) and respiratory muscle strength tests (SNIP) are useful in clinical care and as outcome measure in clinical trials.

Introduction

LAMA2-related muscular dystrophy (LAMA2-MD) and SELENON(SEPN1)-related congenital myopathy (SELENON-RM) are rare neuromuscular diseases with remarkable similarities in clinical phenotype. They are characterized by slowly progressive axial and proximal muscle weakness, respiratory impairment, early-onset spinal rigidity, scoliosis and low bone quality [1-6]. LAMA2-MD and SELENON-RM are caused by pathologic variants in the *LAMA2* and *SELENON* (*SEPN1*) genes, coding for the laminin alpha2 subunit and selenoprotein N, respectively [7, 8]. No curative therapies exist but promising preclinical trials are ongoing. These expected trials emphasize the need to reach trial readiness [9-14]. In order to optimize physical condition and to prevent or treat severe complications, patients receive rehabilitation, respiratory care, orthopedic management and nutritional guidance [15, 16].

Life expectancy is not well documented, but death as early as the first decade has been described in LAMA2-MD and SELENON-RM patients that are severely affected [1, 2, 17]. Respiratory impairment is both in LAMA2-MD and SELENON-RM the leading cause of morbidity and mortality, which makes it a topic of high importance for clinical care and an essential outcome measure for future clinical trials [3]. In LAMA2-MD patients, non-invasive mechanical ventilation is mostly needed in severely affected patients. Respiratory impairment follows a restrictive pattern similar to most other neuromuscular diseases with respiratory involvement [17]. Intercostal muscle weakness, decreased compliance of the chest wall and thoracic deformities related to scoliosis are mainly recognized as the underlying cause of respiratory impairment in LAMA2-MD [3]. Despite that the diaphragm is the most important respiratory muscle, its function has not been well-documented in LAMA2-MD, although it has been hypothesized that diaphragm function is relatively spared [3, 18]. In SELENON-RM, respiratory involvement is strikingly disproportionate to limb weakness: most patients require mechanical ventilation, mainly nocturnal non-invasive mechanical ventilation, while still being ambulant [1]. Weakness of inspiratory and expiratory muscles, scoliosis and thoracic deformities contribute to respiratory failure [1]. Additionally, based on transdiaphragmatic pressure measurements it has been hypothesized that diaphragm weakness plays an important role in the underlying pathophysiology of respiratory impairment [19].

In both LAMA2-MD and SELENON-RM, prevalence estimations on respiratory impairment and mechanical ventilation, and respiratory characterization are lacking. In SELENON-RM, prospective natural history data are also absent. Further, diaphragm ultrasound, which is increasingly used in the diagnosis of diaphragm dysfunction, combined with diaphragm function assessments are missing [20, 21]. The role of the diaphragm in the pathophysiology of respiratory impairment in LAMA2-MD and SELENON-RM is thus not well understood. Moreover, apart from general congenital muscular dystrophy and congenital myopathy guidelines, no disease-specific recommendations on respiratory care and on the selection of outcome measures for clinical

trials in LAMA2-MD and SELENON-RM exist. Finally, correlations between respiratory function, respiratory muscle strength, age and motor function are underreported in the literature. Here we present a prospective 1.5-year natural history study on respiratory involvement in patients with LAMA2-MD and SELENON-RM that aims to fill in these knowledge gaps.

LAMA2-MD and SELENON-RM are jointly discussed in this manuscript since they are both ultrarare and have remarkable similarities in clinical phenotype. Consequently, LAMA2-MD and SELENON-RM fit in the same natural history study protocol and we aimed to use the efficiency of a *basket natural history study* [22]. We expected to learn from differences between these neuromuscular diseases. Moreover, promising new therapies are being developed and there is a high need for trial readiness in both neuromuscular diseases.

Methods

Study design and population

Patients were recruited non-selectively and consecutively in the period from August 2020 to May 2022 as part of the LAST STRONG Study, a 1.5-year prospective natural history study in patients with LAMA2-MD or SELENON-RM. An elaborate description of the protocol can be found elsewhere [23]. We aimed to reach all Dutch-speaking patients in the Netherlands and Flanders. All patients and/or their legal representatives provided informed consent prior to their inclusion in the study and procedures were performed in accordance with the ethical standards laid down in the declaration of Helsinki. Inclusion criteria were a genetic confirmation of LAMA2-MD or SELENON-RM by two recessive (likely) pathologic variants in the *LAMA2* or *SELENON* (*SEPN1*) gene following the American College of Medical Genetics and Genomics (ACMG) guidelines, or typical clinical and histological alterations combined with genetic confirmation in a first degree relative [24]. Exclusion criteria were an insufficient understanding of the Dutch language.

All patients were invited for four visits within 1.5 year (every six months). The protocol included a standardized medical history examination, spirometry, respiratory muscle strength tests and ultrasound of the diaphragm and intercostal muscles. Further, patients underwent an X-ray of the spine at baseline and after one year follow-up. In case patients did not wish or were not able to visit our hospital, they were offered to participate through home visits with only medical history examination and respiratory muscle strength tests.

Clinical features

Demographic data were systematically collected from all patients. Motor function was assessed through the motor function measurement 20/32 (MFM-20/32). Ambulation was defined as being able to walk 10 meters without support. Rigid spine was defined by a decreased flexibility in the neck or lower back. Patients were asked for respiratory symptoms and the use of

mechanical ventilation (none, nocturnal non-invasive, nocturnal and daytime non-invasive or invasive mechanical ventilation).

Spirometry and respiratory muscle strength tests

All patients (age ≥5 years) that visited our hospital performed spirometry with a handheld spirometer (SpiroUSB, Vyaire Medical connected to PC Spirometry software, Spida CareFusion 2.3.0.10 for Windows 7). Forced vital capacity (FVC) and forced expiratory volume in the first second (FEV1) in sitting position were measured, compared with reference values and expressed as percentage predicted (FVC% and FEV%, respectively) [25]. Restrictive pulmonary function was defined as FVC <80% [**Chapter 3**]. Peak cough flow (PCF) was assessed in the sitting position and was considered abnormal if <270 l/min [26]. Further, vital capacity (VC) was assessed both in the sitting and supine position, and percentage decrease in VC between the sitting and supine position was calculated according to the following equation: dVC% = (VCupright – VCsupine)/ VCupright and was considered abnormal if >10% [18]. Respiratory muscle strength tests included maximum inspiratory pressure (PImax), maximum expiratory pressure (PEmax) and sniff nasal inspiratory pressure (SNIP). PImax, PEmax and SNIP were performed in the upright position with a handheld electronic manometer (Micro RPM, Micro Medical, CareFusion, United Kingdom) in all patients (age ≥5 years), and were expressed as absolute values. Both spirometry and respiratory muscle strength tests were performed in accordance with the American Thoracic Society/European Respiratory Society (ATS/ERS) statement on respiratory muscle testing [20, 21, 27]. We used a breathing mask instead of a standard mouth piece in case of macroglossia, insufficient closure of the mouth or in the presence of any other factors that might cause air leakage during spirometry or respiratory muscle strength tests.

Ultrasound of the diaphragm and intercostal muscles

Ultrasound of the diaphragm was performed in the supine position in all visits using an Esaote MyLab Twice ultrasound machine (Esaote SpA, Genoa, Italy) equipped with a 3-13 MHz LA533 linear transducer (Esaote SpA, Genoa, Italy) according to previously described methodology [**Chapter 5**]. In short, diaphragm thickness and thickening were assessed bilaterally in the supine position. The ultrasound probe was placed at the zone of apposition of the diaphragm, typically at the antero-axillary line in the 8th or 9th intercostal space. Thickness was measured at resting end-expiration (DTee), and at maximal end-inspiration (DTei), from the superficial part of the peritoneal layer to the deep part of the pleural layer. A non-identifiable diaphragm was defined as DTee <0.1 mm. Standardized scores (z-scores) of DTee were calculated as the number of standard deviations from the predicted value and were considered abnormal if <-2. Diaphragm thickening ratio (DTR) was calculated as DTei/DTee and was considered abnormal if <1.6 [**Chapter 5**].

Echogenicity of the diaphragm was measured at end-expiration by calculating the mean grayscale level within a manually selected region of interest in three ultrasound images using an

in-house developed software package in MATLAB (version 2013b, Mathworks, Natick, MA, USA) [23]. Standardized scores (z-scores) were calculated as the number of standard deviations from the predicted value and were considered abnormal if >2. In case DTee was <1 mm, echogenicity of the diaphragm could not be reliably measured and was thus excluded for further analysis.

Thickness of the parasternal intercostal muscles was measured 2-3 cm lateral to the sternum in the second or third intercostal space at resting end-expiration (ITee) from the superficial part of the pleural layer to the deep part of the pectoralis major fascia at all visits.

X-ray of the spine

The presence of scoliosis was assessed by X-ray of the spine at baseline and after 12 months, at the 3rd visit, and was dichotomized as present (Cobb Angle ≥10 degrees) or absent. The X-ray of the spine was performed in the sitting position, or in the lying position in case a patient was not able to main the sitting position, and the position was held constant between two consecutive X-rays. Scoliosis was subsequently subdivided into mild (Cobb's angle 10-20 degrees), moderate (Cobb's angle 21-40 degrees) and severe (Cobb's angle >40 degrees), and was classified independent of the presence of scoliosis surgery material [28]. In case only one X-ray was performed (i.e. death, loss from follow-up, practical difficulties), the Cobb's angle measured on this X-ray was used throughout the study.

Data analysis and statistical methods

Descriptive statistics were used to summarize data in IBM SPSS Statistics 25.0.0.1 for Windows (SPSS, Inc., Chicago, IL). Values are median [interquartile range (IQR)], unless otherwise stated. A Wilcoxon signed-rank test was used to compare DTee, DTR and echogenicity between right and left side. In absence of left-to-right differences, the overall DTee, DTR and diaphragm echogenicity in each patient were calculated by averaging the right and left side. The Friedman test was used to test if outcomes changed during 1.5-year follow-up. Spearman's correlation was used to assess correlations between age and MFM-20/32, and respiratory function and respiratory muscle strength tests. The correlation coefficient was considered moderate (r = 0.40–0.59), strong (r = 0.60–0.80), or very strong (r = 0.80–1.0). A p-value <0.05 was considered statistically significant.

Results

Patient characteristics

Twenty-six LAMA2-MD patients (8 males, 18 females) with a median age of 21 [9; 31] (range 3-50) years and a median MFM-20/32 score of 32% [18; 70] were included. Eight (31%) patients were ambulant at the time of the inclusion. Nine patients (33%) had ever reached ambulatory status in their life, i.e. had a limb-girdle muscular dystrophy (LGMD) phenotype, while the remaining patients (66%) had never reached ambulatory status, i.e. had a congenital muscular dystrophy phenotype. All LAMA2-MD patients had a rigid spine. Four patients (three female, one male) did not have the full follow-up due to cardiorespiratory arrest (two hospital visits), burden of participation (one hospital visit, two home visits), personal circumstances (three home visits) and late inclusion (one hospital visit). Eleven SELENON-RM patients (8 males, 3 females) with a median age of 20 [10; 33] (range 3-42) years and a median MFM-20/32 score of 76% [55; 82] participated in this study. Nine (82%) SELENON-RM patients were ambulant. All SELENON-RM patients had a rigid spine. One patient that participated through a home visit (male, 39 years) was lost from follow-up after the first visit due to the burden of participating in this study. Key clinical characteristics can be found in Table 1. A more detailed overview on the clinical features has been previously described [5, 6].

Medical history

LAMA2-MD

At baseline and at follow-up eight (31%) LAMA2-MD patients had non-invasive nocturnal mechanical ventilation and one (3.8%) (male, 21 years) had continuous invasive mechanical ventilation. Nine (35%) patients had respiratory infections before they participated in our study, mostly at paediatric age, of whom eight required admission to the hospital for temporary additional non-invasive or invasive mechanical ventilation and antibiotics. One patient (female, 13 years) needed temporary support from an extracorporeal membrane oxygenation (ECMO) machine after infection with respiratory syncytial virus at pre-school age. During the follow-up period of this study, two (7.7%) patients (female, 3 years; male, 22 years) had several admissions to the intensive care due to bacterial and viral respiratory infections. None of the patients that reported to have been infected with SARS-CoV-2 needed additional treatments or hospital admission (vaccination coverage unknown). At baseline three (12%) patients indicated to suffer from dyspnoea at some moment during a regular day: one patient (male, 22 years) with continuous mechanical ventilation when doing tasks that need invasive mechanical concentration while sitting upright in the chair, and two patients (male, 27 and 23 years) with nocturnal non-ventilation while taking a rest in the supine position. After 1.5-year follow-up, two additional patients indicated dyspnea: one patient (female, 11 years) without mechanical ventilation while walking and one patient (female, 14 years) with nocturnal non-invasive mechanical ventilation while wearing a cloth face mask in the upright position.

Table 1: Demographic characteristics of patients with LAMA2-MD and SELENON-RM.

Demographics	Baseline	After 1,5 year
LAMA2-MD		
Number of patients	26	22
Age at examination (years)	21 [9; 31]	20 [10; 33]
Males (%)	8 (31%)	8 (35%)
(non-)invasive mechanical ventilation	9 (35%)	7 (32%)
BMI – adult (kg/m^2)	21 [18; 24]	21 [18; 25]
BMI – child (kg/m^2)	17 [16; 22]	20 [15; 21]
Number of ambulant patients	8 (31%)	8 (35%)
MFM-20/32 total score (%)	32 [18; 70]	44 [14; 72]
MFM-20/32 D1	3 [2; 45]	10 [0; 44]
MFM-20/32 D2	36 [10; 81]	53 [10; 83]
MFM-20/32 D3	81 [57; 95]	88 [48; 96]
SELENON-RM		
Number of patients	11	10
Age at examination (years)	16 [9; 31]	16 [11; 28]
Males (%)	8 (73%)	7 (70%)
(non-)invasive mechanical ventilation	8 (73%)	9 (90%)
BMI – adult (kg/m^2)	23 [20; 25]	23 [21; 26]
BMI – child (kg/m^2)	15 [14; 20]	15 [13; 21]
Number of ambulant patients	9 (82%)	8 (80%)
MFM-20/32 total score	76 [55; 82]	71 [59; 81]
MFM-20/32 D1	59 [21; 63]	50 [23; 66]
MFM-20/32 D2	83 [69; 86]	81 [76; 85]
MFM-20/32 D3	95 [95; 95]	95 [95; 100]

LAMA2-MD: LAMA2-related muscular dystrophy. SELENON-RM: SELENON-related congenital myopathy. BMI: body mass index. MFM-20/32: motor function measurement 20/32. MFM-20/32 D1: motor function measurement 20/32 domain 1, standing and transfers. MFM-20/32 D2: motor function measurement 20/32 domain 2, axial and proximal motor function. MFM-20/32 D3: motor function measurement 20/32 domain 3, distal motor function. Data is presented as median [p25; p75] or as n (%).

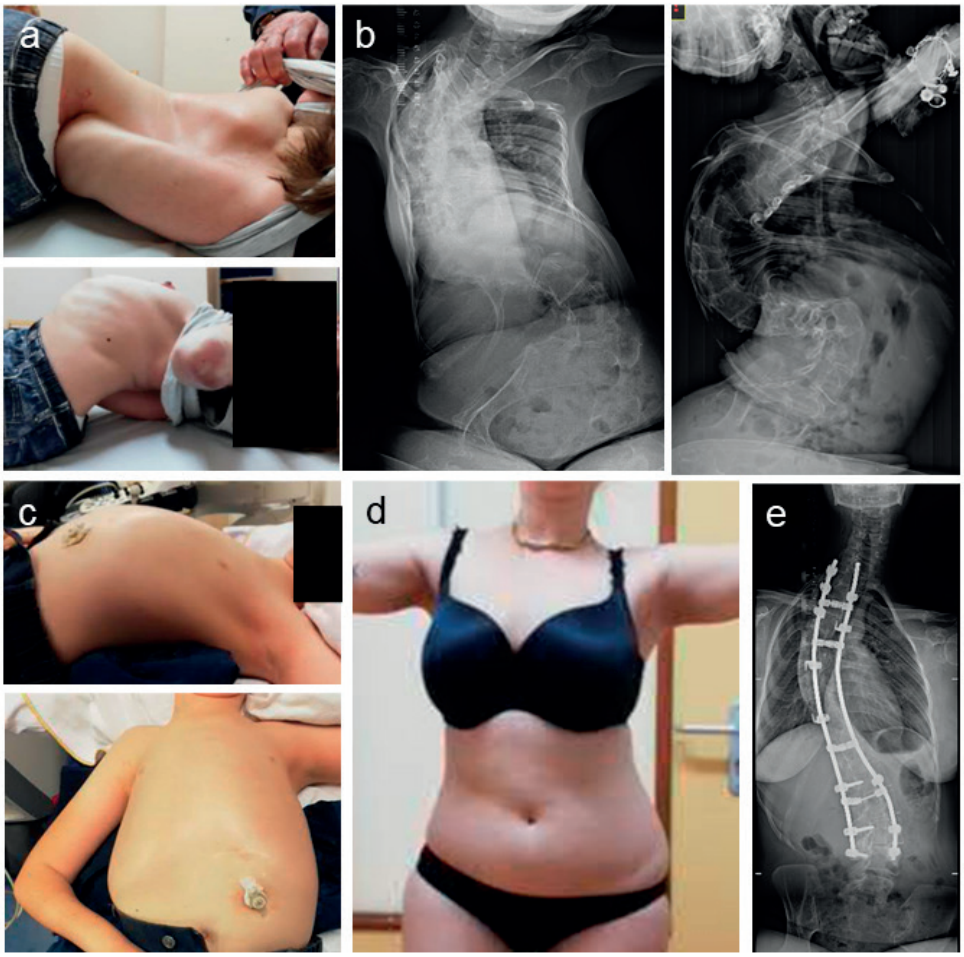


Figure 1: Thorax deformities in LAMA2-MD and SELENON-RM patients.
(a) severe thorax deformity in a LAMA2-MD patient, showing an asymmetric protrusion of the anterior chest wall, an asymmetric retropulsion of the posterior chest wall, a rotation component of the chest wall and scoliosis. (b) X-ray of the spine and thorax of patient shown in a, showing a severe kyphoscoliotic spine with a Cobb's angle of 130 degrees between C7 and L2 and a Cobb's angle of 100 degrees between L2/L3. (c) severe thorax deformities showing pectus carinatum. (d) SELENON-patient, showing from the outside only subtle thorax deformities. (e) X-ray of patient shown in d showing evident thorax deformities secondary to scoliosis.

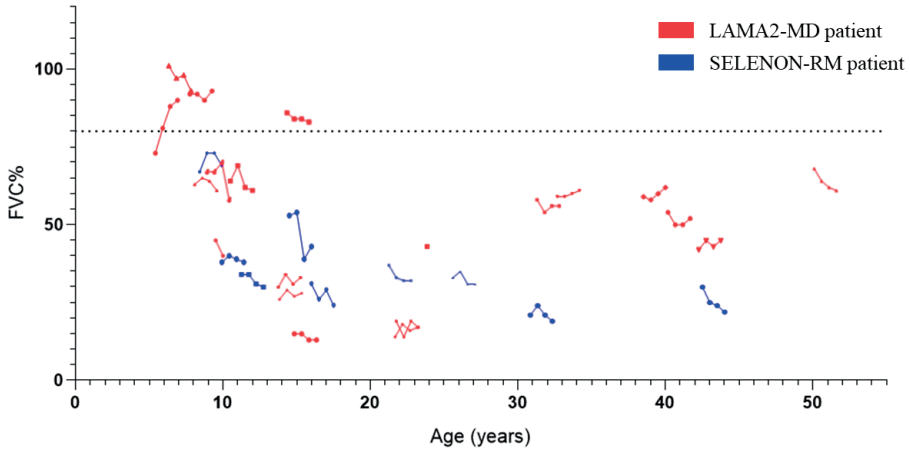


Figure 2: Overview on percentage predicted forced vital capacity (FVC%) in LAMA2-MD and SELENON-RM patients versus age (years). Each line represents one patient followed for 1.5 year. Y = 80% represent the cut-off value for impaired lung function. FVC% = percentage predicted forced vital capacity.

SELENON-RM

At baseline, eight (73%) patients and after 1.5 year follow-up nine (90%) patients were in need of non-invasive, nocturnal mechanical ventilation. In addition, one of them (female, 30 years) used positive air pressure (mouth piece ventilation) during the day. In medical history, three patients reported a respiratory infection that required hospital admission. During follow-up, none of the patients needed antibiotics or hospital admission due to respiratory infection. At baseline seven (64%) patients indicated dyspnoea, all but one using non-invasive mechanical support, mostly while speaking or with physical exercise. No patient developed new dyspnoea at a regular day during the 1.5-year follow-up.

X-ray of the spine

LAMA2-MD

At baseline, 15 (71%) patients had scoliosis, of whom seven had undergone scoliosis surgery. Five patients had a scoliosis that was classified as mild, five as moderate and five as severe (Figure 1). Seventeen patients had a second X-ray of the spine after one year follow-up showing scoliosis in 14 patients, of whom 13 patients already had a scoliosis at baseline. One patient (male, 8 years) developed a new, mild scoliosis and another patient (male, 14 years) progressed from a moderate to a severe scoliosis.

SELENON-RM

At baseline, seven (70%) patients had scoliosis, of whom four patients had undergone scoliosis surgery. Two patients had a scoliosis that was classified as mild, three as moderate and two as severe (Figure 1). All patients had a second X-ray of the spine after one-year follow-up showing scoliosis in eight patients, including one patient who developed a new, mild scoliosis during follow-up. Further, one patient progressed from a mild to a moderate scoliosis and one patient progressed from moderate to severe scoliosis.

Spirometry

A full overview of spirometry, respiratory muscle strength tests and ultrasound of the diaphragm and intercostal muscles can be found in Table 2, Table 3 and Figure 2.

LAMA2-MD

At baseline, spirometry was performed in 20 patients. One patient was too young to perform spirometry (female, 3 years), one patient refrained from spirometry due to complaints of fatigue (female, 31 years) and four patients were seen through home visits (two males, age 27 and 22 and two females, age 22 and 24 years). Seventeen (85%) patients had an impaired respiratory function. Median FVC% was 59% [33; 68], median FEV1% was 64% [34; 71] and median FEV1/FVC was 0.90 [0.86; 0.95], indicating a restrictive pattern. PCF was abnormal in 15 (75%) patients (148 L/min [124.5; 295.8]). One patient (male, 42 years) had an abnormal dVC%. At baseline, the median FVC% was 65 [55; 94] in patients without a scoliosis, 64 [56; 71] with a mild scoliosis, 45 [23; 73] with a moderate scoliosis and 19 [15; 24] with a severe scoliosis. At 1.5-year follow-up, spirometry was performed in 18 patients, of whom 14 (78%) patients had an impaired respiratory function and no patients developed new respiratory impairment. FVC%, FEV1% and dVC% did not change during 1.5-year follow-up period. PCF changed significantly during 1.5-year follow-up (148 L/min [125; 296] at baseline and 191 L/min [135; 309] after 1.5 year, p=0.003).

Table 2: Spirometry, respiratory muscle strength and ultrasound of the diaphragm and intercostal muscles in LAMA2-MD.

LAMA2-MD					
	Baseline (n = 20)	**6 months (n = 19)**	**12 months (n = 18)**	**18 months (n = 18)**	**P value**
Spirometry					
FVC%	59 [33; 68]	58 [34; 69]	60 [30; 74]	60 [32; 67]	ns
FEV1%	64 [34; 71]	63 [34; 70]	61 [32; 71]	61 [31; 68]	ns
dVC%	2.2 [-1.0; 6.5]	0.7 [-9.4; 7.7]	0.6 [-7.8; 4.9]	-3.7 [-8.2; 3.0]	ns
FEV1/FVC	0.90 [0.86; 0.95]	0.89 [0.86; 0.91]	0.90 [0.84; 0.95]	0.87 [0.85; 0.93]	ns
PCF (L/min)	148 [125; 296]	170 [118; 295]	199 [138; 315]	191 [135; 309]	0.003
Respiratory muscle strength					
	Baseline (n = 25)	6 months (n = 24)	12 months (n = 23)	18 months (n = 21)	
PImax (cmH_2O)	49 [29; 63]	43 [28; 58]	50 [25; 62]	52 [25; 64]	ns
PEmax (cmH_2O)	29 [20; 52]	42 [21.; 68]	49 [25; 63]	45 [27; 66]	ns
SNIP (cmH_2O)	40 [28; 60]	40 [16; 60]	36 [23; 46]	48 [33; 66.5]	ns
Diaphragm ultrasound					
	Baseline (n = 22)	6 months (n = 20)	12 months (n = 19)	18 months (n = 18)	
DTee (mm)	1.4 [1.0; 1.5]	1.1 [1.0; 1.3]	1.2 [1.1; 1.4]	1.2 [1.0; 1.2]	ns
DTei (z-score)	0.0 [-0.7; 0.4]*	-0.5 [-0.9; -0.1]	-0.3 [-0.6; -0.2]*	-0.6 [-0.8; -0.3]*	ns
DTR	2.2 [1.8; 2.7]	2.2 [1.8; 2.9]	2.3 [1.8; 2.7]	2.3 [1.8; 2.9]	ns
Echogenicity (z-scores)	2.0 [0.8; 3.3]	2.1 [1.0; 3.1]	1.7 [0.4; 3.2]	2.0 [0.9; 3.1]	ns
Intercostal muscle ultrasound					
ITee (mm)	2.4 [2.0; 2.9]	2.5 [2.1; 3.1]	2.3 [1.7; 3.3]	2.0 [1.6; 3.0]	ns

LAMA2-MD: LAMA2-related muscular dystrophy. FVC%: percentage predicted of forced vital capacity. FEV1%: percentage predicted of forced expiratory volume in the first second. dVC%: percentage decrease in vital capacity from the upright to the supine position. PCF: peak cough flow. PImax: maximal inspiratory pressure. PEmax: maximal expiratory pressure. SNIP: sniff nasal inspiratory pressure. DTee: diaphragm thickness end expiratory. DTR: diaphragm thickening ratio. ITee: intercostal muscle thickness end-expiratory. Data is presented as median [p25; p75]. * z-score could not be calculated in one patient since the diaphragm was not identifiable

Table 3: Spirometry, respiratory muscle strength and ultrasound of the diaphragm and intercostal muscles in SELENON-RM patients

SELENON-RM					
	Baseline (n = 9)	**6 months (n = 9)**	**12 months (n = 9)**	**18 months (n = 9)**	**P value**
Spirometry					
FVC (% predicted)	34 [31; 46]	34 [26; 47]	31 [27; 39]	31 [23; 41]	0.003
FEV1 (% predicted)	37 [33; 50]	37 [28; 50]	33 [28; 41]	33 [24; 43]	0.004
dVC%	30 [7.7; 41]	35 [14; 47]	27 [21; 37]	20 [15; 35]	ns
FEV1/FVC	0.94 [0.91; 0.96]	0.93 [0.90; 0.94]	0.90 [0.85; 0.93]	0.91 [0.90; 0.95]	ns
PCF (L/min)	181 [147; 230]	186 [166; 213]	188 [175; 217]	198 [186; 234]	ns
Respiratory muscle strength					
	Baseline (n = 10)	6 months (n = 9)	12 months (n = 9)	18 months (n = 9)	
PImax (cmH_2O)	34 [26; 40]	34 [27; 47]	30 [25; 42]	27 [24.5; 41]	ns
PEmax (cmH_2O)	50 [43; 62]	52 [37; 65]	50 [43; 65]	56 [43; 72]	ns
SNIP (cmH_2O)	37 [17; 44]	32 [22; 40]	31 [26; 37]	33 [21; 38]	ns
Diaphragm ultrasound					
	Baseline (n = 10)	6 months (n = 10)	12 months (n = 10)	18 months (n = 10)	
DTee (mm)	0.5 [0.3; 0.6]	0.4 [0.1; 0.6]	0.2 [0; 0.6]	0.2 [0; 0.5]	ns
DTee (z-score)	-2.5 [-3.1; -2.1]	-2.6 [-3.3; -2.0]*	-2.3 [-3.6; -1.7]**	-1.7 [-2.6; -1.5]***	ns
DTR	1.2 [1.0; 1.7]	1.2 [1.1; 1.7]	1.2 [1.0; 2.0]	1.1 [1.0; 1.3]	ns
Echogenicity	Not applicable, all patients had DTee < 1 mm in all visits				n.a.
Intercostal muscle ultrasound					
ITee (mm)	2.9 [2.6; 3.6]	2.2 [1.7; 2.9]	2.6 [1.8; 3.4]	3.0 [2.4; 4.2]	0.026

SELENON-RM: SELENON-related congenital myopathy. FVC%: percentage predicted of forced vital capacity. FEV1%: percentage predicted of forced expiratory volume in the first second. dVC%: percentage decrease in vital capacity from the upright to the supine position. PCF: peak cough flow. PImax: maximal inspiratory pressure. PEmax: maximal expiratory pressure. SNIP: sniff nasal inspiratory pressure. DTee: diaphragm thickness end expiratory. DTR: diaphragm thickening ratio. ITee: intercostal muscle thickness end-expiratory. Data is presented as median [p25; p75]. * z-score could not be calculated in one patient since the diaphragm was not identifiable. ** z-score could not be calculated in four patients since the diaphragm was not identifiable. *** z-score could not be calculated in five patients since the diaphragm was not identifiable.

SELENON-RM

Spirometry was performed in 9 patients at baseline. One patient was too young to perform spirometry (male, 3 years) and one patient was seen through home visits (male, 39 years). Respiratory function was impaired in all patients, with a median FVC% of 34% [31; 46], median FEV1% of 37% [33; 50] and median FEV1/FVC of 0.94 [0.91; 0.96], indicating a restrictive pattern. PCF was abnormal in 8 (80%) patients (181 L/min [147; 230]). Seven patients had an abnormal dVC% from the upright to the supine position. At baseline, the two patients without a scoliosis had a FVC% of 67% and 34%, the two patients with a mild scoliosis had a FVC% of 37% and 38%, and the three patients with a moderate scoliosis had a FVC% of 31 [30; 48], and the two patients with a severe scoliosis had a FVC% of 33% and 21%. At 1.5-year year follow-up, respiratory function was still impaired in all patients and all patients had an abnormal dVC%. FVC% and FEV1% significantly decreased during the 1.5-year follow-up (FVC% 34% [31; 46] at baseline and 31% [23; 41] after 1.5 year, p=0.003; FEV1% 37% [33; 50] at baseline and 33% [24; 43] after 1.5 year, p=0.004). The PCF did not change during 1.5-year follow-up (181 L/min [147; 230] at baseline and 198 L/min [186; 234] after 1.5 year, p>0.05).

Respiratory muscle strength

There were no differences in PImax, PEmax and SNIP between baseline and after 1.5-year follow-up for LAMA2-MD and SELENON-RM patients.

Ultrasound of the diaphragm and intercostal muscles

LAMA2-MD

There was no difference in DTee, DTR and echogenicity between the right and the left side of the diaphragm at all visits. At baseline, median DTee was 1.4 [1.0; 1.5] mm, with a median z-score of 0.0 [-0.7; 0.4] and no patients with z-score <-2 except for one patient (male, 42 years) with no identifiable diaphragm. On group level DTR was normal (2.2 [1.8; 2.7]), but four patients had a reduced DTR (<1.6). Median diaphragm echogenicity z-score at baseline was 1.7 [0.6; 3.2]. Eight patients had an elevated echogenicity z-score, which indicates fibrosis or fat infiltration of the diaphragm. Echogenicity of the diaphragm could not be measured in four patients due to DTee <1 mm on the left and/or right side. There was no change in DTee, DTei, DTR, echogenicity and ITee during 1.5-year follow-up.

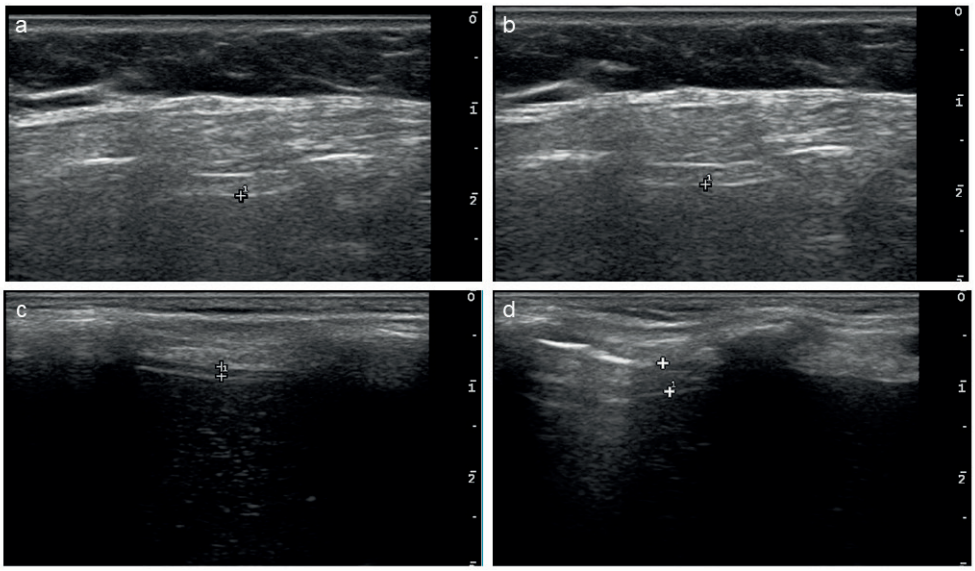


Figure 3: Ultrasound of the diaphragm in LAMA2-MD and SELENON-RM patient.
(a) Ultrasound of the diaphragm of a SELENON-RM at end expiration showing no identifiable diaphragm at end expiration. (b) Ultrasound of the diaphragm of the same SELENON-RM patient showing no identifiable diaphragm at maximal inspiration. The marker in images a and b indicates the position where the diaphragm should be located. Note, that just above the marker a muscle layer is visible. However, through extensive scanning we identified this muscle layer as the intercostal muscles and not the diaphragm. (c) Ultrasound of the diaphragm of a LAMA2-MD patient (DTee = 1.0 mm). (d) Ultrasound of the diaphragm of the same LAMA2-MD patient with evident diaphragm thickening (DTei = 3.2 mm).

SELENON-RM

There was no difference in DTee and DTR between the right and the left side of the diaphragm at all visits. Median DTee was 0.5 [0.3; 0.6] mm at baseline, with a median z-score of -2.5 [-3.1; -2.1], with nine patients having a z-score <-2. Median DTR was 1.2 [1.0; 1.7], with seven patients having a reduced DTR (Fig. 3). All patients had a DTee <1 mm, so diaphragm echogenicity could not be measured. There was no change in DTee, DTei and DTR during 1.5-year follow-up. ITee changes significantly over time (2.9 [2.6; 3.6] at baseline and 3.0 [2.4; 4.2] after 1.5 year follow-up, p = 0.026).

Correlations between spirometry, respiratory muscle strength and motor function

An overview on the observed correlations can be found in Table 4.

LAMA2-MD

In all visits, MFM-20/32 was correlated with FVC%, PImax, PEmax and SNIP. There were no correlations between age and PImax, PEmax and SNIP in all visits, and no correlations between age and FVC% and dVC% in three out of four visits.

SELENON-RM

Age was correlated with FVC%, dVC, PImax and SNIP in all visits. MFM-20/32 was correlated with FVC% and SNIP in three out of four visits.

Table 4: Correlations between spirometry, respiratory muscle strength and motor function measurement 20/32.

	LAMA2-MD						
	Visit	**MFM-20/32 (%)**	**FVC%**	**dVC (%)**	**PImax (cmH_2O)**	**PEmax (cmH_2O)**	**SNIP (cmH_2O)**
Age (years)	1	-0.173	0.390	0.106	0.073	0.241	-0.249
	2	-0.143	-0.485	0.318	0.045	0.100	-0.136
	3	-0.135	-0.526*	0.158	-0.182	0.111	-0.352
	4	-0.164	-0.422	0.557*	-0.145	0.216	-0.123
MFM-20/32 (%)	1	-	0.783**	-0.093	0.716**	0.724**	0.810**
	2		0.784**	-0.115	0.751**	0.752**	0.844**
	3		0.709**	0.257	0.748**	0.696**	0.849**
	4		0.795**	0.308	0.813**	0.647**	0.524*
	SELENON-RM						
Age (years)	1	-0.542	-0.867**	0.950**	-0.733*	0.614	-0.689*
	2	-0.718*	-0.833**	0.683*	-0.717*	0.283	-0.729*
	3	-0.479	-0.824**	0.917**	-0.803**	0.126	-0.932**
	4	-0.413	-0.800**	0.683*	-0.812**	-0.167	-0.711*
MFM-20/32 (%)	1	-	0.669*	-0.418	0.450	-0.015	0.768**
	2		0.695*	-0.407	0.237	0.153	0.828**
	3		0.740*	-0.450	0.293	0.109	0.271
	4		0.552	-0.226	0.282	0.427	0.693*

LAMA2-MD: LAMA2-related muscular dystrophy. SELENON-RM: SELENON-related congenital myopathy. FVC: forced vital capacity. PImax: maximal inspiratory pressure. PEmax: maximal expiratory pressure. SNIP: sniff nasal inspiratory pressure. MFM-20/32: motor function measurement 20/32. * = $p < 0.05$; ** = $p < 0.01$.

Discussion

This study presents a 1.5-year prospective natural history study in patients with LAMA2-MD and SELENON-RM. The major findings of this study are: 1) need for noninvasive mechanical ventilation in a subgroup of LAMA2-MD patients and in the majority of SELENON-RM patients, which was strikingly disproportionate to motor function in SELENON-RM; 2) impaired respiratory function in the majority of the LAMA2-MD patients and in all SELENON-RM patients; 3) progressive decline in respiratory function during 1.5-year follow-up in SELENON-RM patients; 4) a relatively preserved diaphragm thickness and thickening in LAMA2-MD and severe diaphragm atrophy in SELENON-RM patients. 5) strong correlations between motor function, and respiratory function and SNIP in both neuromuscular diseases; and 6) strong to very strong correlations between age, respiratory function, inspiratory muscle strength and diaphragm function in SELENON-RM patients. We discuss the main findings below.

LAMA2-MD

Respiratory function was impaired in the majority of the patients, without a deterioration during 1.5-year follow-up, and was proportionate to ambulatory status and limb muscle weakness. Moreover, nine (35%) LAMA2-MD patients were in need of mechanical ventilation. Remarkable was the large variability in respiratory function and diaphragm function in the cohort of LAMA2-MD patients, ranging from normal to severely impaired. This is congruent with the large variability in motor function and has previously been explained by the variable levels of merosin expression [29]. Our findings are in line with a previous study in LAMA2-MD patients that showed no yearly decrease in FVC% and only a minority of the patients with a decrease in FVC between the sitting and supine position [3, 18]. A linear annual decline in FVC% of 2.9% found in severely affected LAMA2-MD patients in another study cannot be translated to our cohort since we included patients with a variable disease severity based on the MFM-20/32 scores, ambulatory status and age at onset of symptoms [2]. Further, respiratory function was correlated to motor function in our cohort. A similar correlation has been described in spinal muscular atrophy [30, 31], and to a lower extent in nemaline myopathies [**Chapter 3**] and facioscapulohumeral dystrophy [32]. We did not correlate respiratory function (FVC%) to the level of merosin expression for multiple reasons. We did not perform muscle biopsies as part of research due to the burden of this procedure, and the number of patients in whom muscle biopsies with merosin staining was performed in clinical care was limited. In the available muscle biopsies, we were not able to perform reliable quantification of the level of merosin expression since merosin staining was frequently fainted due to the long time interval. Further, the level of merosin expression is not dichotomous, but is a continuous scale, and dividing LAMA2-MD patients into solely two subgroups ‘complete’ or ‘partial’ merosin deficiency is artificial. There was no cross-sectional correlation between age and respiratory function. A likely explanation is that LAMA2-MD patients with severe respiratory impairment have a limited life expectancy and mostly do not survive after the third decade [17]. Consequently, the cohort of patients,

especially at an older age, is biased towards the less severely affected patients. This could give the wrong impression of a stabilization or improvement of respiratory function with increasing age. Moreover, we observed that respiratory function was lower in patients with a more severe scoliosis. We did not perform statistical analysis on respiratory function and severity of scoliosis due to the small subgroups. Scoliosis is known to alter respiratory mechanics in neuromuscular diseases and thereby impairing respiratory function [2, 33]. Low PEmax and low PCF indicate prominent expiratory muscle weakness, which leads to ineffective cough, increasing the risk of respiratory complications including respiratory infections. We consider the variability in PCF during the 1.5-year follow-up as not relevant to assess respiratory disease progression since it is an absolute value, contrarily to other respiratory function variables that are corrected for age, length and weight (FVC%, FEV1%, dVC% and FEV1/FVC). Due to the absence of this correction, an increase in PCF might thus wrongly give the impression of an improvement in PCF.

SELENON-RM

The most noticeable feature in SELENON-RM was severe diaphragm atrophy that was already present at a young age. The youngest patient (male, 3 years) had severe diaphragm atrophy, yet did not need mechanical ventilation. He was able to compensate diaphragm dysfunction with activation of accessory respiratory muscles. In general, due to the severe diaphragm atrophy, caution should be paid to the interpretation of the DTR. Small absolute changes in measurements of DTee and DTei could result in a relatively normal DTR, incorrectly giving the impression of a normal diaphragm function. This study showed a large dVC%, which is a good indication of diaphragm weakness, even in subjects who might have global inspiratory muscle dysfunction [1, 34]. We additionally found a low SNIP, which is predominantly dependent on diaphragm function [35, 36]. Our findings are in line with a previous study using oesophageal and gastric pressure measurements in SELENON-RM patients showing that diaphragm dysfunction is a characteristic feature [19]. Respiratory function was impaired in all patients, with a high need for mechanical ventilation (73% at baseline and 90% at follow-up), which was in line with a previously reported frequencies [37]. Respiratory function was strikingly disproportionate to motor function, with respiratory impairment leading to the need of mechanical ventilation in ambulant patients with relatively preserved limb muscle strength. Patients with a more severe motor function impairment, had an even more severely affected respiratory function. Moreover, we observed that respiratory function was lower in patients with a more severe scoliosis. In SELENON-RM patients, thoracic deformities are known to contribute to respiratory failure [1]. Scoliosis and restrictive respiratory impairment were often diagnosed simultaneously at approximately the end of the first decade, and earlier scoliosis and respiratory failure required earlier non-invasive mechanical ventilatory support [1]. We additionally detected that respiratory function deteriorated during 1,5 year follow-up, despite stable motor function. This was in line with the findings of a retrospective natural history study on SELENON-RM showing an annual decrease in FVC% of -2.04% per year [37]. We also observed strong to very strong correlations between age and respiratory function, respiratory muscle strength and diaphragm function at all visits.

Finally, during the follow-up period, mechanical ventilation was initiated in two additional patients (patient 4, 22 years and patient 10, 12 years), confirming the progressive nature of respiratory impairment. PEmax and PCF were low in all visits, indicating prominent expiratory muscle weakness, which contributes to respiratory complications. ITee changed significantly over time. However, due to small groups and varying absolute thickness, we consider this as an irrelevant change.

Altogether, we conclude that inspiratory and expiratory respiratory function is impaired in the majority of LAMA2-MD and all SELENON-RM patients, and that respiratory impairment is caused by a combination of diaphragm weakness, accessory inspiratory muscle weakness, expiratory muscle weakness and scoliosis [**Chapter 2**]. Our study highlights severe diaphragm atrophy and diaphragm dysfunction in SELENON-RM patients starting at a young age. The study further confirms the characteristic, relatively fast progressive nature of respiratory impairment in SELENON-RM patients.

Recommendations for clinical care

The consensus statements on congenital muscular dystrophies and congenital myopathies, and the clinical care recommendation for LAMA2-MD as published on *GeneReviews* provide a comprehensive overview on respiratory care [15, 16, 38]. Our study supports the expert opinion in these consensus statements and we suggest to implement these recommendations into the clinical care for LAMA2-MD and SELENON-RM. Respiratory function (FVC%, dVC; in upright and supine position) and respiratory muscle strength (SNIP; in upright position) should be performed at least one time per two years in LAMA2-MD patients and annually in SELENON-RM patients order to early detect respiratory impairment and prevent respiratory complications, independent of the motor function, and more often on indication based on clinical symptoms (dyspnoea, headache when waking up). The interval of one year in SELENON-RM is chosen due to the progressive nature of respiratory function in SELENON-RM during the LAST STRONG Study. SNIP should additionally be performed in patients in whom diaphragm dysfunction is present or expected, consequently in all SELENON-RM patients. Since standing height is not reflective of lung growth in patients with scoliosis, serial respiratory function tests are needed to monitor patients over time. Furthermore, since complications during sleep usually precede abnormalities during wakefulness, regular assessment of nocturnal respiratory function through sleep studies is indicated. This is particularly needed in SELENON-RM patients due to their severe diaphragm dysfunction. Non-invasive positive pressure mechanical ventilation is the recommended modality in the treatment of chronic respiratory failure in neuromuscular diseases.

Recommendations for research

We propose to use spirometry and respiratory muscle strength tests as clinical outcome measure in natural history studies and future clinical trials on possible treatment options. In particular FVC% and SNIP showed good correlations with motor function. Diaphragm ultrasound

can help in diagnosis of diaphragm dysfunction in patients with neuromuscular diseases. However, no change during 1.5-year follow-up was found, and therefore we consider ultrasound of the diaphragm not as the first choice for a clinical outcome measure . In patients <5 years that cannot perform spirometry, ultrasound of the diaphragm can nevertheless be used as clinical outcome measures to give an indication of diaphragm function.

We plan to extend the present 1.5-year natural history study to a follow-up of 3 and 5 years (extended LAST STRONG) to assess respiratory function on the longer term and to identify risk factors for developing respiratory impairment.

Strengths and limitations

The major strengths of this study include its standardized and prospective design with an extensive number of clinically available respiratory function tests in an unselected cohort of LAMA2-MD and SELENON-RM patients, with great variability in age and disease severity. Further, we had a high participation rate and only a minor loss from follow-up. The number of patients in this study is nevertheless low, which is inherent to the low prevalence of these neuromuscular diseases. Therefore, future international collaborations are essential. Moreover, the youngest patients were 3 years old, leading to a knowledge gap in younger patients. Finally, a 1.5-year follow-up is too short to detect minor changes in respiratory function and to determine risk factors for developing respiratory impairment on the long-term. Caution should be paid to the interpretation of spirometry and respiratory muscle strength tests in patients with neuromuscular diseases since major fluctuations within a patient might possibly be caused by fatigue or intercurrent respiratory infections [1]. The interpretation might be improved by adequate rest periods between efforts to decrease the influence of fatigability and by regular follow-up respiratory function tests in order to assess the tendency of the respiratory function.

Conclusion

Respiratory impairment was present in the majority of LAMA2-MD patients and in all SELENON-RM patients. In SELENON-RM, severe diaphragm dysfunction, which was strikingly disproportionate to ambulatory status and muscle limb weakness, was present in all patients. Spirometry and respiratory muscle strength tests are useful in respiratory assessment in clinical care and are proposed as clinical outcome measure for natural history studies and future clinical trials starting at a young age (5 years).

References

1. Villar-Quiles, R.N., et al., The clinical, histologic, and genotypic spectrum of SEPN1-related myopathy: A case series. Neurology, 2020. **95**(11): p. e1512-e1527.
2. Zambon, A.A., et al., LAMA2-related muscular dystrophy: Natural history of a large pediatric cohort. Ann Clin Transl Neurol, 2020. **7**(10): p. 1870-1882.
3. Jain, M.S., et al., Longitudinal changes in clinical outcome measures in COL6-related dystrophies and LAMA2-related dystrophies. Neurology, 2019. **93**(21): p. e1932-e1943.
4. Meilleur, K.G., et al., Results of a two-year pilot study of clinical outcome measures in collagen VI- and laminin alpha2-related congenital muscular dystrophies. Neuromuscular disorders : NMD, 2015. **25**(1): p. 43-54.
5. Bouman, K., et al., LAMA2-Related Muscular Dystrophy Across the Life Span: A Cross-sectional Study. Neurol Genet, 2023. **9**(5): p. e200089.
6. Bouman, K., et al., SELENON-Related Myopathy Across the Life Span, a Cross-Sectional Study for Preparing Trial Readiness. J Neuromuscul Dis, 2023. **10**(6): p. 1055-1074.
7. Oliveira, J., et al., LAMA2 gene mutation update: Toward a more comprehensive picture of the laminin-α2 variome and its related phenotypes. Hum Mutat, 2018. **39**(10): p. 1314-1337.
8. Ferreiro, A., et al., Mutations of the selenoprotein N gene, which is implicated in rigid spine muscular dystrophy, cause the classical phenotype of multiminicore disease: reassessing the nosology of early-onset myopathies. Am J Hum Genet, 2002. **71**(4): p. 739-49.
9. Arbogast, S., et al., Oxidative stress in SEPN1-related myopathy: from pathophysiology to treatment. Ann Neurol, 2009. **65**(6): p. 677-86.
10. Arbogast, S., et al., N-acetylcysteine as an effective treatment in vivo and identification of biomarkers in SEPN1-related myopathy: A first preclinical trial. Vol. 24. 2014. 879-880.
11. Smeitink, J., et al., A randomised placebo-controlled, double-blind phase II study to explore the safety, efficacy, and pharmacokinetics of sonlicromanol in children with genetically confirmed mitochondrial disease and motor symptoms ("KHENERGYC"). BMC Neurology, 2022. **22**(1): p. 158.
12. Rooney, J.E., et al., Laminin-111 protein therapy reduces muscle pathology and improves viability of a mouse model of merosin-deficient congenital muscular dystrophy. Am J Pathol, 2012. **180**(4): p. 1593-602.
13. Kemaladewi, D.U., et al., A mutation-independent approach for muscular dystrophy via upregulation of a modifier gene. Nature, 2019. **572**(7767): p. 125-130.
14. Kemaladewi, D., et al., CRISPR/Cas9-mediated exon inclusion in Lama2 gene alleviates dystrophic pathology in MDC1A mouse model. Neuromuscular Disorders, 2016. **26**: p. S190.
15. Wang, C.H., et al., Consensus statement on standard of care for congenital muscular dystrophies. J Child Neurol, 2010. **25**(12): p. 1559-81.
16. Wang, C.H., et al., Consensus statement on standard of care for congenital myopathies. J Child Neurol, 2012. **27**(3): p. 363-82.
17. Sarkozy, A., et al., LAMA2-Related Dystrophies: Clinical Phenotypes, Disease Biomarkers, and Clinical Trial Readiness. Front Mol Neurosci, 2020. **13**: p. 123.
18. Meilleur, K.G., et al., Comparison of sitting and supine forced vital capacity in collagen VI-related dystrophy and laminin α2-related dystrophy. Pediatr Pulmonol, 2017. **52**(4): p. 524-532.

19. Caggiano, S., et al., Diaphragmatic dysfunction in SEPN1-related myopathy. Neuromuscular Disorders, 2017. **27**(8): p. 747-755.
20. ATS/ERS Statement on respiratory muscle testing. Am J Respir Crit Care Med, 2002. **166**(4): p. 518-624.
21. Graham, B.L., et al., Standardization of Spirometry 2019 Update. An Official American Thoracic Society and European Respiratory Society Technical Statement. Am J Respir Crit Care Med, 2019. **200**(8): p. e70-e88.
22. Park, J.J.H., et al., Systematic review of basket trials, umbrella trials, and platform trials: a landscape analysis of master protocols. Trials, 2019. **20**(1): p. 572.
23. Bouman, K., et al., Natural history, outcome measures and trial readiness in LAMA2-related muscular dystrophy and SELENON-related myopathy in children and adults: protocol of the LAST STRONG study. BMC Neurol, 2021. **21**(1): p. 313.
24. Richards, S., et al., Standards and guidelines for the interpretation of sequence variants: a joint consensus recommendation of the American College of Medical Genetics and Genomics and the Association for Molecular Pathology. Genet Med, 2015. **17**(5): p. 405-24.
25. Quanjer, P.H., et al., Multi-ethnic reference values for spirometry for the 3-95-yr age range: the global lung function 2012 equations. Eur Respir J, 2012. **40**(6): p. 1324-43.
26. Birnkrant, D.J., et al., American College of Chest Physicians consensus statement on the respiratory and related management of patients with Duchenne muscular dystrophy undergoing anesthesia or sedation. Chest, 2007. **132**(6): p. 1977-86.
27. Laveneziana, P., et al., ERS statement on respiratory muscle testing at rest and during exercise. Eur Respir J, 2019. **53**(6).
28. Horng, M.H., et al., Cobb Angle Measurement of Spine from X-Ray Images Using Convolutional Neural Network. Comput Math Methods Med, 2019. **2019**: p. 6357171.
29. Geranmayeh, F., et al., Genotype-phenotype correlation in a large population of muscular dystrophy patients with LAMA2 mutations. Neuromuscul Disord, 2010. **20**(4): p. 241-50.
30. Trundell, D., et al., Assessment of the validity and reliability of the 32-item Motor Function Measure in individuals with Type 2 or non-ambulant Type 3 spinal muscular atrophy. PLoS One, 2020. **15**(9): p. e0238786.
31. Chabanon, A., et al., Prospective and longitudinal natural history study of patients with Type 2 and 3 spinal muscular atrophy: Baseline data NatHis-SMA study. PLoS One, 2018. **13**(7): p. e0201004.
32. Teeselink, S., et al., Long-term follow-up of respiratory function in facioscapulohumeral muscular dystrophy. Journal of Neurology, 2022. **269**(7): p. 3682-3689.
33. Mayer, O.H., Scoliosis and the impact in neuromuscular disease. Paediatr Respir Rev, 2015. **16**(1): p. 35-42.
34. Fromageot, C., et al., Supine fall in lung volumes in the assessment of diaphragmatic weakness in neuromuscular disorders. Arch Phys Med Rehabil, 2001. **82**(1): p. 123-8.
35. Wilding, R.J., M. Thynne, and M.M.F. Subhan, Optimization of sniff nasal inspiratory pressure (SNIP) measurement methodology in healthy subjects. BMC Pulmonary Medicine, 2023. **23**(1): p. 66.
36. Prigent, H., et al., Sniff and Muller manoeuvres to measure diaphragmatic muscle strength. Respiratory Medicine, 2008. **102**(12): p. 1737-1743.
37. Silwal, A., et al., Selenoprotein N-related myopathy: a retrospective natural history study to guide clinical trials. Ann Clin Transl Neurol, 2020. **7**(11): p. 2288-2296.

38. Oliveira J, P.F.J., Santos M, and Coelho T, LAMA2 Muscular Dystrophy. In: Adam MP, Feldman J, Mirzaa GM, et al., editors. GeneReviews® [Internet]. Seattle (WA): University of Washington, Seattle; 1993-2023. , 2012 Jun 7 [Updated 2020 Sep 17]; Available from: https://www.ncbi.nlm.nih.gov/books/NBK97333/.

Part II

Critical appraisal



Chapter 5

Association of diaphragm thickness and echogenicity with age, sex and BMI in healthy subjects

Jeroen LM van Doorn
Juerd Wijntjes
Christiaan GJ Saris
Coen AC Ottenheijm
Nens van Alfen
Jonne Doorduin

Published in:
Muscle & Nerve, 2022

Abstract

Introduction/Aims: Diaphragm ultrasound is increasingly used in the diagnosis of diaphragm dysfunction and to guide respiratory management in patients with neuromuscular disorders and those who are critically ill. However, the association between diaphragm ultrasound variables and demographic factors like age, sex and Body Mass Index (BMI) are understudied in the literature. The latter is important for correct interpretation of normative values and comparison with selected patients groups. The aim of this study is to determine the association between diaphragm ultrasound variables and subject characteristics.

Methods: B-mode ultrasound was used to image the diaphragm at the zone of apposition in 83 healthy subjects. Diaphragm thickness at resting end-expiration (DTee), diaphragm thickness at maximal end-inspiration (DTei), diaphragm thickening ratio (DTR), and diaphragm echogenicity were measured. Multivariate linear regression was used to explore the associations between diaphragm ultrasound variables and subject characteristics.

Results: DTee, DTei and DTR do not change with age whereas diaphragm echogenicity increases with age. The thickening ratio had a weak negative association with BMI, while DTee was positively associated with BMI. Men had a larger DTee and DTei than women (DTee 1.6±0.5 and 1.4±0.3 mm; p=0.011, DTei 3.8±1.0 and 3.2±0.9 mm; p=0.004), but similar DTR.

Discussion: Diaphragm thickness, thickening and echogenicity measured with ultrasound are associated with factors such as age, BMI and sex. Therefore, subject characteristics should be considered when interpreting diaphragm ultrasound measurements. In the absence of normative values, matched control groups are a prerequisite for research and in clinical practice.

Introduction

Diaphragm weakness is a common feature in patients with neuromuscular disorders (NMDs) and those who are critically ill. In many NMDs, weakness of the diaphragm leads to dyspnoea, sleep disturbances, and lung infections, and is a major contributor to death [1]. In critically ill patients, mechanical ventilation induces diaphragm injury and atrophy, leading to ventilator dependency and difficult weaning [2]. In both settings, reliable assessment of diaphragm function is to identify early signs of respiratory insufficiency, monitor disease progression and guide individual respiratory management.

Ultrasound is increasingly used as tool to assess diaphragm function and structure in NMD patients and critically ill patients [3, **Chapter 2**]. The costal diaphragm can be visualized at its insertion in the anterior thoracic wall, the so-called zone of apposition. The change in thickness from expiration to inspiration is used to quantify diaphragm function [3, **Chapter 2**]. The assessment of the muscle ultrasound grey level, or echogenicity, reflects structural alterations in muscles due to, for example, fibrosis and inflammation [4]. Echogenicity analysis of skeletal muscles is a well-known and reliable tool for screening, diagnosing, and follow-up of NMDs [4, 5].

Thickness and echogenicity of peripheral muscles are dependent on subject characteristics such as age, Body Mass Index (BMI) and sex [6]. However, it is unknown if diaphragm thickness and echogenicity also depend on these characteristics. The latter is important to identify those subject characteristics that should be taken into account when interpreting diaphragm ultrasound measurements in clinical practice or research. The aim of this study was to determine the association of diaphragm thickness and echogenicity with age, sex and BMI using a standardized approach.

Methods

This is a retrospective study of data collected as part of a project to determine reference limits for clinical practice at the Radboud university medical centre, Nijmegen, the Netherlands and was therefore exempt from ethical approval. All subjects provided their informed consent and procedures were performed in accordance with the ethical standards as laid down in the declaration of Helsinki. Ultrasound examinations were carried out by five laboratory technicians, each with 5-10 years of experience in muscle ultrasound.

Sample size estimation yielded a need for 80 subjects for regression-based reference limits [7]. A decision was made to aim to enrol 10 healthy subjects, five males and five females, for each ten year age category to ensure a balanced age and sex distribution. Subjects with any condition affecting the respiratory or skeletal muscle system were excluded. Demographic factors including age, sex, and BMI were collected. Subjects were recruited via advertisements on social media.

An Esaote MyLab Twice ultrasound machine (Esaote SpA, Genoa, Italy) equipped with a 3-13 MHz LA533 linear transducer was used to assess diaphragm thickness at resting end-expiration (DTee) and at maximal end-inspiration (DTei). Measurements were performed according to previously published methodology (See Supplemental Methods) [8]. Diaphragm thickening ratio (DTR) was calculated as DTei / DTee.

Diaphragm echogenicity values were calculated from the images used for measurements of DTee. Using custom developed software in Matlab (R2018a, Mathworks, Natick, MA, USA) and the trace method, a region-of-interest of diaphragm muscular tissue was manually selected [9]. Echogenicity was calculated as the mean pixel grey-value of this region-of-interest and averaged over three measurements.

After checking linearity, independency, homoscedasticity and normality, a stepwise multivariate linear regression was performed for echogenicity, DTR, DTee, and DTei using R software [10]. A full factorial model was explored with age, sex and BMI as covariates and their quadratic terms. To uphold independence between the covariates and their quadratic terms, age and BMI were centred. Akaike's information criterion (AIC) was used to determine the best fit [11]. This approach allows covariates to be included in the final regression model when they have considerable impact on model fit, even when there is no significant association between the covariate and the dependent variable.

Intraclass correlation coefficients (ICCs) were calculated on the three repeated measures during one session to assess intra-rater reliability. ICC values below 0.50 were considered as poor reliability, 0.50-0.75 moderate, 0.76-0.90 good and 0.91-1.00 excellent [12].

Results

83 healthy subjects were recruited, as listed in Table 1. DTei was missing in one subject. Four diaphragms, with a DTee <1 mm, were too thin to permit determination of a reliable region-of-interest, and were excluded from echogenicity analysis.

Table 2 and Figure 1 present the regression analyses, and the specifications are presented in the supplement. Group average values were different between sexes for DTee and DTei. An increase in age was associated with an increase in echogenicity. Age and age squared were not associated with thickening ratio, although they were included in the regression model based on AIC. An increase in BMI was associated with an increase in thickening ratio and a decrease in DTee.

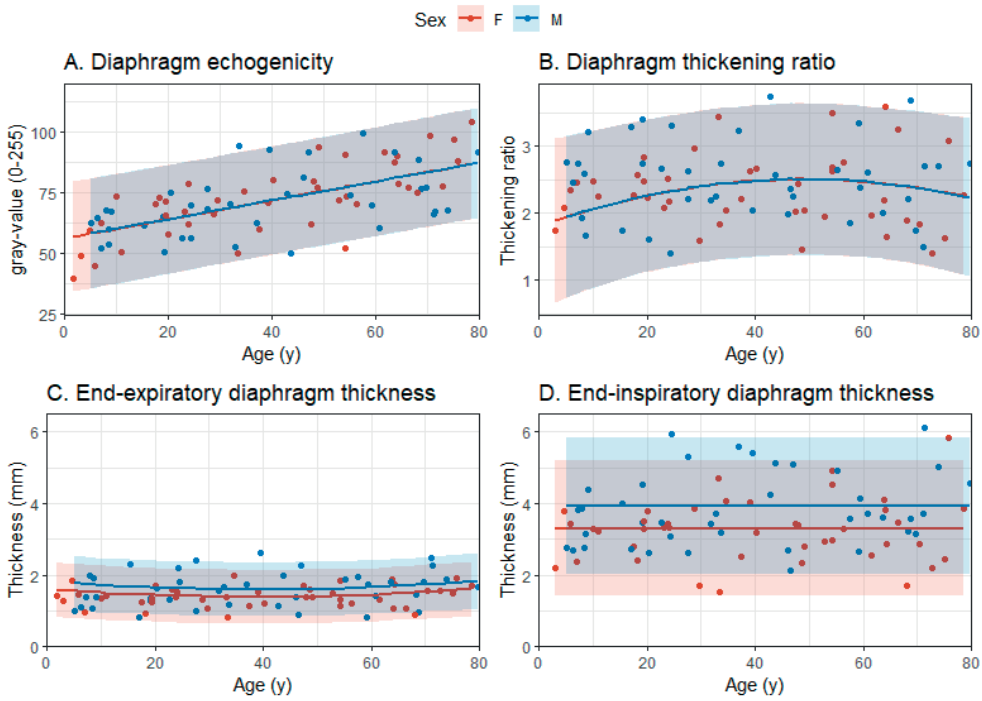


Figure 1: Graphical representation of fitted regression models.
Each dot represent the measurement of a single subject, the line represents predicted values for each subject, where BMI was set fixed at the adult group mean of 23.3 kg/m^2, and the shaded area represents the 95% prediction interval.

Intra-observer reliability of the three echogenicity measurements, $T_{end\text{-}exp}$and $T_{max\text{-}insp}$ were all excellent, with ICCs of 0.93 (0.89-0.96), 0.92 (0.89-0.94), and 0.93 (0.91-0.95), respectively.

Table 1: Subject characteristics and outcomes for different categories.

Category	Sex (M/F)	Age (y)	BMI (kg/m^2)	Echogenicity (0-255)	Thickening ratio	DTee (mm)	DTei (mm)
Age (y): 0-9	7/5	6.2 (2.3)	16.6 (2.8)	56.9 (9.1)	2.4 (0.5)	1.4 (0.4)	3.2 (0.7)
Age (y): 10-19	4/6	16.5 (3.6)	19.0 (2.4)	64.5 (8.9)	2.6 (0.5)	1.3 (0.4)	3.3 (0.6)
Age (y): 20-29	6/6	24.7 (3.1)	21.6 (2.1)	67.2 (7.8)	2.3 (0.6)	1.6 (0.4)	3.5 (1.1)
Age (y): 30-39	5/5	35.3 (2.8)	23.0 (3.0)	69.8 (15.8)	2.5 (0.5)	1.6 (0.5)	3.8 (1.2)
Age (y): 40-49	5/5	45.9 (2.9)	23.7 (2.9)	76.7 (13.6)	2.4 (0.6)	1.5 (0.4)	3.4 (1.1)
Age (y): 50-59	4/5	55.9 (2.3)	24.3 (2.1)	75.3 (14.2)	2.6 (0.5)	1.5 (0.4)	3.8 (0.9)
Age (y): 60-69	5/6	65.4 (3.0)	24.3 (4.3)	81.4 (9.5)	2.4 (0.7)	1.4 (0.4)	3.3 (0.7)
Age (y): 70-80	4/5	74.3 (3.3)	23.0 (1.8)	84.3 (14.8)	2.2 (0.6)	1.8 (0.3)	4.1 (1.4)
Sex: M	40/0	38.2 (23.0)	21.8 (4.0)	70.4 (13.5)	2.5 (0.6)	1.6 (0.5)	3.8 (1.0)
Sex: F	0/43	39.7 (23.2)	21.8 (3.6)	72.3 (15.0)	2.3 (0.5)	1.4 (0.3)	3.2 (0.9)
Age (y): 0-19	9/8	10.9 (6.0)	17.7 (2.8)	60.1 (9.6)	2.5 (0.5)	1.4 (0.4)	3.3 (0.7)
Age (y): 20-80	31/35	49.2 (17.6)	23.3 (2.9)	75.5 (13.5)	2.4 (0.6)	1.6 (0.4)	3.6 (1.1)
Sex: M, age (y): 0-19	9/0	11.2 (5.4)	17.7 (3.2)	60.3 (6.2)	2.6 (0.6)	1.4 (0.5)	3.5 (0.7)
Sex: M, age (y): 20-80	29/0	48.5 (18.1)	23.3 (3.1)	74.2 (13.6)	2.5 (0.6)	1.7 (0.5)	4.0 (1.1)
Sex: F, age (y): 0-19	0/9	10.6 (6.8)	17.7 (2.5)	60.0 (12.2)	2.3 (0.3)	1.3 (0.2)	3.0 (0.6)
Sex: F, age (y): 20-80	0/32	49.8 (17.5)	23.2 (2.8)	76.7 (13.6)	2.3 (0.6)	1.4 (0.3)	3.3 (1.0)
Total	40/43	39.0 (22.9)	21.8 (3.8)	71.4 (14.3)	2.4 (0.6)	1.5 (0.4)	3.5 (1.0)

Data are presented as mean (SD). Total mean values were used to center Age and BMI.

Table 2: Regression models fitted to echogenicity, thickening ratio, DTee and DTei.

Outcome	Regression formula
Echogenicity	71.443 + 0.390 * cAge
Thickening ratio	2.560 – 0.056 * cBMI + 0.006 * cAge + 0.0003 * $cAge^2$
DTee	1.325 + 0.041 * cBMI + 0.211 * Sex(M) + 0.0001 * $cAge^2$
DTei	3.237 + 0.049 * cBMI + 0.613 * Sex(M)

cAge: centred age, calculated by subtracting 39.0 from age in years. cBMI: centred BMI, calculated by subtracting 21.8 from BMI in kg/m^2. $cAge^2$: centred age squared.

Discussion

In healthy subject across a wide age range we found that diaphragm thickness and thickening do not change with age, while diaphragm echogenicity increases with age. Sex and BMI have small effects on diaphragm thickness, but not on diaphragm thickening.

Diaphragm thickness and thickening ratio values presented in this study are comparable to previously reported values [13-17]. Interestingly, Boon and colleagues, using an apparently similar approach reported a DTee of 3.3 mm compared to 1.6 mm in our adult population [8]. Note that BMI in our adult population was considerably lower (23.3 vs. 27.2 kg/m^2). Although we and others [8, 18] found an association between BMI and diaphragm thickness, this cannot fully explain the relatively large difference. Small differences in methodology may also contribute to differences in thickness. The variability in reported values for diaphragm thickness highlights the importance of collecting centre-specific normative values. The larger variation in DTei compared to DTee is in accordance with other reports [19]. This may be attributed to variation in subjects' performance of the manoeuvre to take a deep breath, and affects the level of diaphragm recruitment and the anatomical position of the diaphragm relative to the ultrasound probe.

Our study shows that diaphragm thickness is constant over a wide age range. This differs from skeletal limb muscles that generally increase in thickness until 30-40 years, after which muscle thickness decreases (sarcopenia) [6]. Apparently, changes in respiratory demand with aging, for example due to decreased respiratory compliance, do not seem to be accompanied by changes in diaphragm muscle mass but other mechanisms, like changes in motor control [20].

In agreement with previous studies, diaphragm thickness was larger in men than women [8, 14, 19]. The calculation of thickening ratio cancels out sex differences. We also identified BMI as significant predictor of DTee and thickening ratio, but the size of this effect was small. The latter may result from the narrow range of BMI in our adult population (23.3±2.9 kg/m^2). It has been shown that outside this range BMI has larger effects on diaphragm thickness and thickening ratio [18]. Overall, little variance in thickening ratio was explained by our regression model. Thus

the lower limit of normal (5th percentile) of our healthy population, i.e. 1.6, can be used as cut off value for a normal diaphragm thickening ratio regardless of the subjects' age, sex and BMI [21].

The absence of changes in diaphragm thickening with age is in apparent contrast to age-related changes in pulmonary function and respiratory muscle strength [22, 23]. Furthermore, diaphragm function, as assessed with transdiaphragmatic pressure, is only weakly correlated with diaphragm thickening [24]. Therefore, the relationship between the pressure generating capacity of the diaphragm and diaphragm thickening warrants further research. This may be better reflected by other ultrasound modes such as strain imaging or shear wave elastography [25, 26].

Different ultrasound devices produce different greyscale images, meaning that our diaphragm echogenicity values cannot be used with different ultrasound devices [4, 27]. However, the observed association with age is expected to exist with values obtained from a different machine, as sarcopenia is an inherent property of aging muscle [6]. Normative values should be collected for each different ultrasound device, and age-matched controls should be included when normative values are unavailable. For example, a recent study on diaphragm echogenicity compared mechanically ventilated patients, median age 59 years, with healthy controls, median age 27 years [28]. Our data implies that such a comparison is likely not valid. Furthermore, multiple ultrasound devices were used, complicating comparison of echogenicity values.

This study has limitations. First, the range in BMI was narrow. This impairs the interpretation of diaphragm ultrasound data of a patient outside this range. Second, normative data as presented in this study may have low generalizability to other centres. However, the associations with age, sex and BMI are independent of measurement technique and device settings.

Conclusion

The associations between diaphragm thickness, thickening and echogenicity and age, BMI and sex highlight the importance of taking subject characteristics into account when interpreting diaphragm ultrasound measurements in clinical practice and research.

References

1. Laghi F, Tobin MJ. Disorders of the respiratory muscles. Am J Respir Crit Care Med. 2003;168(1):10-48.
2. Goligher EC, Brochard LJ, Reid WD, Fan E, Saarela O, Slutsky AS, et al. Diaphragmatic myotrauma: a mediator of prolonged ventilation and poor patient outcomes in acute respiratory failure. Lancet Respir Med. 2019;7(1):90-8.
3. Tuinman PR, Jonkman AH, Dres M, Shi ZH, Goligher EC, Goffi A, et al. Respiratory muscle ultrasonography: methodology, basic and advanced principles and clinical applications in ICU and ED patients-a narrative review. Intensive Care Med. 2020;46(4):594-605.
5. Wijntjes J, van Alfen N. Muscle ultrasound: Present state and future opportunities. Muscle Nerve. 2021;63(4):455-66.
6. van Alfen N, Gijsbertse K, de Korte CL. How useful is muscle ultrasound in the diagnostic workup of neuromuscular diseases? Curr Opin Neurol. 2018;31(5):568-74.
7. Pillen S, Arts IM, Zwarts MJ. Muscle ultrasound in neuromuscular disorders. Muscle Nerve. 2008;37(6):679-93.
8. Virtanen A, Kairisto V, Uusipaikka E. Regression-based reference limits: determination of sufficient sample size. Clin Chem. 1998;44(11):2353-8.
9. Boon AJ, Harper CJ, Ghahfarokhi LS, Strommen JA, Watson JC, Sorenson EJ. Two-dimensional ultrasound imaging of the diaphragm: quantitative values in normal subjects. Muscle Nerve. 2013;47(6):884-9.
10. Sarwal A, Parry SM, Berry MJ, Hsu FC, Lewis MT, Justus NW, et al. Interobserver Reliability of Quantitative Muscle Sonographic Analysis in the Critically Ill Population. J Ultrasound Med. 2015;34(7):1191-200.
11. R Core Team. R: A Language and Environment for Statistical Computing. R Foundation for Statistical Computing; 2019.
12. Halsey LG. The reign of the p-value is over: what alternative analyses could we employ to fill the power vacuum? Biology Letters. 2019;15(5):20190174.
13. Koo TK, Li MY. A Guideline of Selecting and Reporting Intraclass Correlation Coefficients for Reliability Research. J Chiropr Med. 2016;15(2):155-63.
14. Hiwatani Y, Sakata M, Miwa H. Ultrasonography of the diaphragm in amyotrophic lateral sclerosis: Clinical significance in assessment of respiratory functions. Amyotrophic Lateral Sclerosis and Frontotemporal Degeneration. 2013;14(2):127-31.
15. Carrillo-Esper R, Pérez-Calatayud Á A, Arch-Tirado E, Díaz-Carrillo MA, Garrido-Aguirre E, Tapia-Velazco R, et al. Standardization of Sonographic Diaphragm Thickness Evaluations in Healthy Volunteers. Respir Care. 2016;61(7):920-4.
16. Sartucci F, Pelagatti A, Santin M, Bocci T, Dolciotti C, Bongioanni P. Diaphragm ultrasonography in amyotrophic lateral sclerosis: a diagnostic tool to assess ventilatory dysfunction and disease severity. Neurological Sciences. 2019;40(10):2065-71.
17. Henke C, Spiesshoefer J, Kabitz HJ, Herkenrath S, Randerath W, Brix T, et al. Characteristics of respiratory muscle involvement in myotonic dystrophy type 1. Neuromuscular Disorders. 2020;30(1):17-27.
18. Ruggeri P, Lo Monaco L, Musumeci O, Tavilla G, Gaeta M, Caramori G, et al. Ultrasound assessment of diaphragm function in patients with late-onset Pompe disease. Neurological Sciences. 2020.

19. Kooragayalu S, Lim L, Aldrich TK. Diaphragm Thickness and Function in Obese Individuals. B29 RESPIRATORY MUSCLE AT WORK: IS IT 'ALL ABOUT THAT BASS'? American Thoracic Society International Conference Abstracts: American Thoracic Society; 2015. p. A2676-A.
20. Boussuges A, Rives S, Finance J, Chaumet G, Vallée N, Risso J-J, et al. Ultrasound Assessment of Diaphragm Thickness and Thickening: Reference Values and Limits of Normality When in a Seated Position. Frontiers in Medicine. 2021;8(1982).
21. Fogarty MJ, Mantilla CB, Sieck GC. Breathing: Motor Control of Diaphragm Muscle. Physiology (Bethesda). 2018;33(2):113-26.
22. Culver BH. How should the lower limit of the normal range be defined? Respir Care. 2012;57(1):136-45; discussion 43-5.
23. Quanjer PH, Stanojevic S, Cole TJ, Baur X, Hall GL, Culver BH, et al. Multi-ethnic reference values for spirometry for the 3–95-yr age range: the global lung function 2012 equations. European Respiratory Journal. 2012;40(6):1324-43.
24. Laveneziana P, Albuquerque A, Aliverti A, Babb T, Barreiro E, Dres M, et al. ERS statement on respiratory muscle testing at rest and during exercise. Eur Respir J. 2019;53(6).
25. Poulard T, Bachasson D, Fossé Q, Niérat MC, Hogrel JY, Demoule A, et al. Poor Correlation between Diaphragm Thickening Fraction and Transdiaphragmatic Pressure in Mechanically Ventilated Patients and Healthy Subjects. Anesthesiology. 2021.
26. Oppersma E, Hatam N, Doorduin J, van der Hoeven JG, Marx G, Goetzenich A, et al. Functional assessment of the diaphragm by speckle tracking ultrasound during inspiratory loading. J Appl Physiol (1985). 2017;123(5):1063-70.
27. Bachasson D, Dres M, Niérat MC, Gennisson JL, Hogrel JY, Doorduin J, et al. Diaphragm shear modulus reflects transdiaphragmatic pressure during isovolumetric inspiratory efforts and ventilation against inspiratory loading. J Appl Physiol (1985). 2019;126(3):699-707.
28. Pillen S, Boon A, Van Alfen N. Muscle ultrasound. Handb Clin Neurol. 2016;136:843-53.
29. Coiffard B, Riegler S, Sklar MC, Dres M, Vorona S, Reid WD, et al. Diaphragm echodensity in mechanically ventilated patients: a description of technique and outcomes. Crit Care. 2021;25(1):64.



Chapter 6

Interplay Between Diaphragm Thickening, Force Generation, and Lung Volume Change: A Physiological Study in Health and Diaphragm Weakness

Jeroen LM van Doorn
Joris SM van Doremalen
Baziel GM van Engelen
Nicol C Voermans
Chris L de Korte
Coen AC Ottenheijm
Jonne Doorduin

Published in:
Thorax, 2026

Abstract

Introduction: Diaphragm ultrasound is increasingly used to assess diaphragm function. Diaphragm thickening (DTF) is widely interpreted as a surrogate of diaphragm force generation. However, the independent contributions of force generation and lung volume change to diaphragm thickening remain unclear. This study aimed to determine the interplay between DTF, force generation and lung volume change.

Methods: Healthy participants and patients with a congenital myopathy performed unloaded concentric contractions, isometric contractions and loaded concentric contractions. Mouth pressure (Pmo), volume and DTF was recorded and transdiaphragmatic pressure (Pdi) was measured in healthy participants. Leakage during isometric efforts was modelled to assess its impact on lung volume change.

Results: Twenty healthy participants and 21 patients completed unloaded concentric contractions and isometric contractions. During isometric contractions, Pmo and Pdi increased without an increase in DTF in either group (5.2%; -13.5%-23.9% to 5.0%; -12.6%-22.4%, p=1.000 and -8.3%; -26.6%-10.0% to -15.8%; -33.0%-1.3%, p=0.999, respectively). However, DTF increased during unloaded concentric contractions (21.9%; 1.2%-42.6% to 105.4%; 88.1%-122.7%, p<0.001 and 7.9%; -12.1%-27.9% to 84.5% ;67.6%-101.5%, p<0.001, respectively). In an additional cohort (21 healthy participants and 21 patients) DTF increased with increasing lung volume (16.5%; 4.2%-28.7%; to 134.9%; 123.1%-146.7%, p<0.001 and 7.4%; -7.0%-21.8% to 49.5%; 36.0%-63.1%, p<0.001, respectively), but did not differ across inspiratory loading up to 50% of maximal inspiratory pressure. Modelling demonstrated that leakage during isometric efforts may induce lung volume changes sufficient to increase DTF.

Discussion: In physiological breathing, diaphragm contraction results in diaphragm thickening and lung volume increase. Diaphragm thickening relates to lung volume change associated with muscle shortening during muscle contraction rather than force generation per se developed by the contraction.

Introduction

Ultrasound has become an increasingly popular technique for evaluating diaphragm function due to its non-invasive nature and the widespread availability of ultrasound machines in hospitals. Currently, diaphragm ultrasound is being utilized in patients with critical illness, neuromuscular disorders, respiratory disorders or COVID-19 [**Chapter 2**][1, 2].

Conventional diaphragm ultrasound can be used to measure diaphragm thickness and excursion. However, there remains considerable debate regarding the physiological and clinical significance of these parameters. The diaphragm thickening fraction (DTF) during inspiration is frequently and widely interpreted as a surrogate of force generation, that is the pressure-generating capacity of the diaphragm [3-5]. Nonetheless, several studies have reported a poor correlation between DTF and inspiratory effort [6, 7], whereas others have demonstrated an association between DTF and changes in lung volume [8, 9]. Given the uncertainty as to whether DTF reflects diaphragm force generation, a lung volume change or a combination of both, ultrasound-derived measures of diaphragm thickening cannot be interpreted unambiguously. A clearer physiological delineation of the determinants of DTF is therefore required to enable valid clinical interpretation and to guide the design and methodological standardization of future studies.

Diaphragm physiology is complex, and the extent of diaphragm thickening is strongly determined by the type of breathing manoeuvre performed during assessment. Different manoeuvres have therefore been used to examine the relation between diaphragm thickening and diaphragm force generation. Isometric contractions, typically performed as voluntary efforts against a closed airway, intend to measure respiratory muscle strength [10, 11]. In contrast, unloaded concentric contractions, such as deep inhalation, are commonly used to evaluate pulmonary function [8, 9, 11]. However, concentric contractions are never truly unloaded due to the respiratory system compliance, and occlusion maneuvers are not strictly isometric due to intentional leakage and compliance-related volume displacement. Inspiratory resistance manoeuvres mitigate these limitations and achieve loaded concentric contractions [6, 7] that provide a better comparison to increased work of breathing in pathology. The use of different breathing manoeuvres that impose distinct mechanical and physiological conditions on the diaphragm likely contributes to the ongoing debate regarding the relationship between diaphragm thickening, force generation, and lung volume.

Therefore, this study aims to determine the complex relationship between diaphragm thickening, force generation, and lung volume change in healthy subjects and patients with respiratory muscle weakness, using different breathing manoeuvres. Furthermore, we evaluate the influence of leakage as a source of bias in the assessment of diaphragm thickening during isometric loading. We hypothesize that DTF is poorly associated with force generation, but is strongly related to changes in lung volume.

Methods

Study population

Healthy participants and patients with a congenital myopathy as a model for diaphragm weakness were included, between 18 and 60 years old. Inclusion criterion for healthy participants was absence of pulmonary disease and/or neuromuscular disease. Healthy participants were recruited through advertisements. Inclusion criteria for patients were a genetically confirmed congenital myopathy [12] and the ability to breathe independently while lying supine during measurements. Patients were recruited by the neurologist at the Neuromuscular Centre of Expertise of the Radboud university medical centre. All participants provided written informed consent and all procedures were carried out in accordance with the ethical principles as laid down in the declaration of Helsinki. This study was approved by the local ethics committee.

Study design

In this prospective physiological study, two experimental phases were performed with different breathing manoeuvres. In phase 1, we evaluated diaphragm thickening in both patients and healthy participants during deep inspiration to evaluate unloaded concentric contractions and (sub)maximal efforts against an occluded airway to evaluate isometric contractions. A nasogastric catheter with an oesophageal and gastric balloon was placed in healthy participants to measure transdiaphragmatic pressure (Pdi), the gold standard for force-generating capacity of the diaphragm [11, 13]. In phase 2, diaphragm thickening was evaluated in both patients and healthy participants during spontaneous breathing under varying levels of resistive load, in order to better replicate physiological loaded breathing.

Experimental procedures

In phase 1, participants were instructed to breathe in as deeply as possible. Diaphragm thickness was obtained at resting end-expiration and at 25%, 50%, 75% and 100% of inspiratory volume in a single manoeuvre. In subsequent manoeuvres, the mouthpiece was occluded, and the participants were presented with their real-time mouth pressure (Pmo) on a screen, together with a target line. The target line was set at 20%, 40% and 60% of the participants' maximal inspiratory pressure (PImax). Participants were instructed to inhale and try to keep their Pmo at the level of the target line. Consecutively, participants were instructed to inhale as forcefully as possible against the occluded airway. Diaphragm thickness was acquired when Pmo was at 20%, 40%, 60% of PImax, and at maximal Pmo. All manoeuvres were repeated three times and the average diaphragm thickness at that level was used for analysis.

In phase 2, participants were instructed to breathe through a tapered flow inspiratory resistance (POWERbreathe KH2, POWERbreathe Internation Ltd, Southam, UK), set at a loading of 10%, 20%, 30%, 40% and 50% of their PImax. The first, third and fifth breath at the target loading were recorded, during which diaphragm thickness was acquired at 10% increments of maximal

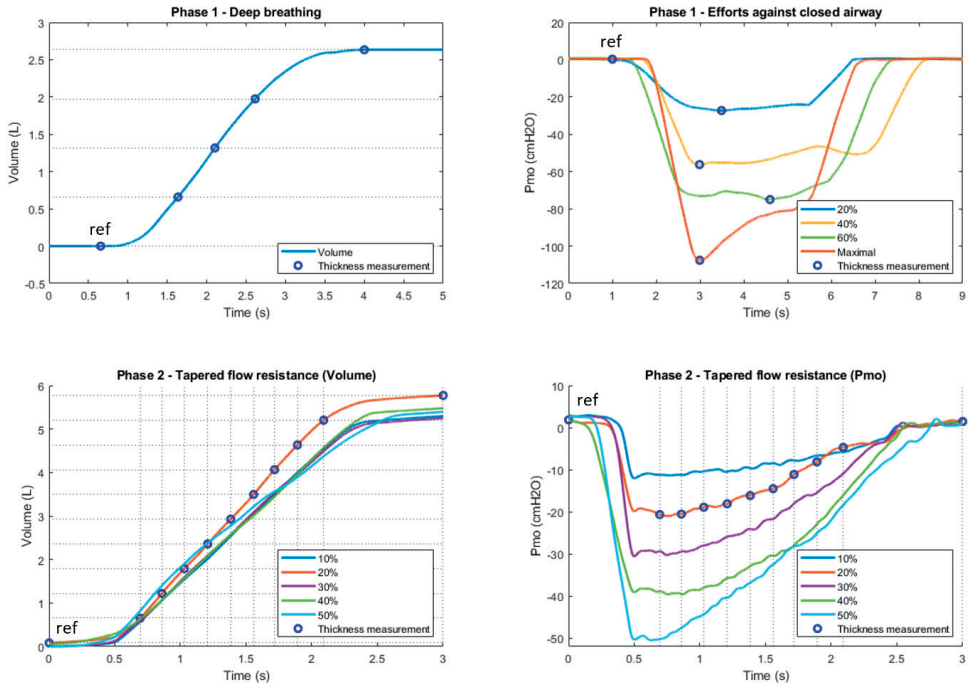


Figure 1: Overview of the study procedures. During deep breathing in phase 1, participants were instructed to inhale as deeply as possible, and diaphragm thickness was measured at the moment of 0%, 25%, 50%, 75% and 100% of maximal inhaled volume (dashed lines). During the efforts against a closed airway in phase 1, four different manoeuvres were performed at 20%, 40%, 60% of PImax and maximal effort, and diaphragm thickness was measured at the maximal pressure. During the tapered flow breathing of phase 2, participants were instructed to inhale deeply against resistance and diaphragm thickness was sampled at the moment (vertical dashed lines) of 10% increments of inhaled volume (horizontal dashed lines). Data are from representative participants, and example methodology was only displayed for 20% loading in phase 2.

inspiratory volume during that breath. Diaphragm thickness acquired at each volume level was averaged over the three breaths and used for analysis. See figure 1 for an overview of the procedures.

Respiratory function testing

Pulmonary function was assessed with a hand-held spirometer. Forced vital capacity (FVC), forced expiratory volume in the first second (FEV1), and Tiffeneau index (FEV1/FVC) were obtained in sitting position and while supine. All values were compared to reference values to derive a predicted value [14]. Maximal inspiratory pressure (PImax) and maximal expiratory pressure (PEmax) were obtained during respiratory muscle strength testing using a portable electronic manometer. All testing was performed in line with the ERS statement on respiratory function testing [11]. In phase 1, the SpiroUSB (Vyaire Medical connected to PC Spirometry software, Spida CareFusion 2.3.0.10 for Windows 7) and Micro RPM (Micro Medical, CareFusion,

United Kingdom) were used for respiratory function testing. Due to malfunction of these devices between the phases, a new device was used for phase 2 (Pneumotrac with RMS connected to Spirotrac, Vitalograph Ltd, Maids Moreton, United Kingdom). The results obtained with the device used in phase 1 were valid up to its malfunction.

Ultrasound scanning and image processing

Ultrasound measurements were performed with the Aplio i800 ultrasound system, equipped with the PLT-1005BT 5-14 MHz linear transducer (Canon Medical Systems Europe BV, Amstelveen, the Netherlands). The diaphragm was scanned at the zone of apposition following a previously published protocol [**Chapter 5**]. In short, the zone of apposition was visualized on the anterior axillary line, typically between the 7^{th} and 9^{th} intercostal space, with the probe oriented craniocaudally. The diaphragm is recognized as a hypoechoic structure between two hyperechoic lines indicating the pleural and peritoneal membranes, between two ribs. Diaphragm thickness (DT) was acquired by placing electronic callipers between the peritoneal and pleural hyperechoic lines. Diaphragm thickening fraction (DTF) was calculated with ((DT – DTref) / DTref) * 100. B-mode video clips were saved, ultrasound settings were standardized during the entire study, and manual compression was kept as minimal as possible. See Figure 2 for example images.

Signal acquisition and processing

During all ultrasound measurements, participants were seated semi-recumbent and were breathing through a mouthpiece while wearing a nose clip. The mouthpiece was connected through a sample port to the DA100C module equipped with TSD160E transducers of the MP160 amplifier system (BIOPAC systems, Inc, Goleta, CA, USA), allowing for continuous measurement of mouth pressure (Pmo). A pneumotachograph was connected to the amplifier through a TSD160A transducer and DA100C module, to continuously measure flow, and therefore, volume. If applicable, a nasogastric catheter with a balloon in the oesophagus and stomach (Type C76080U, Marquat Genie Biomedical, Boissy-Saint-Leger, France) was connected to the amplifier, through custom transducers to additional DA100C modules. After validating the position of the catheter following standard procedures, this allowed for measurement of oesophageal pressure (Pes) and gastric pressure (Pga), and by subtracting Pes from Pga, Pdi [13]. A foot-pedal was used to operate the ultrasound device, that was simultaneously connected to the amplifier, thus allowing offline synchronization of B-mode ultrasound video acquisition with Pmo, Pdi, flow, and volume.

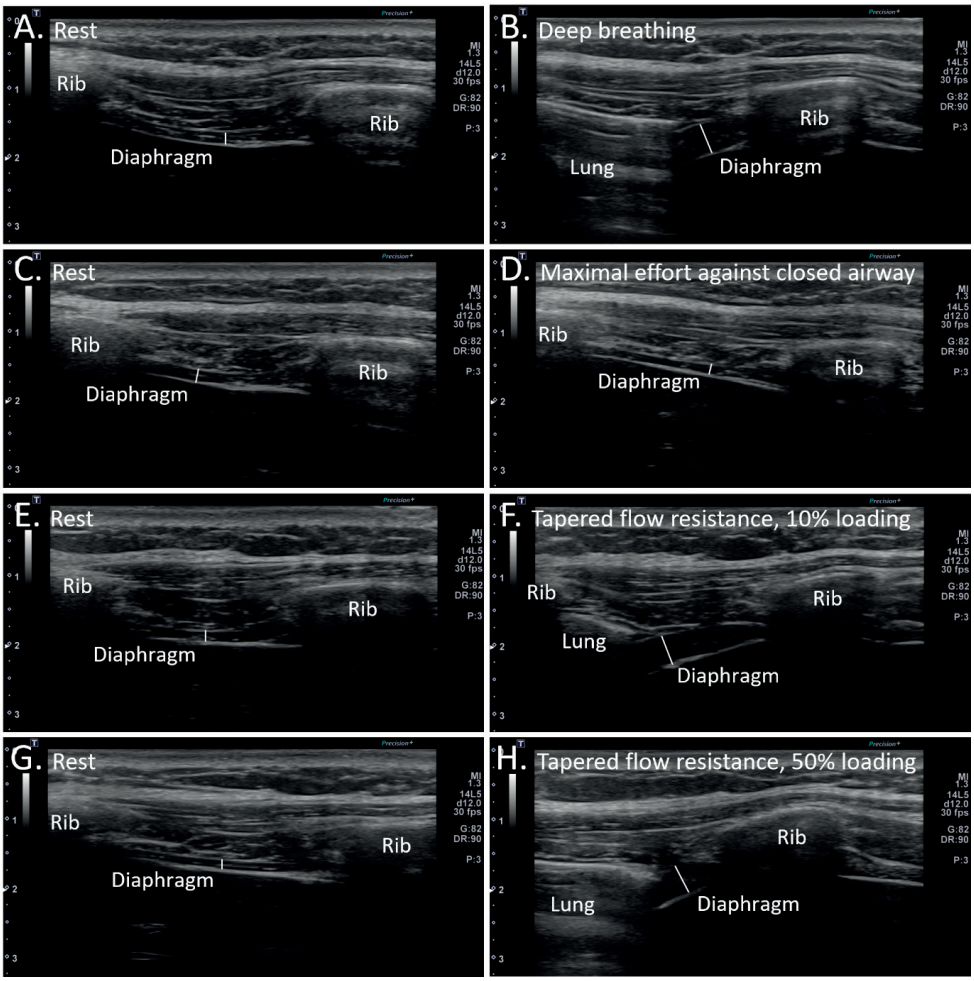


Figure 2: Example images of diaphragm ultrasound during different breathing manoeuvres. The left images represent resting end-expiration before performing the manoeuvre and the right images represent sample moment during the manoeuvre. A, B: deep breathing. C, D: maximal effort against a closed airway. E, F: tapered-flow resistance with 10% loading. G, H: tapered-flow resistance with 50% loading.

Leakage simulation

In phase 1, the efforts against an occluded airway were performed with a small leak to ensure glottal patency and to avoid the use of the cheek muscles [10]. Although small, the leak introduces a volume change which influences the isometric nature of the manoeuvre. To estimate lung volume change during the maximal effort, the leakage was modelled with the orifice flow equation:

$$Q = C_d A \sqrt{\frac{2\Delta P}{\rho}}$$

In this study, the sharp edged orifice had a discharge coefficient C_d of 0.60, the leak area A was a diameter of 1.7 mm, the median PImax of healthy participants in phase 1 was used for pressure differential ΔP and standard air density ρ of 1.226 kg/m^3 at 20˚C and 101.325 kPa was used. Flow per second Q over the orifice was estimated over a standard manoeuvre duration of 4 seconds. Different scenarios were explored: increased discharge coefficient of 0.98 due to different orifice configuration and an increased leak area up to 3.4 mm.

Statistical analysis

This study was part of a larger study into the use of respiratory muscle ultrasound in congenital myopathies for which a sample size estimation was performed, resulting in 21 participants and 21 patient, in phase 1 as well as in phase 2.

Linear mixed modelling was used after checking their assumptions to assess differences between unloaded concentric breathing and isometric contraction in phase 1, and to assess the effect loading on concentric contractions in phase 2, using R software version 4.4.1 with packages lme4 version 1.1-37 and emmeans version 1.11.1 [15].

Starting at a full factorial model with random intercepts and slopes, Akaike's information criterion (AIC) was used to select the optimal set of covariates without overfitting. Analysis of estimated marginal means was used to statistically test the following conditions: 1) the change in diaphragm thickening during unloaded concentric contractions in patients and healthy participants. 2) the change in diaphragm thickening during isometric contractions in patients and healthy participants. 3) the change in diaphragm thickening during the loading conditions in patients and healthy participants in phase 2.

In phase 1, the following model was used:

$$DTR_i = (\beta_0 + u_{0i}) + (\beta_1 + u_{1i}) \bullet Goal_i + (\beta_2 + u_{2i}) \bullet Goal_i^2 + \beta_3 \bullet Manoeuvre_i + \beta_4 \bullet Type_i +$$

$$\beta_5 \bullet (Goal_i \times Manoevre_i) + \beta_6 \bullet \left(Goal_i^2 \times Manoevre_i\right) +$$

$$\beta_7 \bullet (Goal_i \times Type_i) + \beta_8 \bullet \left(Goal_i^2 \times Type_i\right) + \epsilon_i$$

With a random intercept for each participant (u_{0i}), and random slopes for each participant (u_{1i} and u_{2i}). Goal was coded as from 0% to 100% of either deep inspiration or effort against the occluded airway, Manoeuvre was coded as either deep inspiration or effort against the occluded airway and Type was coded as either healthy participant and patient. Goal was centred and scaled. ϵ_i denotes the error term.

In phase 2, the following model was used:

$$DTR_i = (\beta_0 + u_{0i}) + \beta_1 \bullet Loading_i + \beta_2 \bullet Volume_i + \beta_3 \bullet {Volume_i}^2 + \beta_4 \bullet Type_i +$$

$$\beta_5 \bullet (Volume_i \times Type_i) + \beta_6 \bullet \left({Volume_i}^2 \times Type_i\right) + \epsilon_i$$

With a random intercept for each participant (u_{0i}). Loading was coded as 10%, 20%, 30%, 40%, 50%, Volume was normalized from 0% to 100% of individual inspiratory capacity, and Type was coded as either healthy participant and patient. Loading, Volume and Volume^2 were centred and scaled. ϵ_i denotes the error term.

Results

Participants

21 patients and 20 healthy participants were included in phase 1. Patients had variants in the following genes: *RYR1* (n=5), *TTN* (n=5), *DNM2* (n=3), *NEB* (n=2), *COL6A3* (n=1), *BIN1* (n=1), *LMOD3* (n=1), *TPM3* (n=1), *MTM1* (n=1) and *KBTBD13* (n=1). 21 patients and 21 healthy participants were included in phase 2. Patients had variants in the following genes: *RYR1* (n=7), *KBTBD13* (n=6), *SEPN1* (n=3), *MTM1* (n=2), *BIN1* (n=1), *TTN* (n=1), *DNM2* (n=1). Four patients with the *SEPN1* and *DNM2* variants did not tolerate inspiratory loading, and technical failure led to missing data in the patient with the *BIN1* variant in both phases, patients were slightly older than healthy participants, had weaker respiratory muscles, and their pulmonary function was consistent with restrictive pathology. Two healthy participants of phase 1 did not tolerate nasogastric catheterization, resulting in missing Pga, Pes, and Pdi while in two additional healthy participants, technical failure led to those parameters missing. Participant characteristics are presented in Table 1.

Phase 1: isometric contraction and unloaded concentric contraction

As can be seen in Figure 3, DTF increased during deep inspiration in healthy participants (from 21.9%; 1.2%-42.6% to 105.4%; 88.1%-122.7%, p < 0.001), but not during efforts against a closed airway (from 5.2%; -13.5%-23.9% to 5.0%; -12.6%-22.4%, p = 1.000). Also in patients, DTF increased during deep inspiration (from 7.9%; -12.1%-27.9% to 84.5%; 67.6%-101.5%, p < 0.001), but not during efforts against a closed airway (from -8.3%; -26.6%-10.0% to -15.8%; -33.0%-1.3%, p = 0.999).

Phase 2: loaded concentric contractions

As can be seen in Figure 4, DTF increased in healthy participants during inspiration from 10% IC to an average maximum of 71.4% (from 16.5%; 4.2%-28.7% to 134.9%; 123.1%-146.7%, p < 0.001), as well as in patients from 10% IC to an average maximum of 66.2% (from 7.4%; -7.0%-

21.8% to 49.5%; 36.0%-63.1%, p < 0.001). However, the increase in DTF during the inspiratory phase did not differ across loads of 10% to 50% of PImax in either group.

Transdiaphragmatic pressure

There was a strong correlation between Pdi and Pmo during efforts against a closed airway in healthy participants (R = -0.87, p < 0.001, see figure 5), indicating that Pmo may serve as a surrogate for force generated by the diaphragm in the other experimental groups.

Table 1. Participant characteristics.

	Phase 1 – HC (n=20)	**Phase 1 – patient (n=21)**	**p-value**	**Phase 2 – HC (n=21)**	**Phase 2 – patient (n=21)**	**p-value**
Age (y)	22.5 [20.0; 25.5]	34.0 [22.0; 42.0]	**p = 0.047**	28.1 [26.5; 29.5]	42.5 [29.5; 52.3]	**p = 0.006**
BMI (kg/m2)	22.4 [20.9; 25.5]	24.8 [20.5; 27.2]	p = 0.434	22.8 [20.4; 24.2]	24.6 [20.7; 26.2]	p = 0.339
Sex (n male)	8	11	p = 0.630	8	8	p = 1.000
FVC (L)	4.72 [3.97; 5.09]	3.11 [2.33; 4.12]	**p < 0.001**	4.60 [4.16; 5.69]	2.54 [1.76; 3.68]	**p < 0.001**
FVC (%)	96.8 [88.7; 106.8]	62.9 [55.1; 82.6]	**p < 0.001**	98.68 [94.4; 102.3]	73.9 [45.6; 83.6]	**p < 0.001**
FEV1 (L)	3.72 [3.33; 4.57]	2.68 [2.00; 3.28]	**p < 0.001**	3.95 [3.41; 4.52]	2.06 [1.63; 3.10]	**p < 0.001**
FEV1 (%)	94.5 [91.2; 103.7]	64.5 [56.1; 88.4]	**p < 0.001**	96.1 [86.5; 103.4]	68.7 [49.6; 82.0]	**p < 0.001**
FEV1/FVC	0.84 [0.82; 0.86]	0.84 [0.80; 0.86]	p = 0.917	0.83 [0.80; 0.86]	0.83 [0.76; 0.93]	p = 0.529
Drop in FVC sit to supine (L)	0.11 [0.02; 0.21]	0.21 [0.05; 0.33]	p = 0.215	0.18 [0.14; 0.29]	0.21 [0.17; 0.38]	p = 0.320
PCF (L/min)	422.50 [365.75; 492.25]	356.00 [300.00; 394.00]	p = 0.059	411.00 [388.20; 454.80]	396.60 [323.40; 455.40]	p = 0.218
PImax (cmH2O)	101.5 [90.5; 113.5]	81.0 [39.0; 84.0]	**p < 0.001**	95.0 [83.1; 114.6]	65.0 [48.8; 91.4]	**p < 0.001**
PEmax (cmH2O)	122.5 [112.0; 133.3]	81.0 [59.0; 103.0]	**p < 0.001**	104.9 [86.2; 119.0]	62.0 [47.5; 84.0]	**p = 0.002**
Tee (mm)	2.02 [1.75; 2.30]	1.89 [1.66; 2.36]	p = 0.708	1.63 [1.39; 2.02]	1.79 [1.42; 2.69]	p = 0.372
Tei (mm)	4.14 [3.54;5.51]	3.27 [2.44; 4.61]	p = 0.134	5.04 [3.89; 6.18]	3.89 [2.37; 5.08]	**p = 0.040**
DTF	116.8% [75.9%; 131.1%]	53.7% [31.9%; 112.1%]	**p = 0.038**	187.4% [139.8%; 250.6%]	72.6% [18.78%; 110.3%]	**p < 0.001**

Data are presented as median [p25; p75]. p-values were obtained with the Mann-Whitney-U test or the chi-squared test. BMI: Body mass index. FVC: forced vital capacity. FVC%: predicted value of FVC. FEV1: Forced expiratory volume in the first second. FEV1%: predicted value of FEV1. PCF: Peak cough flow. PImax: pressure during a maximal inspiratory effort against a closed airway. PEmax: pressure during a maximal expiratory effort against a closed airway. Tee: Resting end-expiratory diaphragm thickness. Tei: Maximal end-inspiratory diaphragm thickness. DTF: Diaphragm thickening fraction

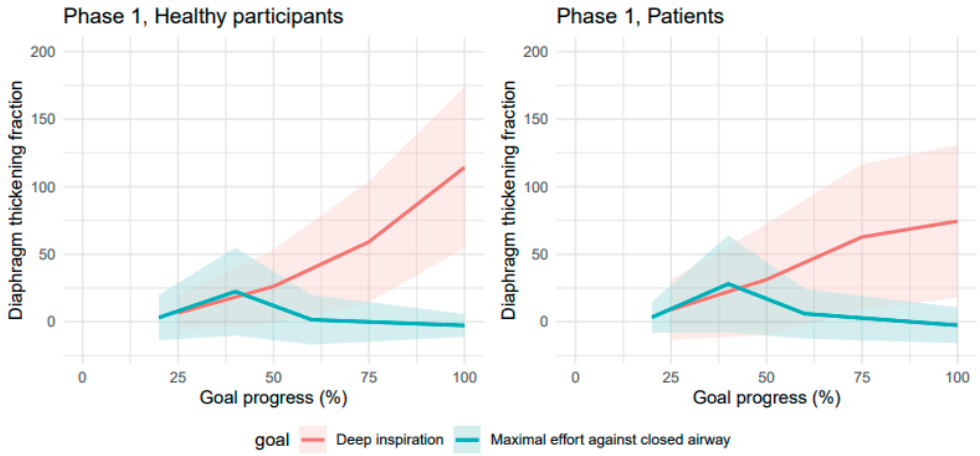


Figure 3: Diaphragm thickening fraction (DTF) during deep inspiration and efforts against a closed airway in phase 1. The left panel presents healthy participants and the right panel presents patients.

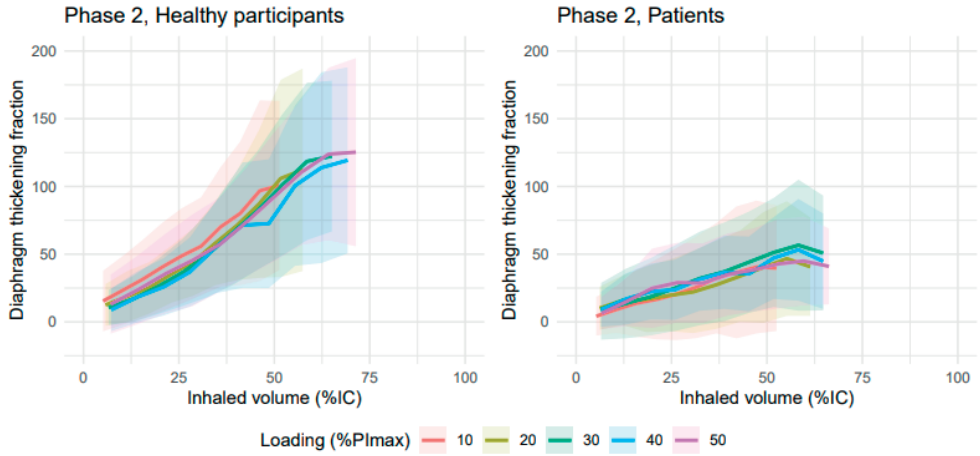


Figure 4: Diaphragm thickening fraction (DTF) during tapered flow resistance breathing in phase 2. The left panel presents healthy participants and the right panel presents patients.

Leakage simulation isometric loading

See Figure 6 for the leakage simulation results. With a discharge coefficient of 0.60 of a sharp edged orifice, leak diameter of 1.7 mm and a median pressure differential of 101.5 cmH_2O, lung volume was estimated to increase with 0.69 L through the leak during a sustained effort of 4 seconds. Under the same conditions, but with a discharge coefficient of 0.98 due to using rounded corners of the orifice, estimated lung volume increase was 1.13 L. Conversely, when only doubling the leak diameter, estimated lung volume increase was 2.78 L. When both doubling the leak diameter and using rounded corners, estimated lung volume increase was 4.54 L. These volumes constitute respectively 15%, 24%, 59% and 96% of FVC in healthy participants of phase 1. When entering that into the mixed effects model that was fitted on the data of phase 1, 15% and 24% of lung volume increase does not result in a significant difference in DTF between deep inspiration and efforts against a closed airway (7.8%; -12.9%-28.5% vs 5.9%; -11.8%-23.5%, p=1.000 for 15% and 17.6%; -0.9%-36.6% vs 5.8%; -10.1%-21.8%, p=0.931 for 24%), but there is a difference at 59% and 96% increase (56.8%; 43.1%-70.5% vs 5.8%; -6.8%-18.3%, p<0.001 for 59% and 98.0%; 81.7%-114.4% vs 5.7%; -10.8%-22.2%, p<0.001 for 96%). This indicates that a manoeuvre that intends to achieve an isometric contraction, may not be considered isometric depending on the leak configuration.

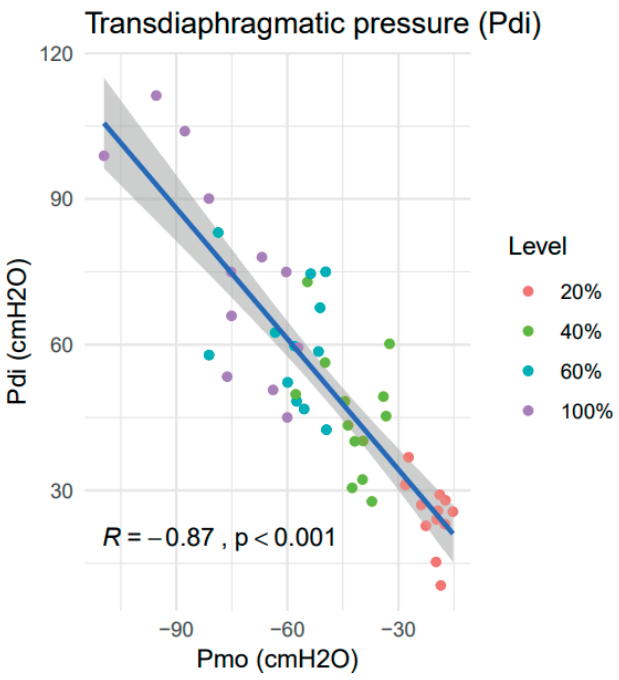


Figure 5: Mouth pressure (Pmo) and transdiaphragmatic pressure (Pdi) during efforts against a closed airway in healthy participants.

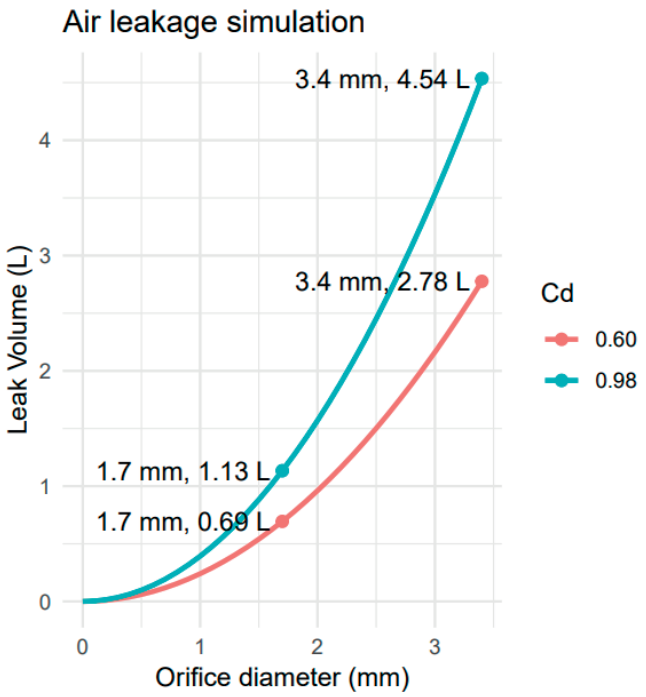


Figure 6: Air leakage simulation during voluntary efforts. Cd: discharge coefficient of the orifice.

Discussion

The present study demonstrated that diaphragm thickening measured by ultrasound is primarily determined by changes in lung volume rather than by the force generated by the diaphragm, during both isometric loading and physiological concentric loading. This relationship was consistently observed in healthy subjects as well as in patients with respiratory muscle weakness, underscoring its physiological robustness across populations. By disentangling the effects of lung volume change and force generation, we provide novel and clinically relevant insight into the determinants of diaphragm thickening. These findings have important implications for the interpretation of diaphragm ultrasound and warrant caution when using diaphragm thickening as a surrogate of diaphragm force generation in research and clinical practice.

Diaphragm thickening during loading

During different levels of isometric loading no thickening of the diaphragm was observed, even at maximal loading, which is in contrast to previous reports [10]. This may be attributed to differences in leak configuration during occlusion manoeuvres. Leak characteristics are rarely specified, yet our modelling demonstrates that even small leaks may induce substantial lung volume displacement, thereby increasing DTF independent of generated force. This may explain

the observed discrepancy between the current and previous studies, and future studies should report leak configuration. The observed relation between DTF and a change in lung volume we found during unloaded deep inspiration is consistent with previous literature [8, 16].

Importantly, we also demonstrate that during physiological tidal breathing, the relationship between lung volume and DTF remains unchanged with increasing inspiratory loads (up to 50% of PImax). This key finding indicates that DTF at a given lung volume is independent of the inspiratory pressure generated by the diaphragm. This strongly suggest that DTF cannot be used as a surrogate of diaphragm force generation. The loaded concentric contraction conditions of phase 2 addressed the methodological challenges of the isometric and unloaded concentric contraction conditions, controlling diaphragm force generation as well as changes in lung volume.

Several studies have investigated the relation between DTF, diaphragm force generation and lung volume change [3, 7, 17]. However, these studies were not specifically designed to disentangle this relationship, lacked comparison across healthy participants and patient populations, failed to tightly control variables, or were based on circumstantial evidence. The strength of the current study is that these factors were included, providing direct evidence for the relation between DTF, diaphragm force generation and lung volume change, confirming the alluded to relation in previous work.

From a physiological perspective, our findings align closely with established muscle physiological concepts. Thickening of a skeletal muscle is a direct result of muscle shortening: as sarcomeres shorten, radial expansion occurs to preserve muscle volume. Accordingly, it is expected that as the diaphragm contracts and the lung expands, the diaphragm shortens and thickens regardless of the inspiratory pressure generated. Conversely, it is also expected that the diaphragm does not shorten when performing an isometric contraction, fiber length does not change and thickening should not occur or minimally due to compliance of the respiratory system. The absence of increased DTF during isometric efforts and its increase during lung expansion confirm this mechanical behavior.

Clinical implications

Our findings indicate that DTF should not be interpreted as a surrogate of diaphragm force generation, but primarily reflect the geometric consequences of muscle shortening and its associated change in lung volume. However, because muscle weakness limits the muscles ability to shorten against the load of the respiratory system, patients with diaphragm weakness will exhibit reduced DTF. This is illustrated by the consistently lower DTF in patients with respiratory muscle weakness in our study. Our findings therefore do not negate the clinical value of diaphragm ultrasound for specific applications. Reduced DTF may still support the diagnosis

of diaphragm dysfunction in patients with unexplained dyspnea, neuromuscular disorders and critically ill patients [18].

In critically ill patients, diaphragm ultrasound can also be used to determine whether the diaphragm is active during mechanical ventilation. Prior studies have consistently shown that DTF increases as ventilatory support is reduced, whereas minimal to no thickening is observed during controlled mechanical ventilation under neuromuscular blockade [3, 19]. Accordingly, diaphragm ultrasound is a reliable tool to assess whether the diaphragm contributes to tidal volume generation in mechanically ventilated patients. However, it does not allow quantification of the magnitude of pressure generated during diaphragm activation, and therefore cannot distinguish between low and high force generation. Indeed, previous findings have demonstrated that there is a poor correlation between Pdi and DTF [6, 7]. However, these papers did not control for changes in tidal volume.

When the objective is to assess force generation, direct pressure measurements - preferably transdiaphragmatic pressure, followed by esophageal or mouth pressure - remain necessary. In this context, indices such as maximal inspiratory pressure in cooperative patients or occlusion pressures in mechanically ventilated patients more accurately reflect diaphragm force generation than diaphragm thickening assessed by ultrasound.

Methodological considerations

Several methodological aspects merits consideration. First, the PImax manoeuvre was performed in the sitting position, while the effort against a closed airway was performed in the semi recumbent position. While Pmo during efforts at 20%, 40% and 60% of PImax were at those intended levels, Pmo during maximal efforts was lower than PImax, and therefore, the Pmo levels during the target pressures were higher than intended. Second, the sample rate of the ultrasound device allowed for measuring DTF at multiple points during deep inspiration, but was not sufficient for measuring DTF at multiple points during the faster efforts against a closed airway. Therefore, the deep inspiration manoeuvre had to be performed only once, while the efforts against a closed airway had to be performed four times. Anticipation of target intensities may have influenced participant performance. Third, our experiment did not included a condition with (partial) passive inflation that can study the effects of changes in tidal volume without diaphragm activation.

In conclusion, ultrasound of the diaphragm is widely used to asses diaphragm function, yet its interpretation requires careful physiological consideration. In physiological breathing, diaphragm contraction results in diaphragm thickening and lung volume increase. Clinicians and researchers should be aware that diaphragm thickening relates to lung volume change associated with muscle shortening during muscle contraction rather than force generation per se developed by the contraction.

References

1. Tuinman, P.R., et al., *Respiratory muscle ultrasonography: methodology, basic and advanced principles and clinical applications in ICU and ED patients-a narrative review.* Intensive Care Med, 2020. **46**(4): p. 594–605.
2. Boussuges, A., et al., *Diaphragm dysfunction after severe COVID-19: An ultrasound study.* Front Med (Lausanne), 2022. **9**: p. 949281.
3. Goligher, E.C., et al., *Measuring diaphragm thickness with ultrasound in mechanically ventilated patients: feasibility, reproducibility and validity.* Intensive Care Med, 2015. **41**(4): p. 642–9.
4. Dubé, B.P., et al., *Ultrasound evaluation of diaphragm function in mechanically ventilated patients: comparison to phrenic stimulation and prognostic implications.* Thorax, 2017. **72**(9): p. 811–818.
5. Vivier, E., et al., *Diaphragm ultrasonography to estimate the work of breathing during non-invasive ventilation.* Intensive Care Med, 2012. **38**(5): p. 796–803.
6. Oppersma, E., et al., *Functional assessment of the diaphragm by speckle tracking ultrasound during inspiratory loading.* J Appl Physiol (1985), 2017. **123**(5): p. 1063–1070.
7. Poulard, T., et al., *Poor Correlation between Diaphragm Thickening Fraction and Transdiaphragmatic Pressure in Mechanically Ventilated Patients and Healthy Subjects.* Anesthesiology, 2022. **136**(1): p. 162–175.
8. Wait, J.L., et al., *Diaphragmatic thickness-lung volume relationship in vivo.* Journal of Applied Physiology, 1989. **67**(4): p. 1560–1568.
9. Cohn, D., et al., *Diaphragm thickening during inspiration.* J Appl Physiol (1985), 1997. **83**(1): p. 291–6.
10. Ueki, J., P.F. De Bruin, and N.B. Pride, *In vivo assessment of diaphragm contraction by ultrasound in normal subjects.* Thorax, 1995. **50**(11): p. 1157–61.
11. Laveneziana, P., et al., *ERS statement on respiratory muscle testing at rest and during exercise.* Eur Respir J, 2019. **53**(6).
12. North, K.N., et al., *Approach to the diagnosis of congenital myopathies.* Neuromuscul Disord, 2014. **24**(2): p. 97–116.
13. Mojoli, F., et al., *Technical aspects of bedside respiratory monitoring of transpulmonary pressure.* Ann Transl Med, 2018. **6**(19): p. 377.
14. Quanjer, P.H., et al., *Multi-ethnic reference values for spirometry for the 3-95-yr age range: the global lung function 2012 equations.* Eur Respir J, 2012. **40**(6): p. 1324–43.
15. *R Core Team. R: A Language and Environment for Statistical Computing*. 2019: R Foundation for Statistical Computing.
16. Cardenas, L.Z., et al., *Diaphragmatic Ultrasound Correlates with Inspiratory Muscle Strength and Pulmonary Function in Healthy Subjects.* Ultrasound in Medicine & Biology, 2018. **44**(4): p. 786–793.
17. Formenti, P., et al., *The Effects of Positive End Expiratory Pressure and Lung Volume on Diaphragm Thickness and Thickening.* Diagnostics (Basel), 2023. **13**(6).
18. Boon, A.J., et al., *Sensitivity and specificity of diagnostic ultrasound in the diagnosis of phrenic neuropathy.* Neurology, 2014. **83**(14): p. 1264–70.
19. Umbrello, M., et al., *Diaphragm ultrasound as indicator of respiratory effort in critically ill patients undergoing assisted mechanical ventilation: a pilot clinical study.* Critical Care, 2015. **19**(1): p. 161.



Chapter 7

Shear wave elastography to assess respiratory muscle function in congenital myopathies

Jeroen LM van Doorn
Dieke Jans
Chris L de Korte
Baziel GM van Engelen
Nicol C Voermans
Nens van Alfen
Coen AC Ottenheijm
Damien Bachasson
Jonne Doorduin

Published in:
Muscle & Nerve, 2026

Abstract

Introduction/Aims: Respiratory muscle dysfunction is prevalent in congenital myopathies and often leads to respiratory failure. Ultrasound shear wave elastography (SWE) measures tissue elasticity and has been proposed as an alternative to invasive measures of respiratory muscle contractility. This study aims to evaluate SWE to assess respiratory muscle function in healthy individuals and congenital myopathy patients, while also determining SWE reliability.

Methods: Shear wave velocity in the diaphragm, parasternal intercostal, sternocleidomastoid, external oblique, internal oblique, and transverse abdominal muscles was acquired in healthy participants and congenital myopathy patients during different manoeuvres . Mouth pressure (Pmo) was acquired simultaneously with SWE acquisition. Furthermore, transdiaphragmatic pressure (Pdi) was acquired in healthy participants. All measurements were repeated by two observers to assess reliability.

Results: Twenty-one congenital myopathy patients and 20 healthy participants were included. Shear wave velocity did not differ between healthy participants and patients during any manoeuvre in any muscle, and Pmo and Pdi were not correlated with shear wave velocity. Intra-observer intra-class correlation coefficients (ICC) varied between 0.28-0.95 for healthy participants and 0.62-0.95 for patients. Inter-observer ICC varied between 0.00-0.87 for healthy participants and 0.00-0.79 for patients. Test-retest ICC varied between 0.00-0.66 for healthy participants and 0.00-0.72 for patients.

Discussion: The absence of differences in shear wave velocity between healthy participants and patients, and the low reliability estimates, indicate that SWE of the respiratory muscles is not suitable in routine clinical care or research. The complex mechanical properties of the respiratory muscles introduce challenges that may require alternative SWE techniques

Introduction

Respiratory muscle dysfunction is common in congenital myopathies, resulting in respiratory symptoms such as dyspnoea, sleep disturbances, and lung infections, and it is often the primary cause of death [1]. For patients, accurate periodic assessment of respiratory muscle function is essential for detecting early signs of respiratory insufficiency, monitoring disease progression, and guiding personalized respiratory care. Current preclinical research focuses on the development of genetic therapies, offering the potential for effective treatment [2]. To evaluate the efficacy of these future treatments, clinical trials are in need of relevant and reliable respiratory outcome measures. Transdiaphragmatic pressure (Pdi) is the gold standard for diaphragm contractility [3]. However, the invasive nature of measuring Pdi - using nasogastric catheters - prevents routine usage, especially in paediatric patients and in those severely affected by neuromuscular disorders (NMD) patients. Furthermore, Pdi measures only the overall contractility of the diaphragm, and does not provide information on local contractile properties or specific other respiratory muscles. While the diaphragm is the primary respiratory muscle, accessory inspiratory muscles and expiratory muscles can be severely affected in NMDs and should be evaluated as well [4]. A non-invasive, quantitative method to assess contractility across the respiratory muscles is therefore needed.

Ultrasound imaging is a non-invasive technique that has been widely used to evaluate respiratory muscle function in NMDs [**Chapter 2**]. The diaphragm thickening ratio is often regarded as a surrogate marker of diaphragm contractility [**Chapter 2**, 5]. However, its correlation with the pressure-generating capacity of the diaphragm is weak [6-9], with limited accuracy in diagnosing diaphragm weakness [10]. More recently, ultrasound shear wave elastography (SWE) has been proposed to evaluate diaphragm contractility [11]. SWE uses an acoustic radiation force push to excite tissue, resulting in propagation of a shear wave originating from the push location. The propagation velocity of the shear wave is proportional to tissue stiffness of large tissues like liver and breast: stiffer tissue results in higher propagation velocity, while softer tissue results in lower propagation velocity [12]. Previously, changes in diaphragm stiffness have been demonstrated to reflect changes in Pdi in healthy participants [13]. However, the potential of SWE for detecting respiratory muscle function in congenital myopathies has not yet been evaluated.

Therefore, this study aimed to investigate SWE of the diaphragm, accessory inspiratory muscles, and expiratory muscles, for evaluating respiratory muscle contractility in patients with congenital myopathies compared to healthy controls. Furthermore, reliability of respiratory muscle SWE was evaluated. We hypothesize that SWE is reliably acquired, is associated with contractility and patients with a congenital myopathy have stiffer respiratory muscles than healthy participants.

Methods

Participants

Patients with congenital myopathies and healthy participants were included. Inclusion criteria for patients were a genetically confirmed diagnosis of any congenital myopathy [14], age between 18 and 60 years and the ability to breathe independently while lying supine during measurements. Respiratory insufficiency was not an inclusion criterion. Patients were recruited through their neurologists at the neuromuscular expertise centre of the Radboud university medical centre. Inclusion criteria for healthy participants were age between 18 and 60 years, and absence of pulmonary disease and neuromuscular disease. Healthy participants were recruited through advertisements. Participants with a contraindication for a nasogastric catheter were excluded. All participants provided written informed consent and all procedures were carried out in accordance with the ethical principles as laid down in the declaration of Helsinki. This study was approved by the local ethics committee.

Study design

An overview of the study is presented in Figure 1. All participants were invited for two study visits, with a period of approximately two weeks between visits. During the first visit, respiratory function testing was performed before starting with the ultrasound measurements by the first observer. Additionally, a nasogastric catheter was inserted in healthy participants only to measure Pdi. During the second visit, ultrasound measurements were repeated by the first observer to assess intra-observer reliability and test-retest reliability.

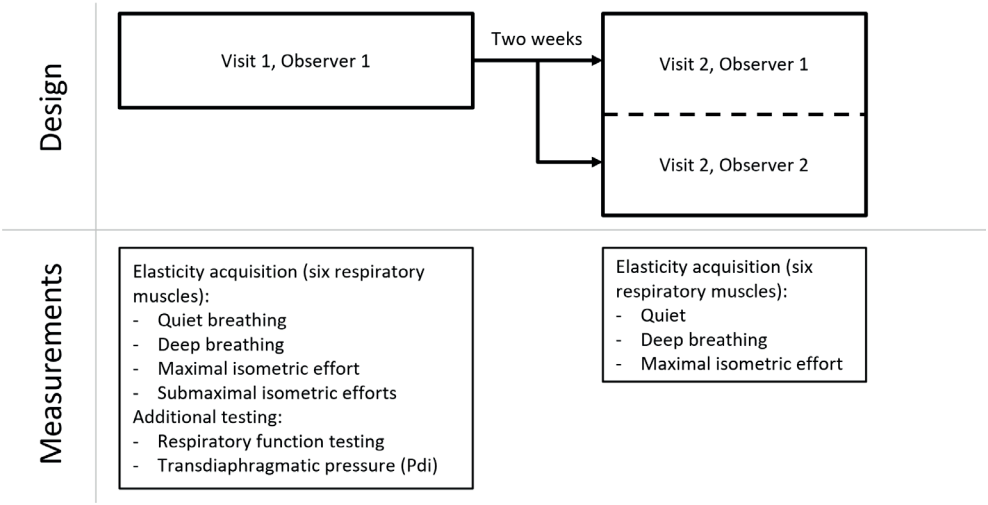


Figure 1: Overview of the study design.

Subsequently, ultrasound measurements were repeated by the second observer to assess inter-observer reliability. Both observers were experienced with respiratory muscle ultrasound scanning through extensive clinical and research practice [**Chapter 2**, **Chapter 5**].

Respiratory function testing

Pulmonary function was assessed with a portable spirometer (SpiroUSB, connected to PC Spirometry software, Spida CareFusion 2.3.0.10 for Windows 7, Vyaire Medical, Mettawa, IL, USA). Forced vital capacity (FVC), forced expiratory volume in the first second (FEV1) and Tiffeneau index (FEV1/FVC) were obtained in the sitting position and while supine. All values were compared to reference values to derive a predicted value [15]. Maximal inspiratory pressure (PImax) and maximal expiratory pressure (PEmax) were obtained during respiratory muscle strength testing using a portable electronic manometer (Micro RPM, Micro Medical, Rhymney, United Kingdom). All testing was performed in line with the ERS statement on respiratory function testing [3].

Ultrasound scanning, shear wave elastography, and image processing

Ultrasound measurements were performed with the Aplio i800 ultrasound system, equipped with the PLT-1005BT 5-14 MHz linear transducer (Canon Medical Systems Europe BV, Amstelveen, the Netherlands). 6 muscles were examined in 4 scanning positions, all on the right side: the diaphragm, parasternal intercostal muscle, sternocleidomastoid muscle, external oblique abdominal muscle, internal oblique abdominal muscle, and transverse abdominal muscle. Ultrasound settings were standardized during the entire study, and manual compression was kept as minimal as possible. See Figure 2 for examples of images of all scanned muscles.

The diaphragm was scanned at the zone of apposition following a previously published protocol [**Chapter 5**]. In brief, the zone of apposition was imaged on the anterior axillary line, typically between the 7th and 9th intercostal space, with the probe oriented craniocaudally. The parasternal intercostal muscle was scanned at the third intercostal space, typically 3-5 cm lateral to the sternum, with the probe oriented craniocaudally. Care was taken to scan lateral to the neurovascular bundle containing the internal thoracic artery. The sternocleidomastoid muscle was scanned halfway on the line between the mastoid process and the sternal clavicular notch, with the probe oriented in line with the muscle fibres. The external oblique abdominal muscle, internal oblique abdominal muscle and transverse abdominal muscle were all scanned halfway between the lowest rib and iliac crest on the anterior axially line, while rotating the probe to be aligned with the muscle fibre direction of each individual muscle.

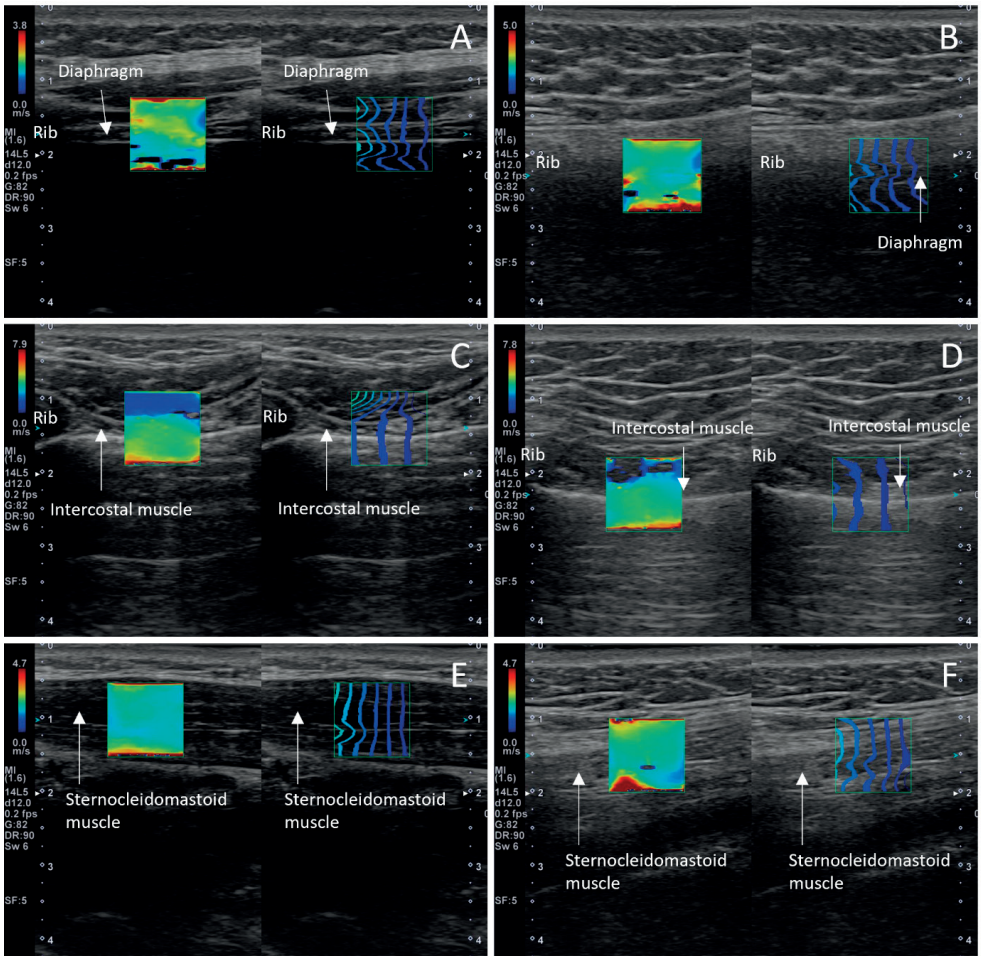


Figure 2: Example images of respiratory muscle shear wave acquisition. Within each panel, a duplicate image is displayed, with two different superimposed boxes. The left box displays the shear wave velocity, while the right box displays the propagation map. The colormap scale to the right of each panel is adapted during each acquisition. Low (blue) shear wave velocity indicates softer tissue, while high (red) shear wave velocity indicates stiffer tissue. A, C, E: examples of a healthy participant. B, D, F: examples of a severely affected patient with a congenital myopathy. A, B: examples of the diaphragm. C, D: examples of the parasternal intercostal muscle. E, F: examples of the sternocleidomastoid muscle.

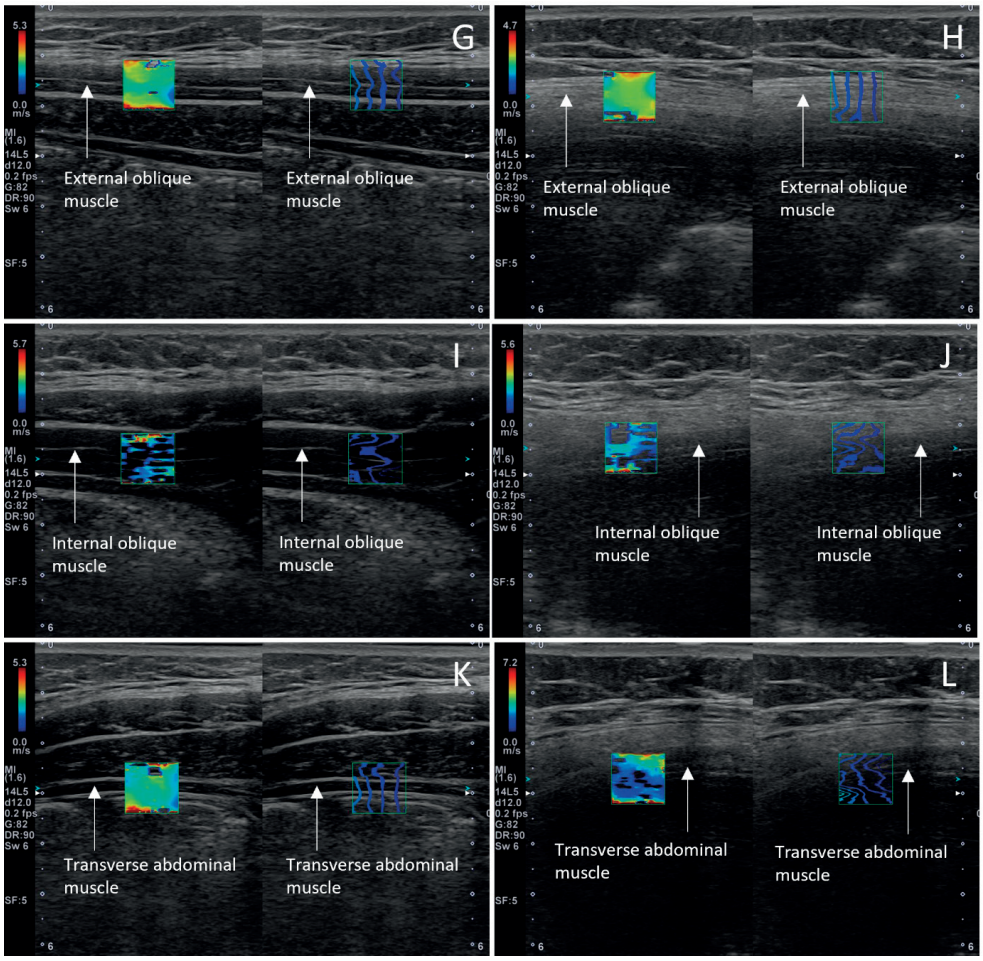


Figure 2 (continued). G, I, K: Examples of a healthy participant. H, J, L: examples of a severely affected patient with a congenital myopathy. G, H: examples of the external oblique abdominal muscle. I, J: examples of the internal oblique abdominal muscle. K, L: examples of the transverse abdominal muscle.

Single SWE measurements were acquired during each manoeuvre and muscle. The SWE box was placed within the muscle as superficially as possible and kept as small as possible, which was 1x1cm for the diaphragm, intercostal and sternocleidomastoid muscles, and 1.07x1cm for the abdominal muscles. Images were stored and exported for offline analysis. Using a custom analysis routine in Matlab (version R2023b, Mathworks, Natick, MA, USA), a region-of-interest was drawn in the SWE box, containing only the muscle of interest. The outer 10% of the SWE box was removed from analysis to exclude any artefacts at the edge of the SWE box. The pixels containing shear wave velocity values inside the region-of-interest were represented with a histogram, on which an optimal kernel density function was modelled. Subsequently, the maximal value of the density function was selected. This permitted obtaining the mode value

of the histogram while excluding any outliers. The mode value was chosen as this identified a representative value in a non-gaussian distribution of shear wave velocity. Each measurement was repeated three times, and the mean of the three measurements was used as outcome.

Data acquisition and signal processing

During all ultrasound measurements, participants breathed through a mouthpiece while wearing a nose clip and lying semi-recumbent. The mouthpiece was connected through a sample port to the DA100C module equipped with TSD160E transducers of the MP160 amplifier system (BIOPAC systems, Inc, Goleta, CA, USA), allowing for continuous measurement of mouth pressure (Pmo). A nasogastric catheter with a balloon in the oesophagus and stomach (Type C76080U, Marquat Genie Biomedical, Boissy-Saint-Leger, France) was connected to the amplifier, and through custom transducers to additional DA100C modules. After validating the position of the catheter following standard procedures, this allowed for measurement of Pdi [16]. A foot-pedal was used to operate the ultrasound device, that was simultaneously connected to the amplifier, thus allowing synchronization of SWE acquisition with Pmo and Pdi measurements.

Experimental procedures

Measurements were divided into 4 blocks, corresponding to the 4 muscle groups scanned. The order of these blocks was randomized, and participants were allowed to rest in between. Each block consisted of SWE acquisition during quiet breathing, deep breathing, and maximal isometric effort. Additionally, during scanning of the diaphragm, a series of submaximal isometric efforts was performed.

Shear wave velocity was acquired at resting end-expiration for the diaphragm, intercostal, and sternocleidomastoid muscles and at end-inspiration for the external oblique, internal oblique, and transverse abdominal muscles during quiet breathing. During deep inspiration or expiration, participants were instructed to inhale as deeply as possible for assessment of the diaphragm, intercostal and sternocleidomastoid muscles. For assessment of the external oblique, internal oblique, and transverse abdominal muscles, participants were instructed to exhale as deeply as possible. Shear wave velocity was acquired at the moment of maximal inspiration or expiration. During a maximal isometric effort, participants were instructed to inhale as forcefully as possible against an occluded airway from functional residual capacity (FRC). For the external oblique, internal oblique, and transverse abdominal muscles, participants were instructed to exhale as forcefully as possible against an occluded airway from FRC. Shear wave velocity was acquired at peak airway pressure.

During submaximal isometric effort, participants were presented with their real-time Pmo on a screen, together with a target line that indicated consecutively 20%, 40% and 60% of their own PImax. During occlusions, participants were instructed to hold their Pmo at the target line for 4 seconds. Shear wave velocity was acquired when the Pmo was at the level of the target line.

Statistical analysis

Shear wave velocity was compared between patients and healthy participants, separately for each manoeuvre. Different manoeuvres were compared pairwise, separately for patients and healthy participants, where each participant acted as their own control. For the submaximal isometric efforts, similar pairwise comparisons were carried out between shear wave velocity as outcome and either Pmo or Pdi. Bonferroni correction was applied. All analyses were carried out using R statistical software, and $p < 0.05$ was considered statistically significant.

Reliability was estimated with intraclass correlation coefficients (ICC). Intra-observer reliability was calculated with the ICC(2, k) model using the data from observer 1 of visit 2, inter-observer reliability with the ICC(3, k) model using the data of both observers of visit 2 and test-retest reliability with the ICC(2) model [17, 19] using the data from observer 1 of both visits. ICC estimates were classified as being poor (ICC <= 0.50), moderate (0.50 < ICC <= 0.75), good (0.75 < ICC <= 0.90) and excellent (ICC > 0.90) [19].

Results

Participants

Twenty-one patients and 20 healthy participants were included. See Table 1 for all participant characteristics. Patients had mutations in the following genes: *RYR1* (n=5), *TTN* (n=5), *DNM2* (n=3), *NEB* (n=2), *COL6A3* (n=1), *BIN1* (n=1), *LMOD3* (n=1), *TPM3* (n=1), *MTM1* (n=1) and *KBTBD13* (n=1). Patients were slightly older than healthy participants, had weaker respiratory muscles, and their pulmonary function was consistent with restrictive pathology. Two healthy participants did not tolerate nasogastric catheterization, resulting in missing Pdi, while in 2 additional healthy participants, technical failure led to missing Pdi.

Shear wave velocity

Shear wave velocity was not different between patients and healthy participants during any manoeuvre in any respiratory muscle (Figure 3), while various small significant changes were observed between manoeuvres. Shear wave velocity in the diaphragm increased during deep inspiration compared to quiet breathing in healthy participants (2.64±0.61 m/s vs 2.12±0.33 m/s, p=0.012), while not in patients. Shear wave velocity in the sternocleidomastoid muscle increased during deep inspiration and maximal voluntary effort compared to quiet breathing in patients (5.02±2.53 m/s vs 2.36±0.65 m/s, p=0.002 and 5.84±2.29 m/s vs 2.36±0.65 m/s, p<0.001, respectively), while not in healthy participants.

Table 1: Participant characteristics.

	Healthy participants (n = 20)	**Patients (n = 21)**	**p-value**
Age (y)	22.5 [20.0; 25.5]	34.0 [22.0; 42.0]	**p = 0.047***
Sex (n Male)	8	11	ns, p = 0.630
BMI (kg/m^2)	22.4 [20.9; 25.5]	24.8 [20.5; 27.2]	ns, p = 0.434
PImax (cmH_2O)	101.5 [90.5; 113.5]	81.0 [39.0; 84.0]	**p = 0.001***
PEmax (cmH_2O)	122.5 [112.0; 133.3]	81.0 [59.0; 130.0]	**p < 0.001***
FVC (L)	4.7 [4.0; 5.1]	3.1 [2.3; 4.1]	**p < 0.001***
FVC %	96.8 [88.8; 106.8]	62.9 [55.1; 82.6]	**p < 0.001***
FEV1 (L)	3.7 [3.3; 4.6]	2.7 [2.0; 3.3]	**p < 0.001***
FEV1 %	95.5 [91.2; 103.9]	64.5 [56.1; 88.4]	**p < 0.001***
FEV1/FVC	0.84 [0.82; 0.86]	0.84 [0.80; 0.86]	ns, p = 0.917
FVC drop in supine position (%)	2.4 [0.6; 0.4.5]	3.9 [1.2; 6.1]	ns, p = 0.197

Data are presented as median [p25; p75]. p-values were obtained with the Mann-Whitney-U test or the chi-squared test. BMI: Body mass index. PImax: pressure during a maximal inspiratory effort against a closed airway. PEmax: pressure during a maximal expiratory effort against a closed airway. FVC: Forced vital capacity. FVC%: predicted value of FVC. FEV1: Forced expiratory volume in the first second. FEV1%: predicted value of FEV1. *: p values < 0.05 are considered statistically significant.

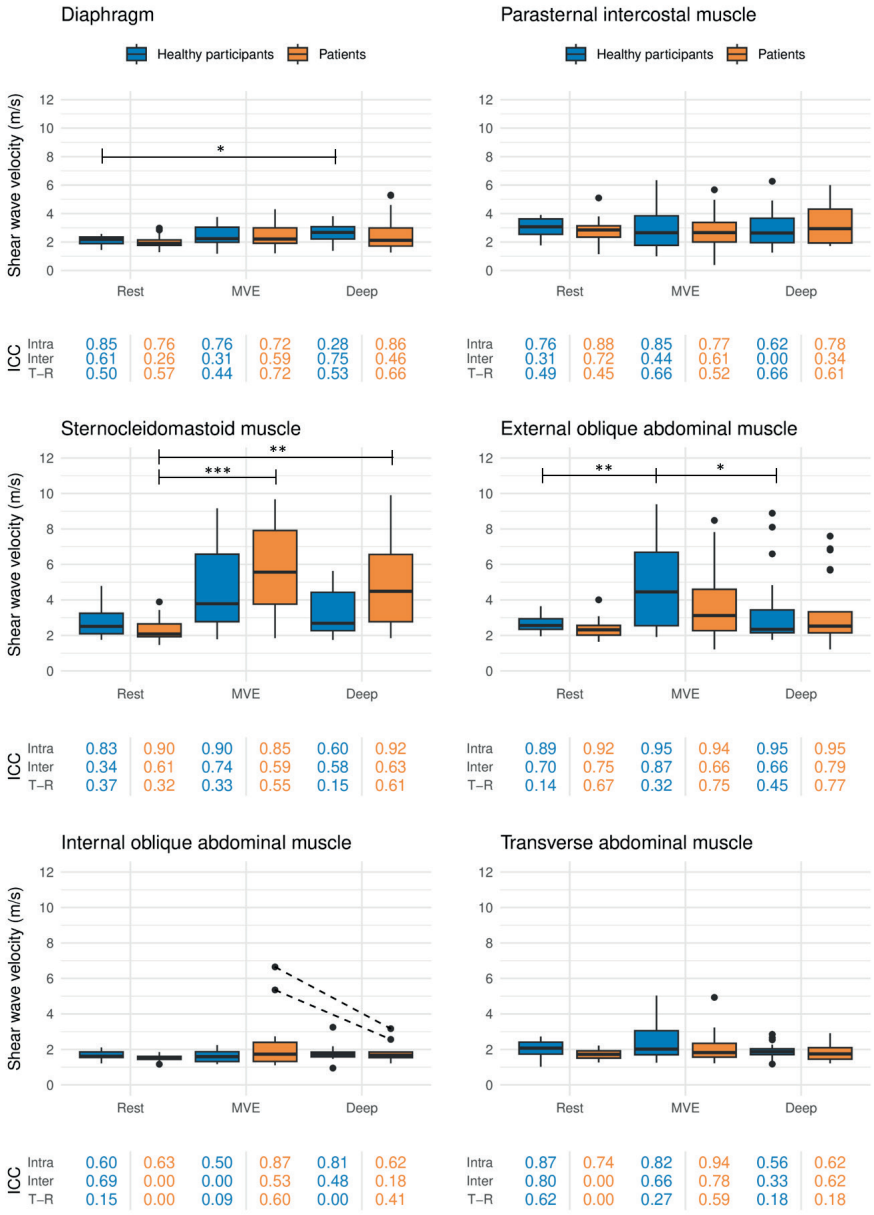


Figure 3: Shear wave velocities and associated ICCs in all measured muscles and manoeuvres. Rest: quiet breathing. MVE: maximal voluntary isometric effort. Deep: deep inhalation or exhalation. Intra: intra-observer reliability. Inter: inter-observer reliability. T-R: test-retest reliability. Dashed lines indicate outliers belonging to the same subject. *: $p < 0.05$, **: $p < 0.01$. ***: $p < 0.001$.

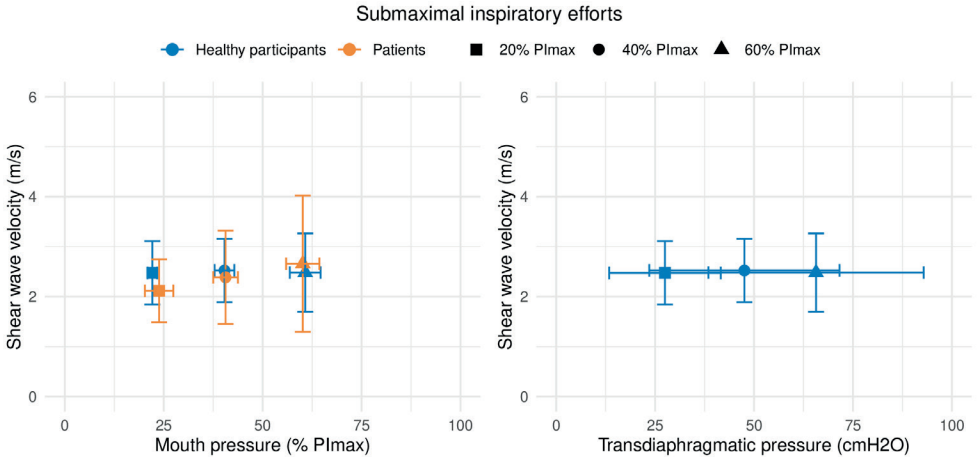


Figure 4: The effect of submaximal inspiratory efforts on shear wave velocity.
Left: shear wave velocity during submaximal inspiratory efforts compared with mouth pressure normalized to PImax for healthy participants and patients. Right: shear wave velocity during submaximal inspiratory efforts compared with transdiaphragmatic pressure in healthy participants only.

Shear wave velocity in the external oblique abdominal muscle increased during maximal voluntary effort compared to deep expiration and quiet breathing in healthy participants (4.91±2.48 m/s vs 3.35±2.15 m/s, p=0.044 and 4.91±2.48 m/s vs 2.66±0.44 m/s, p=0.005, respectively), while not in patients.

Submaximal isometric efforts

Shear wave velocity in the diaphragm at different levels of Pmo and Pdi was not different between patients or healthy participants during all submaximal isometric efforts, nor did it differ between consecutive submaximal isometric efforts (Figure 4).

Reliability

Reliability estimates varied greatly, from very low to very high ICCs, between respiratory muscles, manoeuvres, patients, and healthy participants. Reliability estimates are displayed in Figure 3 and confidence intervals for all reliability estimates can be found in supplemental tables 1 and 2.

Discussion

This study found no difference in shear wave velocity in respiratory muscles between patients with congenital myopathies and healthy participants. Furthermore, shear wave velocity did not reflect changes in Pmo and Pdi during submaximal efforts. The reliability of measuring respiratory muscle SWE was found to be poor.

Muscle fibres of patients with congenital myopathies are impaired in their function by the specific molecular defects in excitation-contraction coupling and sarcomeres, and are eventually replaced by fat and fibrous tissue [19, 20]. This contributes in different ways to tissue elasticity. Fat tissue lowers stiffness and fibrous tissue increases stiffness [21]. A decrease in functional contractile tissue decreases resting muscle tension, which may further decrease tissue stiffness [19, 20]. Defects in specific proteins such as titin conversely increase resting muscle tension [22]. It remains uncertain how these factors interact in individual patients. Nevertheless, it is likely that differences in muscle tissue stiffness exist, given the significant changes that are generally observed in muscle biopsies of congenital myopathy patients, and the wide range in pulmonary function and respiratory muscle strength observed in this study [19, 20]. Therefore, the absence of differences between patients and healthy participants in shear wave velocity in this study raises questions about the validity of measuring respiratory muscle shear wave velocity. This concern is strengthened by the fact that shear wave velocity did not reflect changes in Pdi and Pmo, as was demonstrated previously in healthy participants using a different ultrasound system [13].

The most likely explanation for this contrasting finding is the different WE technique and their implementation across ultrasound manufacturers. The first commercially available SWE system, developed by SuperSonic Imagine (Aix-en-Provence, France), uses successive pushes to generate a mach cone during a single excitation. In comparison to a single push, the mach cone enhances shear wave generation and results in stronger and more detectable shear waves over the full region-of-interest. Furthermore, ultrafast plane wave ultrasound acquisition is used to track the propagation of shear waves, resulting in a sufficient spatiotemporal resolution that is typically needed in muscle [23, 24]. As this approach is patented and requires highly specific electronics, other manufacturers have implemented other SWE techniques. No mach cone is generated in these alternative implementations, resulting in less efficient conversion of acoustic energy from an excitation into mechanical tissue disturbance [25]. Moreover, in the absence of ultrafast plane wave ultrasound acquisition, spatial or temporal resolution must be compromised to be able to track the shear wave. Manufacturers typically do not disclose their alternative method of shear wave generation and tracking, as is the case with the device used in this study.

The original SWE implementation method may be able to overcome the difficulties that respiratory muscle tissue present, in contrast to the implementation that was used in this study. SWE requires isotropic tissue such as liver, breast or thyroid. Muscle is at best directional isotropic when acquiring shear wave velocity parallel to the fibre direction [24]. The diaphragm and the intercostal parasternal muscles, however, present additional difficulties that violates the directional isotropic model. The diaphragm is a complex 3D muscle structure and the muscle fibres of the parasternal intercostal muscles are not homogenous but rather interwoven, resulting in different shear wave velocities for the differently oriented layers. As the excitations may be positioned on specific locations, it is not guaranteed that they are positioned within very thin structures such as the diaphragm, and shear waves will not propagate through that

structure. Moreover, ultrasound acquisition is susceptible to differences in transducer angles, manual pressure applied to the transducer and to signal attenuation when scanning deeper structures, which is the case when scanning the diaphragm or internal and transverse abdominal muscles. This is amplified when scanning muscles deep to other muscles, especially when the superficial muscles are affected in congenital myopathies. Additionally, the SWE box was larger than most of the measured muscles and could not be set smaller. This resulted in tissues other than muscle being imaged, such as fascia or subcutaneous tissue. Due to averaging, this may have influenced the observed shear wave velocity in the region-of-interest. Although this affected all participants equally, this effect cannot be excluded from SWE acquisition. Lastly, while the sternocleidomastoid and the external oblique abdominal muscles do not present these added difficulties, they are prone to disturbance by manual compression.

Any measurement for routine use in clinical practice or scientific research should demonstrate robust reliability and validity. Without these qualities, there is a risk of incorrect diagnoses, misguided clinical decisions, or erroneous conclusions regarding the effectiveness of an investigational drug. ICC estimates were generally observed to be too low for respiratory muscle SWE to be considered reliable. In part, this may be explained by inter- and intra-observer variability that is always associated with tests that are performed manually. However, it is likely that the SWE implementation has the greater impact on the poor reliability estimates. When repeating this study with the original SWE implementation, robust reliability testing should be included.

The data presented in Table 1 is not sufficient to give a full clinical overview of the included patients. In addition to respiratory assessments, skeletal muscle strength was assessed with hand-held dynamometry. However, the device slowly deteriorated in quality until no reliable measurements could be obtained, and it was not possible to determine when this occurred. Therefore, this data was left out. Furthermore, not all patients were diagnosed with a muscle biopsy. Pathogenicity of mutations was confirmed by a neurologist and a clinical geneticist.

In conclusion, respiratory muscle SWE as performed with the ultrasound machine used in our study is neither a valid nor reliable technique for evaluating respiratory muscle contractility in congenital myopathies and healthy participants.

References

1. Laghi, F. and M.J. Tobin, *Disorders of the respiratory muscles.* Am J Respir Crit Care Med, 2003. 168(1): p. 10-48.
2. Gineste, C. and J. Laporte, *Therapeutic approaches in different congenital myopathies.* Curr Opin Pharmacol, 2023. 68: p. 102328.
3. Laveneziana, P., et al., *ERS statement on respiratory muscle testing at rest and during exercise.* Eur Respir J, 2019. 53(6).
4. McCool, F.D. and G.E. Tzelepis, *Dysfunction of the diaphragm.* N Engl J Med, 2012. 366(10): p. 932-42.
5. Boon, A.J., et al., *Two-dimensional ultrasound imaging of the diaphragm: quantitative values in normal subjects.* Muscle Nerve, 2013. 47(6): p. 884-9.
6. Goligher, E.C., et al., *Measuring diaphragm thickness with ultrasound in mechanically ventilated patients: feasibility, reproducibility and validity.* Intensive Care Med, 2015. 41(4): p. 642-9.
7. Poulard, T., et al., *Poor Correlation between Diaphragm Thickening Fraction and Transdiaphragmatic Pressure in Mechanically Ventilated Patients and Healthy Subjects.* Anesthesiology, 2022. 136(1): p. 162-175.
8. Dubé, B.P., et al., *Ultrasound evaluation of diaphragm function in mechanically ventilated patients: comparison to phrenic stimulation and prognostic implications.* Thorax, 2017. 72(9): p. 811-818.
9. Oppersma, E., et al., *Functional assessment of the diaphragm by speckle tracking ultrasound during inspiratory loading.* J Appl Physiol (1985), 2017. 123(5): p. 1063-1070.
10. Friedrich, J., et al., *Poor Correlation between Diaphragm Ultrasound and Invasive Gold Standard Technique Derived Respiratory Muscle Strength Assessment in Patients after Hospitalisation for COVID-19.* Respiration, 2024: p. 1-9.
11. Chino, K., et al., *Diaphragmatic shear modulus at various submaximal inspiratory mouth pressure levels.* Respir Physiol Neurobiol, 2018. 252-253: p. 52-57.
12. Gennisson, J.L., et al., *Ultrasound elastography: principles and techniques.* Diagn Interv Imaging, 2013. 94(5): p. 487-95.
13. Bachasson, D., et al., *Diaphragm shear modulus reflects transdiaphragmatic pressure during isovolumetric inspiratory efforts and ventilation against inspiratory loading.* J Appl Physiol (1985), 2019. 126(3): p. 699-707.
14. North, K.N., et al., *Approach to the diagnosis of congenital myopathies.* Neuromuscul Disord, 2014. 24(2): p. 97-116.
15. Quanjer, P.H., et al., *Multi-ethnic reference values for spirometry for the 3-95-yr age range: the global lung function 2012 equations.* Eur Respir J, 2012. 40(6): p. 1324-43.
16. Mojoli, F., et al., *Technical aspects of bedside respiratory monitoring of transpulmonary pressure.* Ann Transl Med, 2018. 6(19): p. 377.
17. Shrout, P.E. and J.L. Fleiss, *Intraclass correlations: uses in assessing rater reliability.* Psychol Bull, 1979. 86(2): p. 420-8.
18. Koo, T.K. and M.Y. Li, *A Guideline of Selecting and Reporting Intraclass Correlation Coefficients for Reliability Research.* J Chiropr Med, 2016. 15(2): p. 155-63.
19. Cassandrini, D., et al., *Congenital myopathies: clinical phenotypes and new diagnostic tools.* Ital J Pediatr, 2017. 43(1): p. 101.

20. Jungbluth, H., et al., *Congenital myopathies: disorders of excitation-contraction coupling and muscle contraction.* Nat Rev Neurol, 2018. 14(3): p. 151-167.
21. Chavan, R., et al., *On Mechanical Behavior and Characterization of Soft Tissues.* Biomed Eng Comput Biol, 2024. 15: p. 11795972241294115.
22. Linke, W.A., *Stretching the story of titin and muscle function.* J Biomech, 2023. 152: p. 111553.
23. Bercoff, J., M. Tanter, and M. Fink, *Supersonic shear imaging: a new technique for soft tissue elasticity mapping.* IEEE Trans Ultrason Ferroelectr Freq Control, 2004. 51(4): p. 396-409.
24. Gennisson, J.L., et al., *Viscoelastic and anisotropic mechanical properties of in vivo muscle tissue assessed by supersonic shear imaging.* Ultrasound Med Biol, 2010. 36(5): p. 789-801.
25. Urban, M.W., *Production of acoustic radiation force using ultrasound: methods and applications.* Expert Rev Med Devices, 2018. 15(11): p. 819-834.

Supplemental table 1: ICC estimations of healthy participants

Muscle	Manoeuvre	Intra-observer	Inter-observer	Test-retest
Diaphragm	Rest	0.85 (0.69 - 0.94)	0.61 (0.02 - 0.85)	0.50 (0.09 - 0.77)
Diaphragm	Deep	0.28 (-0.47 - 0.69)	0.75 (0.30 - 0.91)	0.53 (0.12 - 0.79)
Diaphragm	MVE	0.76 (0.49 - 0.90)	0.31 (-0.75 - 0.73)	0.44 (0.03 - 0.73)
Intercostal	Rest	0.76 (0.51 - 0.90)	0.31 (-0.74 - 0.73)	0.49 (0.09 - 0.76)
Intercostal	Deep	0.62 (0.20 - 0.84)	0.00 (-1.53 - 0.60)	0.66 (0.32 - 0.85)
Intercostal	MVE	0.85 (0.70 - 0.94)	0.44 (-0.41 - 0.78)	0.66 (0.32 - 0.85)
Sternocleidomastoid	Rest	0.83 (0.64 - 0.93)	0.34 (-0.71 - 0.75)	0.37 (-0.08 - 0.70)
Sternocleidomastoid	Deep	0.60 (0.17 - 0.83)	0.58 (-0.05 - 0.84)	0.15 (-0.30 - 0.55)
Sternocleidomastoid	MVE	0.90 (0.79 - 0.96)	0.74 (0.34 - 0.90)	0.33 (-0.12 - 0.67)
External oblique	Rest	0.89 (0.78 - 0.95)	0.70 (0.23 - 0.88)	0.14 (-0.31 - 0.54)
External oblique	Deep	0.95 (0.89 - 0.98)	0.66 (0.14 - 0.87)	0.45 (0.03 - 0.74)
External oblique	MVE	0.95 (0.89 - 0.98)	0.87 (0.67 - 0.95)	0.32 (-0.13 - 0.66)
Internal oblique	Rest	0.60 (0.16 - 0.83)	0.69 (0.22 - 0.88)	0.15 (-0.28 - 0.54)
Internal oblique	Deep	0.81 (0.60 - 0.92)	0.48 (-0.35 - 0.80)	0.00 (-0.43 - 0.43)
Internal oblique	MVE	0.50 (-0.06 - 0.78)	0.00 (-1.53 - 0.60)	0.09 (-0.35 - 0.50)
Transverse abdominal	Rest	0.87 (0.73 - 0.95)	0.80 (0.48 - 0.92)	0.62 (0.26 - 0.83)
Transverse abdominal	Deep	0.56 (0.08 - 0.81)	0.33 (-0.73 - 0.74)	0.18 (-0.27 - 0.56)
Transverse abdominal	MVE	0.82 (0.63 - 0.92)	0.66 (0.14 - 0.86)	0.27 (-0.18 - 0.63)

ICC estimations with 95% confidence intervals of intra-observer, inter-observer and test-retest reliability during all manoeuvres of all measured muscles of healthy participants.

Supplemental table 2: ICC estimations of patients

Muscle	Manoeuvre	Intra-observer	Inter-observer	Test-retest
Diaphragm	Rest	0.76 (0.46 - 0.90)	0.26 (-0.86 - 0.71)	0.57 (0.20 - 0.81)
Diaphragm	Deep	0.86 (0.70 - 0.94)	0.46 (-0.69 - 0.83)	0.66 (0.27 - 0.86)
Diaphragm	MVE	0.72 (0.38 - 0.89)	0.59 (-0.16 - 0.86)	0.72 (0.37 - 0.89)
Intercostal	Rest	0.88 (0.76 - 0.95)	0.72 (0.32 - 0.89)	0.45 (0.04 - 0.73)
Intercostal	Deep	0.78 (0.54 - 0.90)	0.34 (-0.63 - 0.73)	0.61 (0.26 - 0.82)
Intercostal	MVE	0.77 (0.53 - 0.90)	0.61 (0.04 - 0.84)	0.52 (0.13 - 0.77)
Sternocleidomastoid	Rest	0.90 (0.79 - 0.96)	0.61 (0.01 - 0.84)	0.32 (-0.12 - 0.66)
Sternocleidomastoid	Deep	0.92 (0.84 - 0.97)	0.63 (0.07 - 0.85)	0.61 (0.25 - 0.82)
Sternocleidomastoid	MVE	0.85 (0.68 - 0.93)	0.59 (-0.05 - 0.84)	0.55 (0.16 - 0.79)
External oblique	Rest	0.92 (0.84 - 0.97)	0.75 (0.37 - 0.90)	0.67 (0.35 - 0.85)
External oblique	Deep	0.95 (0.89 - 0.98)	0.79 (0.49 - 0.92)	0.77 (0.51 - 0.90)
External oblique	MVE	0.94 (0.88 - 0.97)	0.66 (0.15 - 0.87)	0.75 (0.47 - 0.89)
Internal oblique	Rest	0.63 (0.23 - 0.84)	0.00 (-1.60 - 0.61)	0.00 (-0.44 - 0.44)
Internal oblique	Deep	0.62 (0.09 - 0.87)	0.18 (-1.83 - 0.77)	0.41 (-0.14 - 0.77)
Internal oblique	MVE	0.87 (0.68 - 0.95)	0.53 (-0.54 - 0.86)	0.60 (0.12 - 0.86)
Transverse abdominal	Rest	0.74 (0.46 - 0.89)	0.00 (-1.67 - 0.63)	0.00 (-0.47 - 0.47)
Transverse abdominal	Deep	0.62 (0.11 - 0.86)	0.62 (-0.31 - 0.89)	0.18 (-0.37 - 0.66)
Transverse abdominal	MVE	0.94 (0.86 - 0.98)	0.78 (0.17 - 0.94)	0.59 (0.07 - 0.86)

Supplemental table 2: ICC estimations with 95% confidence intervals of intra-observer, inter-observer and test-retest reliability during all manoeuvres of all measured muscles of patients.



Chapter 8

General discussion and future perspectives

General discussion

The first part of this thesis – **Current practice** – discusses technical application of respiratory muscle ultrasound in congenital myopathies and its interpretation. The second part of this thesis – **Critical appraisal** – scrutinizes respiratory muscle ultrasound methodology. The current status and future perspectives of respiratory muscle ultrasound in light of the research field is discussed here.

Imaging of skeletal muscles in neuromuscular disorders (NMDs) is increasingly used in diagnosis, clinical management and as outcome measure in clinical research. This aims to quantify atrophy or changes in muscle structure due to replacement of contractile tissue by fat and fibrous tissue: tissue remodelling [1, 2]. In larger skeletal muscles (in limbs and trunk), its diagnostic capabilities and performance as research outcome measure has become evident [3]. These imaging modalities are highly effective in quantifying tissue remodeling through static images, while the assessment of function using dynamic images is still underdeveloped.

The respiratory muscles form a special group of skeletal muscles, where previous research efforts aimed to assess tissue remodelling from static images alongside assessing respiratory function from dynamic images. The value of both approaches are discussed below.

Assessing respiratory muscle tissue remodelling with static ultrasound imaging

Atrophy assessment and echogenicity analysis of the respiratory muscles use the same methodology as in other skeletal muscles [3]. Rigorous standardization of the acquisition protocol is crucial for echogenicity analysis, a requirement that has not always been consistently met in respiratory muscle ultrasound [4-6]. Furthermore, centre-specific normative values for muscle thickness and device specific normal values for echogenicity are needed to interpret these outcomes, as illustrated in **Chapter 2** and **Chapter 5**.

Echogenicity analysis in skeletal muscles tends to assess only the most superficially located muscles. When the muscle of interest is located deep to other structures as is the case with most respiratory muscles, the ultrasound signal is attenuated. This is compounded in NMDs, where the more superficial muscles also get remodelled and reflect more acoustic energy. Ultimately, this leads to the superficial muscle layers appearing unusually bright, reflecting remodeling, while the deeper muscle layers may appear falsely normal or darker [3]. Further limitation is that the diaphragm is already very thin in healthy individuals, and echogenicity analysis might not be feasible when it is severely atrophied as was the case in **Chapter 4**.

Assessing respiratory muscle function with dynamic ultrasound imaging

Movement analysis, thickening analysis, strain imaging and shear wave elastography have been used to derive respiratory muscle function from dynamic ultrasound imaging. The diaphragm has been the focus of these techniques.

Movement of the diaphragm reflects pulmonary function. The diaphragm is an unique muscle without an insertion on a bone, enabling a large range of motion that is not observed in any other muscle. Using the subcostal view with low-frequency ultrasound and relatively low spatial resolution, the outline of the diaphragm is imaged. Absolute displacement during movement and displacement velocities can be measured during different manoeuvres [**Chapter 2**]. Alternatively, displacement velocities can be captured with doppler imaging using the same view [7]. There is a large body of literature assuming that diaphragm thickening as measured at the zone of apposition is a surrogate for diaphragm contractility [8-10]. **Chapter 6** introduced a shift in that interpretation, concluding that analysis of diaphragm thickening is not a suitable method for assessing diaphragm contractility. Instead, the diaphragm contracts and shortens which consequently causes thickening, and leads to an increase in lung volume. Displacement, displacement velocities and thickening of the diaphragm directly reflect a change in lung volume and may therefore be a an alternative for pulmonary function testing.

Strain imaging using speckle tracking is often considered as a separate technique. Using the subcostal view, the outline of the diaphragm can be tracked without the need for manual analysis, but the calculated parameters are the same: absolute displacement and displacement velocities. When imaging the diaphragm at the zone of apposition, technical difficulties are introduced. The diaphragm is a complex 3D structure which is imaged in a 2D plane, and out-of-plane movement constantly introduces new speckles while others are lost. Furthermore, the diaphragm typically moves multiple intercostal spaces during deep inhalation while only one intercostal space is imaged, thus introducing and losing speckles continuously. The lack of additional value of strain imaging of the diaphragm in contrast to strain imaging in cardiac ultrasound is striking. However, speckle loss is considerably less as there is less out-of-plane motion, and the heart stays in the same imaging plane, thus resulting in more stable speckle tracking. The pleural and peritoneal reflections are so strong that they lose the appearance of individual specking and form a continuous line, even when replaced by new speckles. As a result, the pleural and peritoneal reflections are adequately tracked, which can be used to measure diaphragm thickening without manual analysis. Indeed, speckle tracking of the diaphragm carries the same physiological meaning as thickening analysis [11, 12].

Muscle tissue is inherently unsuitable for SWE analysis as the isotropy assumption is violated. At best, fusiform muscle tissue can be considered as directional isotropic. Additionally, the diaphragm is typically very thin, making it susceptible to lamb wave interference and uncertain whether shear wave pushes are positioned between the pleura and peritoneal reflections.

Therefore, the absence of a relation between shear wave propagation speed and diaphragm contractility, and the absence of differences in shear wave propagation speed between congenital myopathy patients and healthy participants in **Chapter 7**, is not unexpected. Given these limitations of SWE, it is surprising that other studies have reported contradictory results [13, 14]. This may be explained by the different SWE-capable ultrasound device used. Most devices implements a SWE algorithm that make use of a push at a single excitation point, which propagates as a sphere. However, the first commercially available system to implement shear wave elastography (SuperSonic Imagine, Aix-en-Provence, France) uses quick successive pushes that are located directly below each other, interfering and resulting in a so-called mach cone. This propagates through the tissue as an enlarging cylinder, which presents like curtains that are opened in the imaged 2D plane. Directional isotropy perpendicular to the propagation direction may be considered as consistent with the isotropy assumption, and lamb waves present less interference. The contradictory results of **Chapter 7** to previous studies highlight the importance of proper validity and reliability testing before a technique such as SWE may be used in clinical practice and research. Furthermore, it remains uncertain whether SWE may act as a surrogate for diaphragm contractility or to assess tissue remodelling.

The value of respiratory muscle ultrasound in congenital myopathies

Given the technical and methodological strengths and limitations of respiratory muscle ultrasound, it raises the question how it can be applied to congenital myopathies. This thesis started with an overview of its current usage, inferring its value from clinical studies, but ended with critical notes on the methodology. Here, the value of respiratory muscle ultrasound in congenital myopathies previous to this thesis is revisited, and the shift in its value that this thesis brings is discussed.

Respiratory muscle contractility (also referred to as muscle strength or effort), in particular diaphragm contractility, has been assessed with diaphragm displacement, displacement velocities and thickening. This operates under the notion that movement of a muscle, or thickening of a muscle equals force generated by that muscle. This is a valid notion in itself, as a muscle has to generate force in order to be able to change its dimension. This has been used to characterize respiratory muscle function in congenital myopathies [**Chapters 3, 4**] and to predict successful weaning from mechanical ventilation in the ICU [15-18], but fails in both settings to do so better than other measures of respiratory function. The results of this thesis shift that paradigm by examining established muscle physiology: a change in thickening of the diaphragm does not indicate a change of diaphragm contractility, but is rather associated with a change in lung volume [**Chapter 6**][19, 20]. The same can be inferred for displacement of the diaphragm, as it directly reflects changes in lung volume. The only method for measuring contractility is transdiaphragmatic pressure (Pdi) as the gold standard for diaphragm contractility, while other non-invasive pressure-based measurements such as maximal inspiratory pressure (PImax),

maximal expiratory pressure (PEmax) and sniff nasal inspiratory pressure (SNIP) provide a global estimate of respiratory muscle contractility [21].

Almost paradoxically, decreased diaphragm thickening does reflect diaphragm weakness in congenital myopathies [**Chapters 3, 4, 6**]. Diaphragm weakness will limit its ability to shorten against the load of the respiratory system and as a consequence, inhaled volume and diaphragm thickening will be decreased. However, the reserve capacity of a healthy diaphragm is far greater than the load of the respiratory system. Therefore, a normal diaphragm thickening ratio does only indicate the generated force is greater than the load imposed by the respiratory system, but not the actual force that is generated for that contraction. Following this reasoning, diaphragm contractility may decrease significantly before that is reflected in decreased thickening.

Respiratory muscle ultrasound may have value in other neuromuscular disorders. Indices of diaphragm movement (displacement, displacement velocities and thickening) are important in diagnostic screening of other neuromuscular disorders. If there is a problem in the neural path to the diaphragm, the diaphragm will not move, or move less. Indeed, ultrasound of the diaphragm is the most sensitive method to diagnose phrenic neuropathy [22]. Echogenicity analysis and atrophy assessment of respiratory muscles has not been part of screening protocols in NMDs. For most NMDs, the respiratory muscles follow axial muscle involvement patterns and specifically screening respiratory muscles does not bring additional diagnostic performance. The exception to this is neuralgic amyotrophy, which may present with isolated respiratory muscle involvement [23].

Ongoing research and future perspectives

Longitudinal studies and accessory respiratory muscles

Chapter 2 identified the current strong focus on the diaphragm with respiratory muscle ultrasound, while the accessory respiratory muscles are also of major relevance in NMDs. Furthermore, to predict a meaningful change in clinical outcome, longitudinal studies have to be conducted. Both need to be addressed for respiratory muscle ultrasound to be considered as a surrogate endpoint in clinical drug-evaluating trials.

Therefore, our research group is currently performing a longitudinal study with 42 healthy participants and 42 patients with a congenital myopathy that addresses both. See Figure 1 for an overview of this study. This study resulted in **Chapter 6** and **Chapter 7** and will lead to several additional insights. First, thickness, thickening and echogenicity analysis can be conducted on the extra-diaphragmatic respiratory muscles. Second, the follow-up visits enables longitudinal analysis of thickness, thickening and echogenicity data on all respiratory muscles. Third, more insight into progression of respiratory symptoms in congenital myopathies will be obtained, and if respiratory muscle ultrasound compares in sensitivity to change to pulmonary function

tests and respiratory muscle strength testing. Fourth, clinical trial design may be informed with data from this study. Knowing the rate at which respiratory symptoms progress, sample size estimations can be made and study length can be determined.

As thickening of the diaphragm is associated with increasing lung volume, thickening analysis may be used as an alternative to pulmonary function testing. However, this remains hypothetical. To explore this hypothesis, our group recently initiated a longitudinal study in children with NMDs during which pulmonary function testing and respiratory muscle ultrasound is performed. This study is expected to provide more insight in which pulmonary function tests can be reliably performed in children at different ages, whether respiratory muscle ultrasound can be performed reliably at younger ages and if respiratory muscle ultrasound can serve as alternative to pulmonary function testing in this subgroup. A different cross-sectional study is performed by our group in patients with Duchenne Muscular Dystrophy which includes the same measurements.

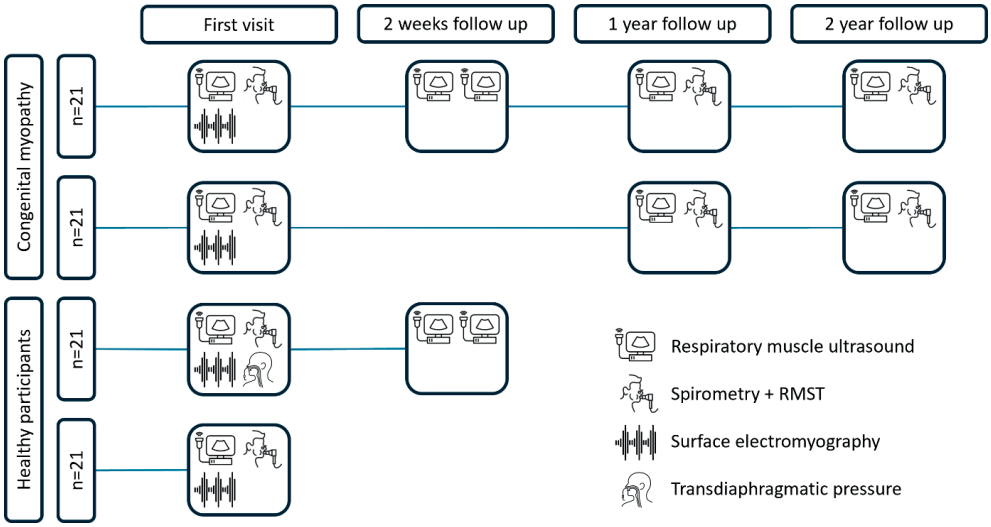


Figure 1: Overview of the longitudinal study that is currently performed. The respiratory muscle ultrasound protocol consists of measurement of thickness, thickening, echogenicity and shear wave propagation speed. The diaphragm, parasternal intercostal muscle, the sternocleidomastoid muscle, the external oblique abdominal muscle, the internal oblique abdominal muscle and the transverse abdominal muscle are assessed. All measurements are done during quiet breathing, deep inhalation or exhalation, and a maximal effort against a closed airway. The ultrasound protocol is repeated by two independent observers during the 2 weeks follow up visit. RMST: respiratory muscle strength testing.

Novel developments

An exciting new methodology has recently emerged in the form of contrast enhanced ultrasound (CEUS), which has the potential to study tissue remodeling, also in the respiratory muscles. This technique measures tissue perfusion, which can be affected by microvascular changes during tissue remodeling in NMDs [24]. It has been used to measure perfusion of the diaphragm in healthy participants and in mechanically ventilated patients in the ICU, but not in NMDs [25]. This technique relies on the administration of small bubbles composed of a biodegradable shell and filled with a gas that are introduced in the blood as contrast agent. The interface between the gas in the bubbles and the surrounding blood has a very high acoustic impedance, resulting in a strong reflection of acoustic energy. This results in an image of high echogenicity when imaging tissue that has been perfused with this contrast agent. Subsequently, the bubbles can burst when sufficient acoustic energy is utilized, resulting in a release of the gas with a subsequent very high ultrasound reflection, the so-called flash. As a result, the imaged tissue will appear less bright after this flash. However, since the tissue is perfused by blood containing contrast agent from the feeding arteries, tissue brightness will gradually increase until it is at the level before the flash. The rate at which brightness increases is related to perfusion with a fast echogenicity increase for highly perfused tissue. Whether there is a difference between healthy participants and patients with a neuromuscular disorder as measured by CEUS, how reliable this is and whether CEUS can play a role in the assessment of tissue remodeling remains to be studied.

Conclusion

This thesis shows that respiratory muscle ultrasound offers valuable insight into tissue remodeling but provides limited information on respiratory function in congenital myopathies. Diaphragm thickening and shear wave elastography were found to lack validity for assessing diaphragm contractility, underscoring persistent methodological challenges. Muscle tissue remodeling assessments, particularly thickness and echogenicity, remain the most reliable applications. Ultrasound continues to hold diagnostic relevance in other neuromuscular disorders. The comparison with established techniques highlights that spirometry remains more sensitive for functional assessment, while pressure-based measures remain essential for quantifying contractility.

References

1. Cassandrini, D., et al., *Congenital myopathies: clinical phenotypes and new diagnostic tools.* Ital J Pediatr, 2017. 43(1): p. 101.
2. Jungbluth, H., et al., *Congenital myopathies: disorders of excitation-contraction coupling and muscle contraction.* Nat Rev Neurol, 2018. 14(3): p. 151-167.
3. Wijntjes, J. and N. van Alfen, *Muscle ultrasound: Present state and future opportunities.* Muscle Nerve, 2021. 63(4): p. 455-466.
4. Coiffard, B., et al., *Diaphragm echodensity in mechanically ventilated patients: a description of technique and outcomes.* Crit Care, 2021. 25(1): p. 64.
5. Umbrello, M., et al., *Qualitative and quantitative muscle ultrasound changes in patients with COVID-19-related ARDS.* Nutrition, 2021. 91-92: p. 111449.
6. Formenti, P., et al., *Respiratory and peripheral muscular ultrasound characteristics in ICU COVID 19 ARDS patients.* J Crit Care, 2022. 67: p. 14-20.
7. Fayssoil, A., et al., *Diaphragm sniff ultrasound: Normal values, relationship with sniff nasal pressure and accuracy for predicting respiratory involvement in patients with neuromuscular disorders.* PLoS One, 2019. 14(4): p. e0214288.
8. Goligher, E.C., et al., *Measuring diaphragm thickness with ultrasound in mechanically ventilated patients: feasibility, reproducibility and validity.* Intensive Care Med, 2015. 41(4): p. 642-9.
9. Dubé, B.P., et al., *Ultrasound evaluation of diaphragm function in mechanically ventilated patients: comparison to phrenic stimulation and prognostic implications.* Thorax, 2017. 72(9): p. 811-818.
10. Vivier, E., et al., *Diaphragm ultrasonography to estimate the work of breathing during non-invasive ventilation.* Intensive Care Med, 2012. 38(5): p. 796-803.
11. Hatam, N., et al., *A novel application for assessing diaphragmatic function by ultrasonic deformation analysis in noninvasively ventilated healthy young adults.* Ultraschall Med, 2014. 35(6): p. 540-6.
12. Oppersma, E., et al., *Functional assessment of the diaphragm by speckle tracking ultrasound during inspiratory loading.* J Appl Physiol (1985), 2017. 123(5): p. 1063-1070.
13. Fossé, Q., et al., *Ultrasound shear wave elastography for assessing diaphragm function in mechanically ventilated patients: a breath-by-breath analysis.* Crit Care, 2020. 24(1): p. 669.
14. Flatres, A., et al., *Real-time shear wave ultrasound elastography: a new tool for the evaluation of diaphragm and limb muscle stiffness in critically ill patients.* Crit Care, 2020. 24(1): p. 34.
15. Li, C., et al., *Diaphragmatic ultrasonography for predicting ventilator weaning: A meta-analysis.* Medicine (Baltimore), 2018. 97(22): p. e10968.
16. Medrinal, C., et al., *ICU outcomes can be predicted by noninvasive muscle evaluation: a meta-analysis.* Eur Respir J, 2020. 56(4).
17. Llamas-Álvarez, A.M., E.M. Tenza-Lozano, and J. Latour-Pérez, *Diaphragm and Lung Ultrasound to Predict Weaning Outcome: Systematic Review and Meta-Analysis.* Chest, 2017. 152(6): p. 1140-1150.
18. Tuinman, P.R., et al., *Respiratory muscle ultrasonography: methodology, basic and advanced principles and clinical applications in ICU and ED patients-a narrative review.* Intensive Care Med, 2020. 46(4): p. 594-605.

19. Hodges, P.W., et al., *Measurement of muscle contraction with ultrasound imaging.* Muscle Nerve, 2003. 27(6): p. 682-92.
20. Wait, J.L. and R.L. Johnson, *Patterns of shortening and thickening of the human diaphragm.* J Appl Physiol (1985), 1997. 83(4): p. 1123-32.
21. Laveneziana, P., et al., *ERS statement on respiratory muscle testing at rest and during exercise.* Eur Respir J, 2019. 53(6).
22. Boon, A.J., et al., *Sensitivity and specificity of diagnostic ultrasound in the diagnosis of phrenic neuropathy.* Neurology, 2014. 83(14): p. 1264-70.
23. Gabet, J.M., et al., *Neuralgic amyotrophy: An update in evaluation, diagnosis, and treatment approaches.* Muscle Nerve, 2025. 71(5): p. 846-856.
24. Margeta, M., *Neuromuscular disease: 2022 update.* Free Neuropathol, 2022. 3: p. 5.
25. Bird, J.D., et al., *Quantifying Diaphragm Blood Flow With Contrast-Enhanced Ultrasound in Humans.* Chest, 2024. 166(4): p. 821-834.

Appendices



Appendix I - Summary

General introduction

Congenital myopathies, the respiratory muscles and ultrasound are outlined in **Chapter 1**. Ultrasound is increasingly used to assess respiratory muscle function in neuromuscular disorders, the intensive care unit and pulmonary medicine, both in clinical practice and as outcome measure in research. The first part of this thesis – **Current practice** – discusses technical application of respiratory muscle ultrasound in congenital myopathies and its interpretation. The second part of this thesis – **Critical appraisal** – scrutinizes respiratory muscle ultrasound methodology. This thesis thus aimed to determine the current status and future perspectives of respiratory muscle ultrasound in clinical practice and research.

Part 1 – Current practice

Chapter 2 is a review of the literature on methodology, technological developments, clinical applications and limitations of ultrasound and magnetic resonance imaging of the respiratory muscles in neuromuscular disorders. Accessory respiratory muscle weakness has been identified as clinically significant in patients with neuromuscular disorders, however, the majority of studies only aimed at measuring the diaphragm. Furthermore, a lack of standardization in methodology lead to large variability in reported data and longitudinal studies with respiratory muscle imaging are lacking. Ultrasound has been used to characterize respiratory muscle function in several neuromuscular disorders, but is rarely used in clinical practice. Echogenicity assessment, strain imaging through speckle tracking, and ultrafast shear wave elastography are identified as promising methods to assess the respiratory muscles in neuromuscular disorders.

Chapter 3 evaluated respiratory function in the Dutch cohort of nemaline myopathies (NM). Median diaphragm thickening in typical NM was below the centre-specific lower limit of normal (**Chapter 5**) together with an increased median echogenicity z-score, while not in mild NM or Childhood-onset NM with slowness. No statistical differences were found between NM types, in contrast to pulmonary function testing and respiratory muscle strength testing, indicating that these volitional tests may be more sensitive to differences in diaphragm function than diaphragm ultrasound. When stratifying on pulmonary function and ventilation status, patients with impaired pulmonary function and used mechanical ventilation had decreased diaphragm thickening and increased diaphragm echogenicity, in line with differences in pulmonary function and respiratory muscle strength. Both these findings lead to the hypothesis that diaphragm ultrasound reflect pulmonary function as well as diaphragm strength. No differences in diaphragm and intercostal resting end-expiration thickness were found in both analyses, indicating that an increase of respiratory muscle involvement does not lead to atrophy in NM.

Chapter 4 evaluated respiratory function in the Dutch cohort of *LAMA2* related muscular dystrophy (LAMA2-MD) and *SEPN1* related congenital myopathy (SELEONON-RM), and the

change in respiratory function during a 1.5 year follow-up period. There were no changes in respiratory function in LAMA2-MD during the follow-up period, both as assessed with pulmonary function tests, respiratory muscle strength tests and respiratory muscle ultrasound. The diaphragm as measured with ultrasound was normotrophic and thickening was normal, while median echogenicity z-score ranged between 1.7 and 2.1, where 2.0 marks an increase. In contrast, the diaphragm was atrophic and diaphragm thickening was decreased in SELENON-RM. As a result, diaphragm echogenicity could not be analysed. However, these parameters did not change during the follow-up period in line with respiratory muscle strength tests but in contrast to pulmonary function tests. The analyses in both patient groups reinforces the hypothesis that diaphragm ultrasound reflects diaphragm strength testing and pulmonary function testing, but may be less sensitive to change as volitional tests.

Part 2 – Critical appraisal

In **Chapter 5**, diaphragm thickness, thickening and echogenicity data are collected with ultrasound in a representative sample of young to old healthy participants. Diaphragm echogenicity is strongly influenced by age. Echogenicity that would be normal in older individuals would be substantially increased in younger individuals, leading to the need for controlling age as a statistical variable in interpretation of diaphragm echogenicity analysis. Diaphragm thickness is influenced by sex and body mass index (BMI), although less pronounced as with echogenicity. Diaphragm thickening is not influenced by age, sex, or BMI, and a lower limit of normal is provided. Normative data or matched controls have to be available for valid interpretation of diaphragm ultrasound in clinical practice or research. We provided a detailed protocol for acquisition and analysis of diaphragm ultrasound, as well as methods to calculate reference data, as the proposed standard.

In **Chapter 6**, the complex relationship between diaphragm thickening as measured with ultrasound, force generated by the diaphragm and changes in lung volume is elucidated. The relation has been subject of considerable scientific debate and with the experiments performed in this chapter, an in-depth physiological analysis is performed. Diaphragm thickening has been considered as a surrogate of force generated by the diaphragm. Participants that performed maximal isometric contractions had no increase in diaphragm thickness, while diaphragm thickness increased substantially during unloaded concentric contractions. This suggested that diaphragm thickening did not reflect diaphragm force generation, but rather an increase in lung volume. however, intended leakage in the system prevented the isometric manoeuvre from being strictly isometric, and physiological resistance in the respiratory system prevented the unloaded concentric manoeuvre from being strictly unloaded. Therefore, tapered flow resistance breathing was used to control force generation as well as inspiratory volume simultaneously at different loading levels. Diaphragm thickening did not change between different loading levels, but increased along increasing lung volume. Diaphragm thickening should not be interpreted as surrogate measure of force effort generated by the diaphragm.

The use of shear wave elastography (SWE) was assessed as an alternative to measure respiratory effort in **Chapter 7**. Previous studies that used SWE in the diaphragm indicated that it is a surrogate of inspiratory effort generated by the diaphragm. This study was repeated with healthy participants, and was extended with congenital myopathy patients, reliability analyses and the accessory respiratory muscles. SWE had poor intra-observer, inter-observer and test-retest reliability, did not show differences between healthy participants and patients with congenital myopathies and did not correlate with the gold standard of inspiratory effort generated by the diaphragm, transdiaphragmatic pressure. Therefore, SWE was not a suitable method to assess respiratory muscle function. Importantly, the SWE methodology used by the manufacturer may have had considerable impact on these results and may be different to devices from different manufacturers.

General discussion

Chapter 8 discussed the methodological value to assess respiratory muscle tissue remodelling with static ultrasound imaging and to asses respiratory muscle function with dynamic ultrasound imaging. Furthermore, the value of respiratory muscle ultrasound in congenital myopathies are discussed. Echogenicity analysis and atrophy assessment are reliable and valid methods to assess tissue remodelling. Assessing respiratory muscle function, in particular diaphragm function, is difficult with analysis of diaphragm movement, thickening and shear wave elastography. Spirometry and pressure-based measurements remain more sensitive for functional assessment in congenital myopathies, while reduced diaphragm thickening as measured with ultrasound is indicative of diaphragm weakness. Current research efforts focus on assessing the accessory respiratory muscle and performing long-term follow-up studies.



Appendix II - Nederlandse samenvatting | Dutch summary

Introductie

Hoofdstuk 1 introduceert congenitale myopathieën, de ademhalingsspieren en echografie. Echografie wordt in toenemende mate ingezet om de functie van de ademhalingsspieren te beoordelen bij spierziekten, op de intensive care en de longgeneeskunde, zowel in de klinische praktijk en als uitkomstmaat in onderzoek. Het eerste deel van dit proefschrift – **Current practice** – behandelt de technische toepassing van echografie van de ademhalingsspieren bij congenitale myopathieën en de interpretatie daarvan. Het tweede deel – **Critical appraisal** – reflecteert kritisch op de methodologie van echografie van de ademhalingsspieren. Dit proefschrift had derhalve als doel om de huidige status en toekomstperspectieven van echografie van de ademhalingsspieren in de kliniek en in onderzoek vast te stellen.

Deel 1 – Current practice

Hoofdstuk 2 is een review van de literatuur over methodologie, technologische ontwikkelingen, klinische toepassingen en beperkingen van echografie en MRI van de ademhalingsspieren bij mensen met een spierziekte. Zwakte van hulpademhalingsspieren is klinisch relevant, maar de meeste studies richtten zich uitsluitend op het diafragma. Daarnaast leidt een gebrek aan standaardisatie tot grote variabiliteit in de gerapporteerde uitkomstmaten en longitudinale studies ontbreken. Echografie is gebruikt om de functie van ademhalingsspieren te karakteriseren bij mensen met een spierziekte, maar wordt zelden toegepast in de klinische praktijk. Echogeniciteitsanalyse, strain imaging met speckle tracking en shear wave elastografie zijn veelbelovende methoden om de ademhalingsspieren te beoordelen bij mensen met een spierziekte.

Hoofdstuk 3 onderzocht de ademhalingsfunctie in het Nederlandse cohort van nemaline myopathie (NM). De mediane diafragma-verdikking bij typische NM was lager dan de centrum-specifieke ondergrens van normaal (**Hoofdstuk 5**), met een verhoogde mediane echogeniciteit z-score. Dit gold niet voor milde NM of childhood-onset NM met traagheid. Er werden geen statistisch significante verschillen gevonden tussen NM-typen, in tegenstelling tot longfunctieonderzoek en ademhalingsspierkrachtmetingen. Dit suggereert dat deze testen gevoeliger zijn voor verschillen in diafragmafunctie dan echografie. Wanneer gestratificeerd werd op longfunctie en ventilatiestatus, hadden patiënten met verminderde longfunctie en patiënten die mechanische ventilatie gebruikten een lagere diafragma-verdikking en hogere echogeniciteit, in lijn met verschillen in longfunctie en spierkracht. Deze bevindingen leiden tot de hypothese dat diafragma-echografie zowel longfunctie als diafragmakracht weerspiegelt. Er werden geen verschillen gevonden in dikte van diafragma en intercostale spieren, wat suggereert dat toename van spierbetrokkenheid niet leidt tot atrofie bij NM.

Hoofdstuk 4 onderzocht we de ademhalingsfunctie in de Nederlandse cohorten van *LAMA2*-gerelateerde spierdystrofie (LAMA2-MD) en *SEPN1*-gerelateerde congenitale myopathie (SELENON-RM), evenals veranderingen over een follow-upperiode van 1,5 jaar. Bij LAMA2-MD traden geen veranderingen op in longfunctie, ademhalingsspierkracht of echografie. Het diafragma had een normale dikte en de verdikking was normaal, terwijl de mediane echogeniciteit z-score tussen 1,7 en 2,1 lag, waarbij 2,0 een toename markeert. Bij SELENON-RM was het diafragma atrofisch en de verdikking verminderd, waardoor echogeniciteit niet betrouwbaar kon worden geanalyseerd. Deze parameters veranderden niet gedurende de follow-up, in overeenstemming met spierkrachtmetingen maar in tegenstelling tot longfunctie. Deze analyses versterken de hypothese dat diafragma-echografie diafragmakracht en longfunctie weerspiegelt, maar mogelijk minder gevoelig is voor verandering dan conventionele testen.

Deel 2 – Critical appraisal

Normaalwaarden voor diafragma-dikte, verdikking en echogeniciteit werden verzameld in **Hoofdstuk 5** in een representatieve groep gezonde deelnemers van jong tot oud. Echogeniciteit bleek sterk afhankelijk van leeftijd: waarden die normaal zijn bij ouderen zouden bij jongeren duidelijk verhoogd zijn. Diafragma-dikte wordt beïnvloed door geslacht en BMI, zij het minder sterk dan echogeniciteit. Diafragma-verdikking wordt niet beïnvloed door leeftijd, geslacht of BMI; hiervoor is een ondergrens van normaal vastgesteld. Normatieve data of gematchte controles zijn essentieel voor een valide interpretatie van diafragma-echografie. We presenteerden een gedetailleerd protocol voor acquisitie en analyse, evenals methoden om referentiewaarden te berekenen.

In **hoofdstuk 6** werd de complexe relatie tussen diafragma-verdikking, contractiliteit van het diafragma veranderingen in longvolume onderzocht. Deze relatie is onderwerp van wetenschappelijke discussie. Bij maximale isometrische contracties nam de diafragma-dikte niet toe, terwijl deze wel toenam bij onverzwaarde concentrische contracties. Dit suggereerde dat verdikking eerder longvolume weerspiegelt dan kracht. Door lekkage in het systeem waren de manoeuvres echter niet strikt isometrisch of strikt onverzwaard. Daarom werd tapered-flow-weerstand gebruikt om kracht en volume gelijktijdig te controleren. Diafragma-verdikking veranderde niet tussen verschillende inspanningsniveaus, maar nam toe met stijgend longvolume. Diafragma-verdikking moet niet geïnterpreteerd worden als een surrogaatmaat voor contractiliteit.

Shear wave elastografie (SWE) werd onderzocht als alternatief om contractiliteit te meten in **Hoofdstuk 7**. Eerdere studies suggereerden dat SWE een surrogaat is voor inspanning van het diafragma. Deze studie werd herhaald bij gezonde deelnemers en werd uitgebreid met patiënten met een congenitale myopathie, betrouwbaarheidsanalyses, en de hulpademhalingsspieren. SWE bleek een slechte intra-observer, inter-observer en test-retest betrouwbaarheid te hebben, toonde geen verschillen tussen gezonde deelnemers en patiënten, en correleerde niet met de

gouden standaard voor contractiliteit van het diafragma: de transdiafragmale druk. Daarom is SWE geen geschikte methode om ademhalingsspierfunctie te beoordelen. De gebruikte SWE-methodologie van de fabrikant kan hierbij een belangrijke rol hebben gespeeld en kan verschillen van andere systemen.

Algemene discussie

Hoofdstuk 8 bespreekt de methodologische waarde van het beoordelen van structurele veranderingen van de ademhalingsspieren met statische echografie en het beoordelen van de functie van de ademhalingsspieren met dynamische echografie. Daarnaast wordt de waarde van echografie van de ademhalingsspieren bij congenitale myopathieën besproken. Analyse van echogeniciteit en beoordeling van atrofie zijn betrouwbare en valide methoden om structurele veranderingen vast te stellen. Het beoordelen van de functie van de ademhalingsspieren, in het bijzonder de diafragmafunctie, is echter uitdagend wanneer dit gebeurt op basis van diafragmabeweging, dikteverandering en shear wave elastografie. Spirometrie en drukmetingen blijven gevoeliger voor functionele beoordeling bij congenitale myopathieën, terwijl een verminderde verdikking van het diafragma, gemeten met echografie, wel indicatief is voor diafragmazwakte. Huidige studies richten zich op het beoordelen van de hulpademhalingsspieren en lange-termijn follow-up.



Appendix III - Samenvatting in begrijpelijk Nederlands

Algemene inleiding

Hoofdstuk 1

Veel mensen met een congenitale myopathie hebben problemen met de ademhaling. Dit komt doordat de spieren die helpen bij het ademen minder sterk worden. Om te kijken hoe goed iemand kan ademen, gebruiken artsen en onderzoekers nu longfunctietesten en metingen van de kracht van de ademhalingsspieren. Maar deze testen zijn in veel situaties niet precies genoeg of zijn niet altijd betrouwbaar.

Daarom wordt er steeds vaker echografie gebruikt om de ademhalingsspieren te onderzoeken. Echografie is een techniek waarbij geluidsgolven worden gebruikt om beelden van de spieren te maken. Toch zijn er nog veel vragen. Wat meten we precies met echografie? En hoe kunnen we deze techniek op de beste manier gebruiken?

Dit proefschrift geeft antwoord op deze vragen en bestaat uit twee delen:

1. Hoe echografie in de huidige praktijk wordt gebruikt bij mensen met een congenitale myopathie.

2. Een kritische blik op hoe goed echografie van de ademhalingsspieren werkt.

Deel 1 – De huidige praktijk

Hoofdstuk 2

We hebben bekeken wat er al bekend is over het gebruik van echografie van de ademhalingsspieren bij mensen met een spierziekte. In veel onderzoeken wordt alleen gekeken naar het middenrif, omdat dit de belangrijkste spier is om mee te ademen. Maar bij mensen met een spierziekte zijn ook andere spieren belangrijk, zoals de borstspieren, nekspieren en buikspieren. Er zijn grote verschillen in hoe onderzoekers echografie gebruiken. Ze meten niet allemaal op dezelfde manier. Daardoor kun je de resultaten van verschillende studies niet goed met elkaar vergelijken. Ook is er nog geen onderzoek dat laat zien hoe de echografiemetingen veranderen over meerdere jaren. Verder wordt echografie van de ademhalingsspieren in de reguliere zorg nog maar weinig toegepast.

Hoofdstuk 3

We onderzochten mensen in Nederland met nemaline myopathie. Bij de groep mensen met de wereldwijd meest voorkomende vorm van nemaline myopathie werkt het middenrif minder

goed. In Nederland wonen echter veel mensen die een andere vorm van nemaline myopathie hebben Bij hen is het nog niet duidelijk of het middenrif ook minder goed werkt.

De resultaten van de echografie komen goed overeen met andere testen, zoals longfunctietesten en metingen van de kracht van de ademhalingsspieren. Dit laat zien dat echografie waarschijnlijk een goed beeld geeft van hoe goed iemand kan ademhalen. We zien geen duidelijke afname van de dikte van de spieren. Dit betekent dat de ademhalingsspieren bij mensen met nemaline myopathie niet altijd dunner worden, ook al werken ze soms wel minder goed.

Hoofdstuk 4

We onderzochten ook twee andere spierziekten: LAMA2-dystrofie en SELENON-myopathie. Bij mensen met LAMA2-dystrofie blijft de ademhaling stabiel gedurende de onderzoeksperiode van anderhalf jaar. Bij SELENON-myopathie is het middenrif wel dunner en zwakker, maar dit wordt gedurende de onderzoeksperiode niet erger. De longfunctie neemt in diezelfde periode echter wel af in deze groep.

Uit deze resultaten blijkt dat echografie niet heel goed werkt om kleine veranderingen in de ademhalingsspieren te vinden. Andere testen, zoals longfunctietesten en metingen van de kracht van de ademhalingsspieren, zijn daar gevoeliger voor.

Deel 2 – Een kritische blik

Hoofdstuk 5

In **Hoofdstuk 2** zagen we dat er grote verschillen zijn tussen onderzoeken die echografie van de ademhalingsspieren gebruiken. Daardoor verschillen ook de uitkomsten van die onderzoeken. Om dit probleem aan te pakken, hebben we bij een grote groep gezonde mensen het middenrif gemeten met echografie. Deze metingen kunnen we gebruiken als normaalwaarden: waarden die laten zien wat normaal is bij gezonde mensen.

Uit dit onderzoek blijkt dat sommige uitkomsten afhangen van leeftijd, lengte, gewicht en geslacht. Dit geldt bijvoorbeeld voor hoe helder het beeld is en voor de dikte van het middenrif. Andere maten zijn juist voor iedereen ongeveer gelijk. Een voorbeeld daarvan is hoeveel het middenrif dikker wordt tijdens het inademen.

Hoofdstuk 6

Veel onderzoekers meten de verdikking van het middenrif met echografie om te bepalen hoe sterk het middenrif is. Dat hebben wij in **Hoofdstuk 3** en **Hoofdstuk 4** ook gedaan. Maar er is veel discussie over de vraag of die verdikking echt iets zegt over de kracht van het middenrif.

Daarom hebben we dit onderzocht bij mensen met een congenitale myopathie en bij gezonde mensen. We zagen dat de verdikking van het middenrif niet samenhangt met de kracht van het middenrif. De verdikking blijkt wél samen te hangen met hoeveel lucht iemand inademt. Daarom adviseren wij andere onderzoekers om de verdikking van het middenrif niet meer te gebruiken als maat voor spierkracht.

Hoofdstuk 7

We willen graag de kracht van het middenrif goed kunnen meten. Daarom onderzochten we een andere echografie-techniek: shear wave elastografie (SWE). Dit is een nieuwe methode die de stijfheid van spieren kan meten. We onderzochten SWE bij mensen met een congenitale myopathie en bij gezonde mensen. Daarbij keken we naar alle ademhalingsspieren: het middenrif, de borstspieren, de nekspieren en de buikspieren. Uit het onderzoek bleek dat de metingen met SWE niet betrouwbaar zijn. De resultaten kwamen ook niet overeen met andere testen die iets zeggen over de kracht van de ademhalingsspieren. Daarom is SWE op dit moment geen geschikte methode om de kracht van de ademhalingsspieren te meten.

Algemene discussie

Hoofdstuk 8

Uit eerder onderzoek weten we dat echografie kan helpen om verschillende functies van de ademhalingsspieren te meten. In dit proefschrift laten we zien dat dit in de praktijk juist erg moeilijk is. Zo kunnen we met echografie nog niet goed meten hoe sterk de ademhalingsspieren zijn. Longfunctietesten of krachtmetingen van de ademhalingsspieren blijven de eerste keuze om de functie van de ademhalingsspieren te bepalen bij mensen met een congenitale myopathie. Veranderingen in de ademhalingsspieren door een congenitale myopathie zijn daarentegen wel goed zichtbaar met echografie.

In **Hoofdstuk 2** zagen we dat er meer onderzoek nodig is naar echografie van alle ademhalingsspieren, en naar hoe deze metingen veranderen over een langere periode. Dit soort langlopend onderzoek hebben we in dit proefschrift niet of slechts beperkt uitgevoerd. Op dit moment zijn we bezig met een nieuw onderzoek. Daarin volgen we mensen met een congenitale myopathie twee jaar lang. We meten tijdens die periode alle ademhalingsspieren met echografie. Hiermee hopen we de openstaande vragen alsnog te kunnen beantwoorden.



Appendix IV – Research data management

Ethics and approval

This thesis is based on the results of research involving human participants, which were conducted in accordance with relevant national and international legislation and regulation, and were in accordance with the ethical standards as laid down in the declaration of Helsinki. All participants provided written informed consent before study procedures were conducted.

Chapters 3, 4, 6 and 7 were approved by the local ethics committee (METC Oost-Nederland) under file numbers 2018-4252 (**Chapter 3**), 2017-3911 (**Chapter 4**) and 2021-7368 (**Chapters 6 and 7**). **Chapter 5** was at the time exempt from ethical approval as these data were collected as part of a project to determine reference limits for clinical practice.

Privacy

Privacy of study participants was ensured with pseudonymized participant codes. For **Chapters 3-5**, the key was stored separately from the data on a secured network rive and was only accessible to the researchers who needed access because of their role in the project. For **Chapters 6 and 7**, Participant Identity Management System (PIMS) was used, an in-house developed system designed to comply with all relevant legislation and regulations regarding access, audit trail and storage.

Data collection and storage

Clinical data was directly entered into Castor EDC or from the electronic patient file, while everything with raw source data such as imaging or signal files was stored on the department server, analysed and the outcome measures was entered into Castor EDC afterwards. All data is archived in a Data Acquisition Collection (DAC) with closed access in the Radboud Data repository for 15 years.

Data sharing

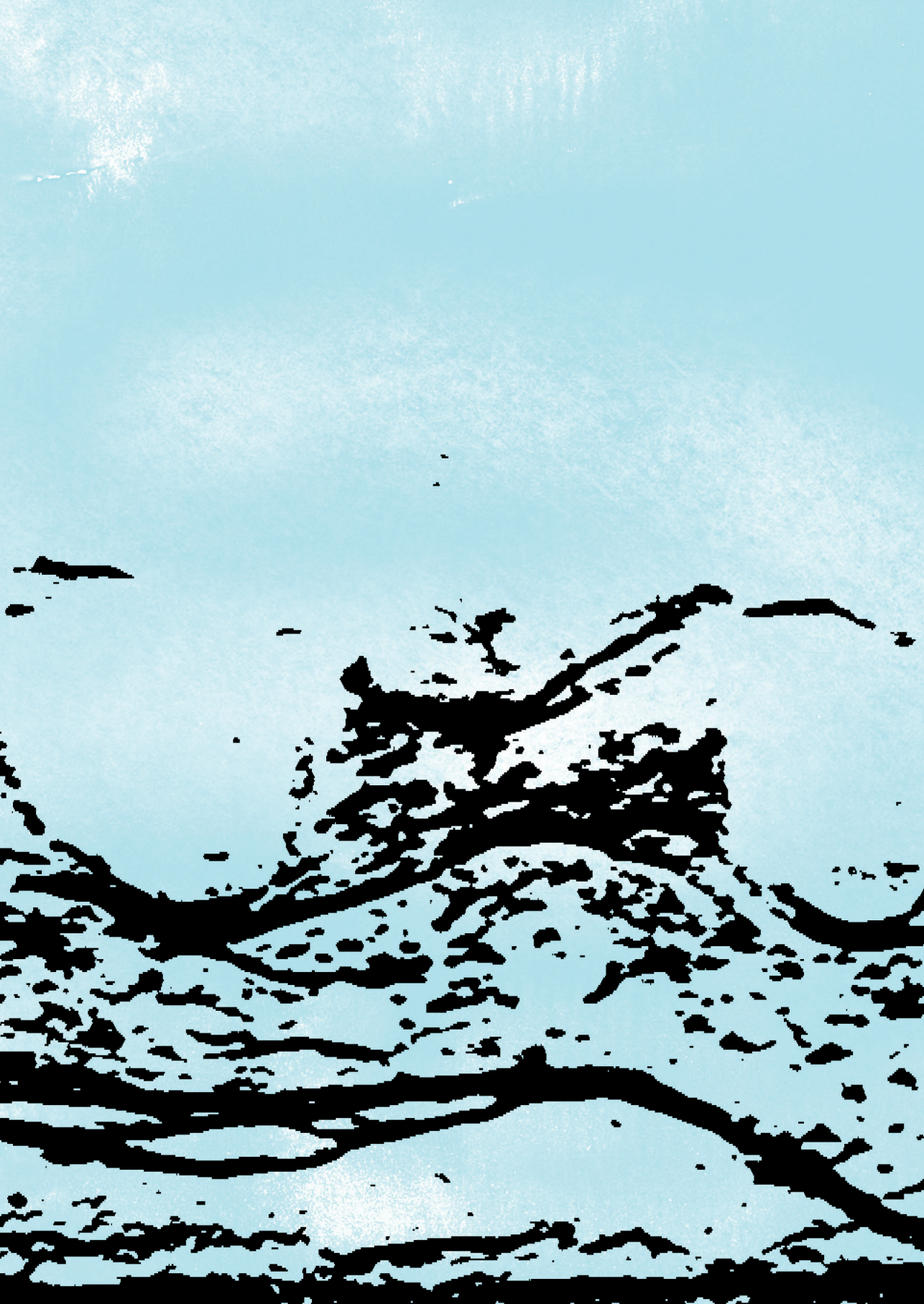
Participants did not give explicit consent for data sharing and therefore, the data cannot be shared. The data will be archived with closed access in a DAC of the Radboud Data Repository (DOI: 10.34973/aj3m-mt93) for 15 years after termination of the study



Appendix V - Author's scientific contributions to this thesis

	Study design	Data acquisition	Data analysis	Writing
CHAPTER 1	N/A	N/A	N/A	X
CHAPTER 2	X*	X*	N/A	X*
CHAPTER 3			X*	X*
CHAPTER 4			X*	X*
CHAPTER 5	X*		X	X*
CHAPTER 6	X*	X	X	X*
CHAPTER 7	X*	X*	X	X*
CHAPTER 8	N/A	N/A	N/A	X

* (One of the) Coauthors also contributed



Appendix VI – List of publications

This thesis

van Doorn JLM, van Doremalen JSM, van Engelen BGM, Voermans NC, de Korte CL, Ottenheijm CAC, Doorduin J. Interplay between diaphragm thickening, force generation and lung volume change: a physiological study in health and diaphragm weakness. Thorax. 2026:thorax–2026–225036.

van Doorn JLM, Jans D, de Korte CL, van Engelen BGM, Voermans NC, van Alfen N, Ottenheijm CAC, Bachasson D, Doorduin J. Shear Wave Elastography to Assess Respiratory Muscle Function in Congenital Myopathies. Muscle Nerve. 2026;74(1):103–10.

Bouman K, **van Doorn JLM**, Groothuis JT, Wijkstra PJ, van Engelen BGM, Erasmus CE, Doorduin J, Voermans NC. Respiratory function in LAMA2-related muscular dystrophy and SELENON-related congenital myopathy, a 1.5-year natural history study. Eur J Paediatr Neurol. 2024;48:30–9.

van Kleef ESB, **van Doorn JLM**, Gaytant MA, de Weerd W, Vosse BAH, Wallgren-Pettersson C, van Engelen BGM, Ottenheijm CAC, Voermans NC, Doorduin J. Respiratory muscle function in patients with nemaline myopathy. Neuromuscul Disord. 2022;32(8):654–63.

van Doorn JLM, Wijntjes J, Saris CGJ, Ottenheijm CAC, van Alfen N, Doorduin J. Association of diaphragm thickness and echogenicity with age, sex, and body mass index in healthy subjects. Muscle Nerve. 2022;66(2):197–202.

van Doorn JLM, Pennati F, Hansen HHG, van Engelen BGM, Aliverti A, Doorduin J. Respiratory muscle imaging by ultrasound and MRI in neuromuscular disorders. Eur Respir J. 2021;58(5).

Other publications

van de Camp S, Brenninkmeijer R, **van Doorn JLM**, de Laat ECM, Pomp L, Stinissen L, Cameron D, Groothuis JT, van Alfen N, Jungbluth H, Erasmus CE, Bartels B, Wadman RI, Voet NBM, van der Pol WL, Voermans NC. READYCOM: protocol for a 2-year prospective natural history and cross-sectional muscle-fatigability study for improving trial readiness in congenital myopathies. BMJ Open. 2026;16(8):e119529.

Ijland MM, **van Doorn JLM**, Beukman A, van der Hoeven JG, Lemson J, Heunks LMA, Doorduin J. The effect of mechanical ventilation on respiratory muscle echogenicity in critically ill children: an observational cohort study. BMC Pediatr. 2025;25(1):502.

de Laat ECM, Houwen-van Opstal SLS, Bouman K, **van Doorn JLM**, Cameron D, van Alfen N, Dittrich ATM, Kamsteeg EJ, Smeets HJM, Groothuis JT, Erasmus CE, Voermans NC. A 5-year natural history study in LAMA2-related muscular dystrophy and SELENON-related myopathy: the Extended LAST STRONG study. BMC Neurol. 2024;24(1):409.

Vincenten SCC, **van Doorn JLM**, Teeselink S, Rasing NB, Padberg GW, Voermans NC, van Engelen BGM, van Alfen N, Mul K. The other face of facioscapulohumeral muscular dystrophy: Exploring orofacial weakness using muscle ultrasound. Muscle Nerve. 2024;70(5):1062–71.

Hermans BP, **van Doorn JLM**, Roesthuis LH, Hofland J, Li WWL, van Dort DIM, van der Heijden E, van Goor H, Verhagen A. Characterisation of pulmonary air leak measurements using a mechanical ventilator in a bench setup. J Med Eng Technol. 2024;48(3):81–91.

Jonkman AH, Warnaar RSP, Baccinelli W, Carbon NM, D'Cruz RF, Doorduin J, **van Doorn JLM**, Elshof J, Estrada-Petrocelli L, Graßhoff J, Heunks LMA, Koopman AA, Langer D, Moore CM, Nunez Silveira JM, Petersen E,

Poddighe D, Ramsay M, Rodrigues A, Roesthuis LH, Rossel A, Torres A, Duiverman ML, Oppersma E. Analysis and applications of respiratory surface EMG: report of a round table meeting. Crit Care. 2024;28(1):2.

Bouma S, Cobben N, Bouman K, Gaytant M, van de Biggelaar R, **van Doorn JLM**, Reumers SFI, Voet NB, Doorduin J, Erasmus CE, Kamsteeg EJ, Jungbluth H, Wijkstra P, Voermans NC. Respiratory features of centronuclear myopathy in the Netherlands. Neuromuscul Disord. 2023;33(7):580–8.

Kramer JJ, Boon HTM, Leijten QH, Ter Laak H, Eshuis L, Kusters B, **van Doorn JLM**, Kamsteeg EJ, Eymard B, Doorduin J, Voermans NC. Dystrophic Myopathy of the Diaphragm with Recurrent Severe Respiratory Failure is Congenital Myasthenic Syndrome 11. J Neuromuscul Dis. 2023;10(2):271–7.

Lagarde MLJ, **van Doorn JLM**, Weijers G, Erasmus CE, van Alfen N, van den Engel-Hoek L. Tongue movements and teat compression during bottle feeding: A pilot study of a quantitative ultrasound approach. Early Hum Dev. 2021;159:105399.

A



Appendix VII – Dankwoord | Acknowledgements

Allereerst wil ik alle deelnemers bedanken die met hun inzet hebben bijgedragen aan dit proefschrift. In het speciaal iedereen met een congenitale myopathie, die tot wel vier keer langs zijn geweest voor een onderzoeksbezoek. De gesprekken met jullie hebben mij veel inzicht gegeven hoe het is om te leven met een spierziekte, en wat wij als onderzoekers eigenlijk allemaal wel van jullie vragen. Die waardevolle lessen neem ik mee.

Prof. dr. Voermans, beste **Nicol**, je was pas 'echt' bij dit proefschrift betrokken nadat Baziel met emeritaat ging en jij benoemd werd tot hoogleraar. Maar stiekem was je al vanaf het begin beschikbaar om je inzicht in congenitale myopathieën te delen. Zonder jouw inzet had ik waarschijnlijk geen patiënten gevonden die graag mee wilden doen met mijn onderzoek. Je kijkt als neuroloog met een hele andere blik naar klinisch onderzoek dan ik, en daarin heb ik heel veel van je geleerd. Bedankt voor alle momenten waarop je mee kon denken en manuscripten kon bekijken, zelfs als je agenda overvol zat.

Prof. dr. Ottenheijm, beste **Coen**, hoewel jouw rol wat meer op afstand lag, heeft jouw inzet er toe geleid dat dit promotietraject tot stand kwam. Je zocht de verbinding tussen mijn werk en jouw werk op het lab en dat leidde vaak tot interessante inzichten. Met de nieuwe stappen die we nu aan het zetten zijn bij de muizen hoop ik nog vaak met je samen te kunnen werken.

Prof. dr. ir. de Korte, beste **Chris**, ook jouw rol lag wat meer op afstand. Desalniettemin waren al onze meetings, in de agenda altijd vermomd als 'een kop koffie drinken', voor mij bijzonder waardevol. Waar ik met name kijk naar de toepassing van een techniek, kijk jij veel kritischer naar de techniek zelf. Die reflectie op meerdere niveaus hebben verschillende manuscripten naar een hoger niveau getild. We konden erg enthousiast negatief over nieuwe technieken zijn, en ik denk dat die instelling me nu tot een betere onderzoeker maakt. Dank voor alle koppen koffie en hopelijk kunnen we dat nog vaak doen.

Dr. Doorduin, beste **Jonne**, toen ik jou en Nens in 2019 een mailtje stuurde met 'heb je toevallig werk voor me', had ik niet verwacht hier nu een dankwoord te schrijven. Net afgestudeerd en je bood me een project aan dat eigenlijk bedoeld was voor een postdoc. Dit project was als een achtbaan: ik had nooit verwacht dat we uiteindelijk schapen stonden te opereren om een zelf ontwikkelde diafragmapacemaker te testen. En al helemaal niet dat mijn collega's me alleen maar schaap-gerelateerde cadeaus zouden geven. Helaas konden we geen vervolgsubsidie vinden, maar bood je me een ander project samen met Coen aan dat uiteindelijk zou uitmonden in dit proefschrift. Gedurende dit traject heb je gefungeerd als mijn mentor en heb je me alle facetten van het zijn van onderzoeker geleerd. Ook nu, best een tijd na je vertrek naar de IC, merk ik dat nog vaak de vaardigheden toepas die ik van jou heb overgenomen. Dank voor de rol die je voor mij hebt gespeeld, ik had me geen betere begeleider kunnen wensen.

Gedurende mijn promotietraject zijn er een aantal wisselingen van de wacht geweest in mijn promotieteam. **Prof. dr. Van Engelen**, beste **Baziel**, bedankt voor jouw input in de eerste fase. Je hebt vaak een verrassende kijk op zaken die snel tot hele nieuwe inzichten leiden. Bedankt voor je interesse in alle zaken rondom de onderzoeker. **Dr. Hanssen**, beste **Rik**, bedankt voor jouw nuchtere en pragmatische kijk op het gebruik uitdagende echografietechnieken bij mensen. Ik hoop dat je het naar je zin hebt bij Maastro!

Ik wil graag de leden van de manuscriptcommissie bedanken voor hun deskundige beoordeling van dit proefschrift. Ik kijk er naar uit om met jullie in discussie te gaan tijdens mijn verdediging.

Prof. dr. Van Alfen, beste **Nens**, gek genoeg ben jij nooit formeel betrokken geweest bij mijn promotietraject. Desalniettemin speel jij sinds het begin van mijn onderzoekscarrière een enorme rol. Ik ben heel blij en dankbaar dat ik de afgelopen jaren steeds meer bekend mocht raken met de kwantitatieve spierechografie, en dat we dat nu verder door kunnen ontwikkelen. Ik ben heel enthousiast over de volgende stappen die we nu aan het zetten zijn bij de muizen! Dank voor je vertrouwen in mij.

Tijdens mijn verdediging heb ik twee fantastische collega's naast me staan. **Odette**, jij bent ooit aangeschaft als maatje voor mij toen ik eenzaam op de onderzoekskamer weg zat te kwijnen en die taakomschrijving heb je ter harte genomen. Ik heb zelden iemand ontmoet die jouw passie voor wijn heeft. **Eline**, je kwam pas later bij Odette en mij op de kamer zitten, maar je persoonlijkheid maakt dat meer dan goed. Ik heb zelden iemand ontmoet die met jouw passie kan klagen. Met zijn drieën versterken we elkaar alleen maar en dat is voor niemand leuk – behalve voor ons. Dank voor de zwarte aura.

Onderzoek doe je niet alleen, onderzoek doe je individueel op een gezellig kantoor. Dank aan alle onderzoekers die dat mogelijk hebben gemaakt. **Esmee**, voordat ik die rol van je overnam, heette jij mij welkom in de onderzoeksgroep in afwezigheid van Jonne. Leuk dat we samen een artikel hebben geschreven, dat in het proefschrift van ons beiden terecht is gekomen. En we klaren de klus met een week ertussen! **Roderick**, **Carlijn** en **Lieneke**, bedankt voor de fijne sfeer in onze eigen bubbel en voor mijn eerste schaap. **Karlijn**, je nam de plek van Esmee over, en ook met jou heb ik een artikel geschreven dat in het proefschrift van ons beiden terecht is gekomen. Jij hebt de klus echter een stuk sneller geklaard. Bedankt dat ik jouw paranimf mocht zijn! **Sjan**, fijn dat je altijd een baken van positiviteit bent. Hopelijk kunnen we nog lang samen onderzoeken. Bedankt dat ik jouw paranimf mag zijn! **Joost**, **Sanne**, **Luuk** en **Nick**, soms wat meer op afstand, soms via gelach door de muur, maar jullie andere kijk op dingen was waardevol en vermakelijk. **Ilse**, bij dezen toch een losse boodschap. Heeft dat kamergenootschap toch nog ergens toe geleid! Sorry voor mijn constante geklaag. **Lizan**, het was nooit saai als jij er was, en die wervelwind zorgt ervoor dat jij een week later de klus klaart. Succes op je nieuwe plek! **Sanne**, mijn excuses voor hoe vaak ik aan jou vroeg om dingen voor onze gezamenlijke

deelnemers te regelen. Dat was voor mij echter wel heel waardevol, bedankt! **Marit**, het is heel leuk om te zien hoe je Spieren voor Lucht als een soort opvolger van mijn onderzoek oppakt, en met jou op veel plekken samen te werken. Desondanks hebben we gelukkig zelden een echte meeting, maar weten we alles te vermommen als koffiemomenten en lunch. Dank voor het tegenlezen van mijn discussie en je hulp met het ontwerp van mijn proefschrift! **Iris**, **Ronne**, **Dirk**, **Elise**, **Stacha**, **Amir**, **Kiki**, **Marloes** en **Riemke**, als iedereen er is lopen de werkplekken over en duren de koffiemomenten erg lang. Desondanks hebben we zo een erg leuke groep en blijf ik nog graag lang op mijn plek tussen jullie zitten.

Verschillende studenten hebben mij geholpen tijdens dit proefschrift. **Tim**, **Douwe**, **Dieke**, **Nora** en **Joris**, jullie hulp was van onschatbare waarde. Jullie zullen me af en toe vast vervloekt hebben, waarvoor excuses, maar ik vond het juist erg leuk en waardevol om jullie te begeleiden. Jullie hielden me (bijna allemaal) jong.

De afdeling Klinische Neurofysiologie, in het bijzonder alle **laboranten**, jullie zijn een warme thuishaven. Het is altijd heel fijn om bij jullie binnen te komen lopen en te kijken of er nog een koekje in de trommel zit. Jullie zijn een leuke groep en het is altijd leuk om met dat koekje nog lang bij jullie te blijven kletsen. Ik wil specifiek **Sander** bedanken voor al zijn hulp met alles wat een apparaat genoemd mag worden, en **Juerd** voor het tegenlezen van mijn discussie.

Alle medewerkers van het **spierziekten expertise centrum** en het **kinderspiercentrum**, jullie zijn een fijne groep collega's die samen de zorg en het onderzoek voor mensen met een spierziekte vormgeven op alle leeftijden. Ik blijf graag nog lang met jullie samenwerken. In het bijzonder wil ik **Donnie** bedanken (dit keer in het Nederlands) als vaste sparringpartner als het aankomt op imaging. Ik leer heel veel van jou over MRI, onderzoek en mooi Schots taalgebruik. **Marloes**, mijn laatste masterstage bij jou bleek een schot in de roos, en de opstap naar een plek in deze groep. Je was destijds een hele fijne begeleider en het was heel leuk om je ons artikel te zien verdedigen bij jouw promotie. Ik ben blij dat wij nog steeds samenwerken.

Ik heb geluk met de vele vrienden om mij heen. De trouwe kijkers van **Ex on the beach** (we lopen wat achter), de **Stamgasten** (al een tijd niet meer in de Aesculaaf geweest), de **Krassantjes** (hoe spreek je dat nu eigenlijk uit?), de **D&D** en **Gloomhaven** avonden, ik kan altijd op jullie steunen en stoom afblazen waar nodig. Dit dankwoord wordt veel te lang als ik jullie allemaal individueel ga benoemen, maar jullie zijn heel belangrijk voor mij.

Natuurlijk wil ik ook graag mijn familie bedanken. **Bart**, **Ria**, **Martijn**, **Youngmee** en **Rick**, het is altijd heerlijk om het 'drukke' Nijmegen even te ontsnappen als ik bij jullie ben. Dank voor jullie steun en interesse, zonder jullie was ik niet gekomen waar ik nu ben. Tijdens mij promotietraject heb ik daar nog een extra familie bij gekregen met **Peter**, **Nanny**, **Bart** en **Joëlle**. Dank voor het warme welkom en jullie enthousiasme voor mijn proefschrift.

Bregje, de laatste woorden hier zijn voor jou. Meer dan je door hebt ben je voor mij een steun en toeverlaat. Hoewel je het begin van dit promotietraject niet hebt meegemaakt, voelt het voor mij alsof je er de hele weg bij was. Ik ben je enorm dankbaar voor het aanhoren van mijn tirades bij tegenslagen, het tonen van interesse in mijn successen en hoe jij altijd achter mij staat als ik weer eens iets heb verzonnen. Ik hoop dat ik nog veel successen en mijlpalen met jou mag vieren, nu in ons eigen thuis. Ik hou van jou.

A



Appendix VIII – Curriculum Vitae

Jeroen van Doorn werd geboren op 1 september 1994 te Oss. In 2012 haalde hij zijn VWO diploma aan het Maaslandcollege te Oss. Hierna volgde hij de bachelor biomedische wetenschappen aan de Radboud Universiteit te Nijmegen, welke hij afsloot met een wetenschappelijke stage op de afdeling revalidatiegeneeskunde van het Radboudumc en het Donders Centre for cognitive Neuroimaging. Vervolgens volgde hij de master biomedical sciences aan de Radboud Universiteit te Nijmegen, waarin hij twee wetenschappelijke stages volbracht, één bij het SMA expertisecentrum van het UMCU en één bij het team kinderlogopedie van de afdeling Revalidatiegeneeskunde van het Radboudumc.

Na zijn afstuderen is hij als wetenschappelijker onderzoeker gaan werken op de afdeling Neurologie – Klinische Neurofysiologie van het Radboudumc onder begeleiding van Dr. Jonne Doorduin. Zijn eerste project was het ontwikkelen van een voorloper van een prototype van een neuraal aangestuurde diafragmapacemaker. Daarna is hij gestart met zijn promotieonderzoek, hetgeen heeft geresulteerd in dit proefschrift. Tijdens zijn promotieonderzoek heeft hij zich gespecialiseerd in (kwantitatieve) neuromusculaire echografie, waar hij onderzoek naar doet sinds het afronden van zijn promotieonderzoek onder begeleiding van prof. dr. Nens van Alfen.

Jeroen woont samen met zijn partner, Bregje, in Nijmegen.



Radboudumc
university medical center

IN DEI NOMINE FELICITER

Radboud University